

DIRECT DISTRIBUTIONAL OPTIMIZATION FOR PROV- ABLE ALIGNMENT OF DIFFUSION MODELS

Anonymous authors

Paper under double-blind review

ABSTRACT

We introduce a novel alignment method for diffusion models from distribution optimization perspectives while providing rigorous convergence guarantees. We first formulate the problem as a generic regularized loss minimization over probability distributions and directly optimize the distribution using the Dual Averaging method. Next, we enable sampling from the learned distribution by approximating its score function via Doob’s h -transform technique. The proposed framework is supported by rigorous convergence guarantees and an end-to-end bound on the sampling error, which imply that when the original distribution’s score is known accurately, the complexity of sampling from shifted distributions is independent of isoperimetric conditions. This framework is broadly applicable to general distribution optimization problems, including alignment tasks in Reinforcement Learning with Human Feedback (RLHF), Direct Preference Optimization (DPO), and Kahneman-Tversky Optimization (KTO). We empirically validate its performance on synthetic and image datasets using the DPO objective.

1 INTRODUCTION

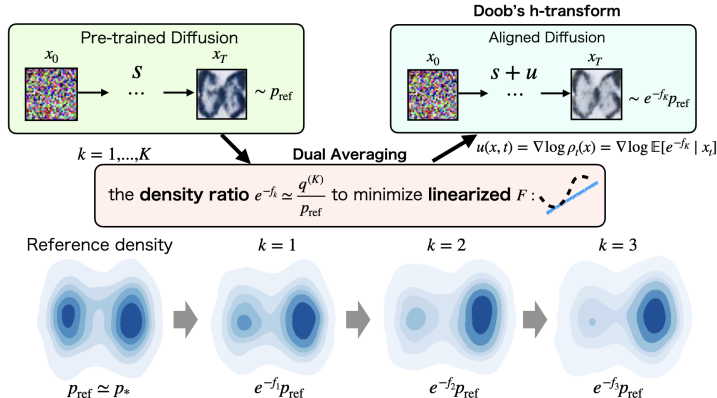
Diffusion models (Sohl-Dickstein et al., 2015; Ho et al., 2020; Song et al., 2021) have recently emerged as powerful tools for learning complex distributions and performing efficient sampling. Within the framework of foundation models, a common approach involves pre-training on large-scale datasets, followed by adapting the model to downstream tasks or aligning it with human preferences (Ouyang et al., 2022). This alignment is typically formalized as nonlinear distribution optimization, with a regularization term that encourages proximity to the pre-trained distribution. Examples of such alignment methods include Reinforcement Learning with Human Feedback (RLHF) (Ziegler et al., 2020), Direct Preference Optimization (DPO) (Rafailov et al., 2023; Wallace et al., 2024), and Kahneman-Tversky Optimization (KTO) (Ethayarajh et al., 2024; Li et al., 2024).

Specifically, these methods solve the minimization problems of a regularized functional $F(q) + \beta D_{\text{KL}}(q||p_{\text{ref}})$ over q in the probability space \mathcal{P} , where p_{ref} is the probability density corresponding to the pretrained diffusion model. However, this type of distributional optimization problem over the density q is challenging because the output density governed by the reference model cannot be evaluated and neither is the aligned model q . They are accessible only through samples generated from their corresponding generative models. Existing distributional optimization methods such as *mean-field Langevin dynamics* (Mei et al., 2018) and *particle dual averaging* (Nitanda et al., 2021) resolved this problem by adapting a Langevin type sampling procedure to calculate a functional derivative of the objective without explicitly evaluating the densities. However, the distributions q and p_{ref} are highly complex and multimodal from which it is extremely hard to generate data by a standard MCMC type methods including the Langevin dynamics. This difficulty can be mathematically characterized by isoperimetric conditions, such as logarithmic Sobolev inequality (LSI) (Bakry et al., 2014), that has usually exponential dependency on the data dimension d for multimodal data yielding the curse of dimensionality. Unfortunately, the existing distribution optimization methods mentioned above are sensitive to the LSI constant, so they suffer from severely slow convergence, failing to align diffusion models.

That is to say, alignment of diffusion models has two challenges: (i) inaccessibility of the output densities and (ii) multimodality of the densities. This naturally leads to a fundamental question:

054 *Can we develop an alignment algorithm for diffusion models from distribution optimization*
 055 *perspectives, while ensuring rigorous convergence guarantees without isoperimetric conditions?*
 056

057 We address this question by developing a diffusion-model based distribution optimization method
 058 and providing rigorous convergence and sampling error guarantees, and demonstrate its applicability
 059 to several tasks involved with diffusion model alignment. **Our method represents the aligned model**
 060 **by a diffusion model that can be described by merely adding a correction term to the score function**
 061 **of the original reference model. During optimizing the model, we don't rely on any MCMC sampler**
 062 **but only use samples generated by the original reference model (and the aligned diffusion model).**
 063 **This characteristics is helpful to resolve the issue of isoperimetric condition.**
 064



072 Figure 1: Overview of the proposed method integrating Dual Averaging and Doob’s h-transform.

073 1.1 OUR CONTRIBUTIONS

074 To tackle the two challenges mentioned above: absence of (i) sampling guarantee and (ii) isoperime-
 075 try, we propose a general framework that integrates dual averaging (DA) method (Nesterov,
 076 2009) and diffusion model (Sohl-Dickstein et al., 2015; Ho et al., 2020; Song et al., 2021). The DA
 077 method is an iterative algorithm that constructs the Gibbs distribution converging to the optimal
 078 distribution (i.e., alignment). A key advantage of this DA scheme is its ability to bypass isoperime-
 079 tric conditions with the help of high sampling efficiency of the reference diffusion model, enabling
 080 isoperimetry-free sampling from an aligned distribution. Specifically, an aligned diffusion process
 081 that approximately generates the Gibbs distribution obtained by DA method can be constructed
 082 through the Doob’s *h*-transform (Rogers & Williams, 2000) and density ratio estimation with re-
 083 spect to a reference distribution using neural networks (see Figure 1 for illustration).
 084

085 We summarize our contribution below.

- 086 • We establish a model alignment method to align diffusion models, with convergence guaran-
 087 tees for both convex and nonconvex objectives, based on distribution optimization theory and
 088 Doob’s *h*-transform. Notable distinctions from other mean-field optimization methods are that
 089 our method works without isoperimetry conditions such as LSI and allows for sampling from
 090 multimodal distributions.
- 091 • We also analyze the sampling error due to the approximation of the drift estimators with neural
 092 networks and the discretization of the process, and evaluate how these errors affect the final
 093 sampling accuracy.
- 094 • Our general framework encompasses several major alignment problems such as RLHF, DPO,
 095 and KTO, establishing a provable alignment method for these scenarios. We demonstrate
 096 the applicability of our framework to these settings and empirically validate its performance
 097 on both synthetic and image datasets, aiming at data augmentation for a specific mode of
 098 distribution, using DPO objective.

099 We also emphasize that our method has the potential to be applied to general distribution opti-
 100 mization problems beyond alignment tasks such as density ratio estimation under the covariate shift
 101 setting (Sugiyama et al., 2008; Tsuboi et al., 2009) and climate change tracking (Ling et al., 2024).
 102

1.2 RELATED WORK.

Mean-field optimization. PDA method (Nitanda et al., 2021; Nishikawa et al., 2022), an extension of DA method (Nesterov, 2009) to the distribution optimization setting, was the first method that proves the quantitative convergence for minimizing entropy regularized convex functional. Subsequently, P-SDCA method (Oko et al., 2022), inspired by the SDCA method (Shalev-Shwartz & Zhang, 2013), achieved the linear convergence rate. Mean-field Langevin dynamics (Mei et al., 2018) is the most standard particle-based distribution optimization method, derived as the mean-field limit of the noisy gradient descent, and its convergence rate has been well studied by Mei et al. (2018); Hu et al. (2021); Nitanda et al. (2022); Chizat (2022); Suzuki et al. (2023); Nitanda (2024). Additionally, several mean-field optimization methods such mean-field Fisher-Rao gradient flow (Liu et al., 2023b) and entropic fictitious play (Chen et al., 2023a; Nitanda et al., 2023) have been proposed with provable convergence guarantees. We note that the convergence rates of these methods were established under isoperimetric conditions such as log-Sobolev and Poincaré inequalities, which ensure concentration of the probability mass. IKLPD method (Yao et al., 2024) shares similarities with our method, as it employs the normalizing flow to solve intermediate subproblems in the distributional optimization procedure, and its convergence does not depend on isoperimetric conditions. However, the applicability of IKLPD to alignment tasks remains uncertain since handling the proximity to the reference distribution is non-trivial.

Fine-tuning of diffusion models. Recently, alignment of diffusion models have been investigated, inspired by LLM fine-tune methods, such as RLHF (Ziegler et al., 2020), DPO (Rafailov et al., 2023), and KTO (Ethayarajh et al., 2024). Applying them to diffusion models entails additional difficulty since the output density p_{ref} of the diffusion model is not available, and hence several techniques have been developed to circumvent the explicit calculation of p_{ref} . For instance, Fan et al. (2023); Black et al. (2024); Clark et al. (2024) invented the maximization algorithm of the reward in each diffusion time step. Uehara et al. (2024b) used Doob’s h -transform to compute the correction term that can be automatically derived from the density ratio between the generated and the reference distributions. Instead of optimizing original DPO and KTO objectives, Wallace et al. (2024) considered the evidence lower bound (ELBO) and Li et al. (2024) defined a new objective function to replicate KTO. Marion et al. (2024) also studied fine-tuning of diffusion models as distributional optimization within the RLHF framework and conducted convergence analysis for the one-dimensional Gaussian distribution.

2 PROBLEM SETTING

Distributional Optimization. Let \mathcal{P} be the space of probability density functions with respect to the Lebesgue measure on $(\mathbb{R}^d, \mathcal{B}(\mathbb{R}^d))$. Let $F : \mathcal{P} \rightarrow \mathbb{R}$ be a functional and $p_{\text{ref}} \in \mathcal{P}$ be the reference density. In this work, we consider the regularized loss minimization problem over \mathcal{P} :

$$\min_{q \in \mathcal{P}} \{L(q) := F(q) + \beta D_{\text{KL}}(q \| p_{\text{ref}})\}, \quad (1)$$

where $D_{\text{KL}}(q \| p_{\text{ref}}) := \mathbb{E}_q[\log \frac{q}{p_{\text{ref}}}]$ is the Kullback-Leibler divergence, and $\beta > 0$ is a regularization coefficient. We assume that F is differentiable. That is, the functional F has *first order variation* $\frac{\delta F}{\delta q} : \mathcal{P} \times \mathbb{R}^d \ni (q, x) \rightarrow \frac{\delta F}{\delta q}(q, x) \in \mathbb{R}$ such that for all $q, q' \in \mathcal{P}$,

$$\left. \frac{dF(q + \epsilon(q' - q))}{d\epsilon} \right|_{\epsilon=0} = \int \frac{\delta F}{\delta q}(q, x)(q' - q)(x) dx.$$

In the following we assume that there exists a unique minimizer $\hat{q}_{\text{opt}} := \arg \min_{q \in \mathcal{P}} L(q)$.

Diffusion Models. p_{ref} is the output density of a pre-trained diffusion model (Sohl-Dickstein et al., 2015; Song & Ermon, 2019; Ho et al., 2020; Song et al., 2021; Vahdat et al., 2021), while $p_* \in \mathcal{P}$ is the target distribution of pre-training. A “noising” process $\{\bar{X}_t\}_{t \geq 0}$ denotes the Ornstein-Uhlenbeck (OU) process from $p_*(x)$. The law of \bar{X}_t can be written as $p_t(x) = \int \mathcal{N}(m_t \bar{X}_0, \sigma_t) dp_*(\bar{X}_0)$ with $m_t = e^{-t}$, $\sigma_t^2 = 1 - e^{-2t}$. Then, the reverse process $\{\bar{X}_t^{\leftarrow}\}_{0 \leq t \leq T}$ ($T \geq 0$) can be defined as

$$\bar{X}_t^{\leftarrow} \sim p_t, \quad d\bar{X}_t^{\leftarrow} = \{\bar{X}_t^{\leftarrow} + 2\nabla \log p_{T-t}(\bar{X}_t^{\leftarrow})\} dt + \sqrt{2} dB_t.$$

Then it holds that $\text{Law}(\bar{X}_t^{\leftarrow}) = \text{Law}(\bar{X}_{T-t})$, which enables us to sample from p_* . In practice, we approximate the score $\nabla \log p_{T-t}(\bar{X}_t^{\leftarrow})$ function by a score network $s : \mathbb{R}^{d+1} \rightarrow \mathbb{R}^d : (x, t) \mapsto$

162 $s(x, t)$. In addition, we initialize $X_0^{\leftarrow} \sim \mathcal{N}(0, I_d) \simeq p_T$ and the process is time-discretized. The
 163 random variable generated by the following dynamics with step size h is denoted by $\{X_t^{\leftarrow}\}_{0 \leq t \leq T}$.

164 $X_0^{\leftarrow} \sim \mathcal{N}(0, I_d)$, $dX_t^{\leftarrow} = \{X_{lh}^{\leftarrow} + 2s(X_{lh}^{\leftarrow}, lh)\}dt + \sqrt{2}dB_t$, $t \in [lh, (l+1)h]$, $l = 1, \dots, L = T/h$.

165 In the same way, we define q_t as the density of the diffusion process corresponding to q_* , and
 166 $\{\bar{X}_t\}_{t \geq 0}$ and $\{X_t^{\leftarrow}\}_{0 \leq t \leq T}$ as the corresponding noising and the backward process.

167 Now we have two challenges in this problem (1):

- 168 (A). **Multimodality of p_{ref} and \hat{q}_{opt} .** Our goal is to obtain samples from \hat{q}_{opt} . Now we tackle
 169 with the case that p_{ref} and \hat{q}_{opt} have high *multimodality*: p_{ref} and \hat{q}_{opt} have multiple modes
 170 or maxima, in other words, the potentials $-\log p_{\text{ref}}$ and $-\log \hat{q}_{\text{opt}}$ are extremely far from
 171 concave. Probability distributions of real-world data like images often have such complex
 172 structures, which implies that LSI is significantly weak.
 173 (B). **Inaccessibility to the density p_{ref} .** We cannot directly calculate the density p_{ref} because
 174 diffusion models only have the score network. We only have information of p_{ref} as samples
 175 from p_{ref} .

176 **Inapplicability of Mean-Field Langevin Dynamics.** Mean-field Langevin dynamics
 177 (MFLD) (Mei et al., 2018) is the most standard particle-based optimization method tailored
 178 to solve the special case of the problem (1) where F is convex functional and p_{ref} is a strongly
 179 log-concave distribution such as Gaussian distribution. The convergence rate of MFLD (Nitanda
 180 et al., 2022; Chizat & Bach, 2018) has been established under the condition where the proximal
 181 distribution: $p_q \propto p_{\text{ref}} \exp\left(-\beta^{-1} \frac{\delta F}{\delta q}(q, \cdot)\right)$ associated with MFLD iteration q satisfies logarithmic
 182 Sobolev inequality (LSI), which says sufficient concentration of p_q . Typically, LSI for p_q should
 183 rely on the isoperimetry of the reference distribution p_{ref} with Holley-Strook argument (Holley &
 184 Stroock, 1987) since $\frac{\delta F}{\delta q}(q, \cdot)$ is not expected to encourage it in general. Therefore, the replacement
 185 of p_{ref} to a pre-trained distribution, which is highly complex and has multi-modality, leads to
 186 failure or weak satisfaction of LSI. As a result, the convergence of MFLD is significantly slowed
 187 down. Additionally, MFLD is practically implemented so that finite particles approximately follow
 188 the ideal dynamics of MFLD, and it is not intended for resampling from the final distribution
 189 represented by these particles. In short, the lack of (i) a sampling guarantee and (ii) a isoperimetric
 190 condition limits the applicability of MFLD in our problem setting.

191 To address these challenges, we employ the following strategy, which will be detailed in Section 4.

- 192 (A). **Modifications of diffusion models for sampling from a multimodal distribution.** First,
 193 we obtain samples from p_{ref} using a diffusion model which works for a broad range of
 194 probability distributions that have complex structures such as multimodality. **Then, we**
 195 **reconstruct the diffusion model to sample from \hat{q}_{opt} by simply adding a correction term.**
 196 (B). **A distributional optimization algorithm that does not require the density p_{ref} .** Sec-
 197 ond, following the dual averaging (DA) method in the distribution optimization setting,
 198 we construct a sequence of distributions $\hat{q}^{(k)}$ converging to the optimum, which guides an
 199 aligned diffusion process in combination with the density ratio estimation using neural net-
 200 works with Doob’s h -transform. We only have to calculate the density ratio between $\hat{q}^{(k)}$
 201 and p_{ref} and the samples from p_{ref} to run our algorithm.

202 3 APPLICATIONS

203 Our framework of the distributional optimization for the pre-trained diffusion models includes im-
 204 portant fine-tuning methods for diffusion models. The first term $F(q)$ in (1) represents *the human*
 205 *preference*, acting as feedback from the outputs of p_{ref} . Note that $F(q)$ can be dependent of p_{ref} .
 206 The second term $\beta D_{\text{KL}}(q \| p_{\text{ref}})$ in (1) provides regularization to prevent q from collapsing.

207 **Example 1** (Reinforcement Learning). *Our study includes the case F is limited to be a linear*
 208 *functional:*

$$209 \min_{q \in \mathcal{P}} \{\mathbb{E}_q[-r(x)] + \beta D_{\text{KL}}(q \| p_{\text{ref}})\},$$

210 where $r(x)$ is a reward function. In this case, the optimal distribution is obtained as $q_*(x) \propto$
 211 $\exp\left(\frac{r(x)}{\beta}\right) p_{\text{ref}}(x)$. This type of the problems has been studied as the Reinforcement Learning (Fan
 212 et al., 2023; Black et al., 2024; Clark et al., 2024; Uehara et al., 2024b).

213 The following two examples have not been directly solved via diffusion models:

Example 2 (DPO). *Direct Preference Optimization (DPO) (Rafailov et al., 2023) is an effective approach for learning from human preference for not only language models but also diffusion models. Our algorithm can directly minimize the DPO objective, while Wallace et al. (2024) tried applying DPO to diffusion models via minimization of an upper bound of the original objective. In DPO, humans decide which sample is more preferred given two samples from p_{ref} . Let x_w and x_l be “winning” and “losing” samples from p_{ref} . $x_w \succ x_l$ denote the event that x_w is preferred to x_l . The DPO objective can be written as*

$$L_{\text{DPO}}(q) := -\mathbb{E}_{x_w \sim p_{\text{ref}}} \mathbb{E}_{x_l \sim p_{\text{ref}}} \left[\log \sigma \left(\gamma \log \frac{q(x_w)}{p_{\text{ref}}(x_w)} - \gamma \log \frac{q(x_l)}{p_{\text{ref}}(x_l)} \right) \mathbb{1}_{x_w \succ x_l}(x_w, x_l) \right],$$

where $\mathbb{E}_{x \sim p}$ denotes expectation with respect to x whose probability density is $p \in \mathcal{P}$, σ is a sigmoid function, $\mathbb{1}_{x \succ y}(x, y)$ is one if $x \succ y$ and is zero otherwise. Precisely, the functional derivative of $L_{\text{DPO}}(q)$ is calculated as

$$\begin{aligned} \frac{\delta L_{\text{DPO}}}{\delta q}(q, x) = & -\gamma \mathbb{E}_{x_l \sim p_{\text{ref}}} \left[(1 - \sigma(-\gamma f(x) + \gamma f(x_l))) \frac{\int e^{-f} dp_{\text{ref}}}{e^{-f(x)}} \mathbb{1}_{x \succ x_l}(x, x_l) \right] \\ & + \gamma \mathbb{E}_{x_w \sim p_{\text{ref}}} \left[(1 - \sigma(-\gamma f(x_w) + \gamma f(x))) \frac{\int e^{-f} dp_{\text{ref}}}{e^{-f(x)}} \mathbb{1}_{x_w \succ x}(x_w, x) \right], \end{aligned} \quad (2)$$

where $q = e^{-f} p_{\text{ref}} / \int e^{-f} dp_{\text{ref}}$. See Appendix B for the derivation. Therefore, we only need samples from p_{ref} and the log-density ratio or the potential f to calculate the functional derivatives.

Example 3 (KTO). *Our algorithm can also minimize L_{KTO} directly. Assume that the whole data space \mathbb{R}^d is split into a desirable domain \mathcal{D}_D and an undesirable domain \mathcal{D}_U . The objective of the original KTO (Ethayarajh et al., 2024) is formulated as*

$$\begin{aligned} L_{\text{KTO}}(q) = & \mathbb{E}_{x \sim p_{\text{ref}}} \left[\gamma_D \left(1 - \sigma \left(\kappa \log \frac{q}{p_{\text{ref}}} - D_{\text{KL}}(q \| p_{\text{ref}}) \right) \right) \mathbb{1}_{\{x \in \mathcal{D}_D\}} \right. \\ & \left. + \gamma_U \left(1 - \sigma \left(D_{\text{KL}}(q \| p_{\text{ref}}) - \kappa \log \frac{q}{p_{\text{ref}}} \right) \right) \mathbb{1}_{\{x \in \mathcal{D}_U\}} \right], \end{aligned}$$

where γ_D , γ_U , κ are hyper parameters, and σ is a sigmoid function. Li et al. (2024) defined objectives compatible with diffusion models based on KTO, but our algorithm can directly minimize L_{KTO} . Like the DPO objective, we only have to calculate samples from p_{ref} and the potential f of the density ratio (f is defined as $q = e^{-f} p_{\text{ref}} / \int e^{-f} dp_{\text{ref}}$) to calculate the functional derivatives. Please refer to Appendix B for the concrete formulation of $\frac{\delta L_{\text{KTO}}}{\delta q}$.

4 THE NONLINEAR DISTRIBUTIONAL OPTIMIZATION ALGORITHM

Now we make a concrete introduction of our proposed approach. Our goal of the distribution optimization (1) is to train a neural network that approximates $\hat{f}_{\text{opt}} = \log \frac{q_{\text{opt}}}{p_{\text{ref}}} + (\text{const.})$. To achieve this, we utilize the *Dual Averaging* (DA) algorithm (Nesterov, 2009; Nitanda et al., 2021; Nishikawa et al., 2022), and we iteratively construct a tentative local potential f_k by approximating the update the DA algorithm. After we obtain f_k , we estimate the diffusion model that generates the desired output (approximately) following q_* , through *Doob’s h-transform technique*.

Phase 1: Dual Averaging. Let f_1 be a randomly initialized potential. First, we initialize $q^{(1)} \propto \exp(-f_1) p_{\text{ref}}$, where f_1 is a randomly initialized neural network. Then, the distribution $q^{(k)}$ is updated recursively by pulling back the weighted sum of gradients from the dual space to the primal space. There are two options of DA methods. For a given hyper-parameter $\beta' > 0$, the update of Option 1 is given as

$$\begin{aligned} \text{(Opt. 1)} \quad \hat{q}^{(k+1)} = & \arg \min_{q \in \mathcal{P}} \left\{ \frac{2}{k(k+1)} \sum_{j=1}^k j \left(\mathbb{E}_q \left[\frac{\delta F}{\delta q}(q^{(j)}) \right] + \beta D_{\text{KL}}(q \| p_{\text{ref}}) \right) + \frac{2\beta'}{k} D_{\text{KL}}(q \| p_{\text{ref}}) \right\} \\ = & \exp(-\bar{g}^{(k)}) p_{\text{ref}}, \end{aligned} \quad (3)$$

where $\bar{g}^{(k)}(x) = \sum_{j=1}^k w_j^{(k)} \frac{\delta F}{\delta q}(q^{(j)}, x)$, $w_j^{(k)} = \frac{j}{\beta k(k+1)/2 + \beta'(k+1)}$ ($j = 1, \dots, k$). By Lemma 4 in Appendix A.2, $\bar{g}^{(k)}$ can be explicitly determined. We train a neural network f_{k+1} to approximate $\bar{g}^{(k)}$ ¹ and define the next step as $q^{(k+1)} \propto \exp(-f_{k+1}) p_{\text{ref}}$. Similarly, the update of Option 2 is

¹For DPO and KTO, it suffices to obtain the neural network $\bar{g}^{(k)}$ to minimize $\mathbb{E}_{p_{\text{ref}}} [(f - \bar{g}^{(k)})^2]$ where the expectation with respect to p_{ref} is simulated by generating data from p_{ref} , while obtaining $\bar{g}^{(k)}$ for general settings requires Doob’s h-transform similar to Phase 2. Please also refer to Section 6.

given as

$$\text{(Opt. 2)} \quad \hat{q}^{(k+1)} = \arg \min_{q \in \mathcal{P}} \left\{ \frac{2}{k(k+1)} \sum_{j=1}^k j \left(\mathbb{E}_q \left[\frac{\delta F}{\delta q}(q^{(j)}) - \beta \bar{g}^{(j)} \right] \right) + \frac{2\beta'}{k} D_{\text{KL}}(q \| p_{\text{ref}}) \right\}. \quad (4)$$

Here, we again express as $\hat{q}^{(k+1)}(x) \propto \exp(-\bar{g}^{(k)}(x)) p_{\text{ref}}(x)$ where $\bar{g}^{(k)}(x) = \sum_{j=1}^k w_j^{(k)} \left(\frac{\delta F}{\delta q}(q^{(j)}, x) - \beta \bar{g}^{(j)}(x) \right)$ with $w_j^{(k)} = \frac{j}{\beta'(k+1)}$. Then, $q^{(k+1)}$ is obtained in the same manner as Option 1. This phase of DA update is summarized in Algorithm 4. [For the more detailed algorithm in Option 1, please refer to Algorithm D.1.](#)

Algorithm 4.1 Dual Averaging (DA)

Input: s : pre-trained score, f_1 : initialized neural networks

Output: f_K : a trained potential.

Set $q^{(1)} \propto \exp(-f_1) p_{\text{ref}}$.

for $k = 1, \dots, K - 1$ **do**

 Obtain $\bar{g}^{(k)}$ via the DA algorithm with Option 1 (Eq. (3)) or Option 2 (Eq. (4)) using the recurrence formula (47), where $\hat{q}^{(k+1)} \propto \exp(-\bar{g}^{(k)}) p_{\text{ref}}$ is the ideal update.

 Train a neural network f_{k+1} to approximate $\bar{g}^{(k)}$, and set $q^{(k+1)} \propto \exp(-f_{k+1}) p_{\text{ref}}$.

end for

Phase 2: Sampling with Doob’s h-transform. After we obtain the solution f_K , we want to sample from $q_K \propto \exp(-f_K) p_{\text{ref}}$, which approximates the optimal solution of (1). When sampling from q_K , it is necessary to obtain the score function related to this distribution. However, constructing the score function of q_* only from the score function of p_{ref} and f_K requires a particular technique. Specifically, we apply Doob’s h-transform (Rogers & Williams, 2000; Chopin et al., 2023; Uehara et al., 2024b; Heng et al., 2024). By introducing the correction term $u_*: \mathbb{R}^{d+1} \rightarrow \mathbb{R}^d$ defined by

$$u_*(y, t) = \nabla \log \mathbb{E}[\exp(-f_*(\bar{X}_T^{\leftarrow})) \mid \bar{X}_t^{\leftarrow} = y],$$

the score function of q_* at (x, t) is written as $\nabla \log q_t(y) = \nabla \log p_t(X_t^{\leftarrow}, T - t) + u_*(y, t)$, where q_t is the law of the backward process at time t whose output distribution is the optimal solution q_* . We provide the derivation in Lemma 12 and refer readers to Rogers & Williams (2000); Chopin et al. (2023) for more details and a formal treatment of Doob’s h-transform. By approximating $\log p_t(X_t^{\leftarrow}, T - t)$ by the score network $s(x, t)$ and the correction term $u_*(x, t)$ by $u(x, t)$ and discretizing the dynamics, we obtain the following update

$$Y_0^{\leftarrow} \sim \mathcal{N}(0, I_d), \quad dY_t^{\leftarrow} = \{Y_t^{\leftarrow} + 2(s(Y_{lh}^{\leftarrow}, lh) + u(Y_{lh}^{\leftarrow}, lh))\} dt + \sqrt{2} dB_t, \quad t \in [lh, (l+1)h],$$

where $u(x, t)$ can be computed as $u(x, t) = \nabla_x \log \mathbb{E}[\exp(-f_K(X_T^{\leftarrow})) \mid X_t^{\leftarrow} = x]$, which can be estimated by running the reference diffusion model (X_t^{\leftarrow}) . The practical treatment for this is discussed in Appendix C. [For experimental information, please have a look at Section 6 and Algorithm D.2 in Appendix D.2.](#)

5 THEORETICAL ANALYSIS

In this section, we give theoretical justification of our proposed algorithm. More concretely, we show the rate of convergence of the (inexact) DA method and give an approximation error bound on the diffusion model based on the h-transform.

5.1 CONVERGENCE RATE OF THE DA METHOD

We give the convergence rate of the DA algorithm in the two settings: when F is (I) convex and (II) non-convex, respectively.

(I): Convex objective F . First, we show the rate when F is convex. We basically follow the proof technique of Nitanda et al. (2021); Nishikawa et al. (2022). In the analysis, we put the following assumption on F .

Assumption 1. *The loss function F satisfies the following conditions:*

- (i) $\frac{\delta F}{\delta q}$ is bounded: There exists $B_F > 0$ such that $\|\frac{\delta F}{\delta q}(q)\|_\infty \leq B_F$ for any $q \in \mathcal{P}$,

- 324 (ii) $\frac{\delta F}{\delta q}$ is Lipschitz continuous with respect to the TV distance: There exists $L_{\text{TV}} > 0$ such that
 325 $\|\frac{\delta F}{\delta q}(q) - \frac{\delta F}{\delta q}(q')\|_{\infty} \leq L_{\text{TV}} \text{TV}(q, q')$ for any $q, q' \in \mathcal{P}$.
 326
 327 (iii) F is convex: $F(q) \geq F(q') + \int \frac{\delta F}{\delta q}(q') d(q - q')$ for any $q, q' \in \mathcal{P}$,
 328

329 Then, we can show that the (inexact) DA algorithm achieves the following convergence rate that
 330 yields $\mathcal{O}(K^{-1})$ convergence of the objective.

331 **Theorem 1 (Convergence of the objective in Option 1)**. Suppose that $\beta' \geq \beta$ and we train the
 332 potential f_{k+1} so that it is sufficiently close to $\bar{g}^{(k)}$ as $\text{TV}(\hat{q}^{(k)}, q^{(k)}) \leq \epsilon_{\text{TV}}$ for all k . Then, under
 333 Assumption 1, Option 1 satisfies the following convergence guarantee:

$$334 \frac{2}{K(K+1)} \sum_{k=1}^K k \left[L(\hat{q}^{(k)}) - L(\hat{q}_{\text{opt}}) \right] \leq 2L_{\text{TV}}\epsilon_{\text{TV}} + \left(\frac{2B_F}{K(K+1)} + \frac{2\beta' D_{\text{KL}}(q_* \| p_{\text{ref}}) + 2B_F^2 \beta^{-1}}{K} \right).$$

338 See Appendix A.1 for the proof. From this theorem, we see that the DA algorithm with Option
 339 1 achieves $\mathcal{O}(1/K)$ convergence. The assumption (ii) in Assumption 1 is required to bound an
 340 expectation of $\bar{g}^{(k)}$ in the bound. The assumption (iii) is required to bound the difference between the
 341 exact update $\hat{q}^{(k)}$ and the inexact update $q^{(k)}$. If the update is exact, we don't need this assumption.

342 **(II): Non-convex objective F .** We also give a convergence for a non-convex loss F . Here, we put
 343 the following assumption.

344 **Assumption 2.** The loss function F satisfies the following conditions:

- 345 (i) $\frac{\delta F}{\delta q}$ is bounded: There exists $B_F > 0$ such that $\|\frac{\delta F}{\delta q}(q)\|_{\infty} \leq B_F$ for any $q \in \mathcal{P}$,
 346
 347 (ii) $\frac{\delta F}{\delta q}$ is Lipschitz continuous with respect to the TV distance: $\|\frac{\delta F}{\delta q}(q) - \frac{\delta F}{\delta q}(q')\|_{\infty} \leq L_{\text{TV}} \text{TV}(q, q')$
 348 for any $q, q' \in \mathcal{P}$,
 349
 350 (iii) F is lower bounded.

351 Assumptions (i) and (ii) are the same as the convex case (Assumption 1), and lower boundedness (iii)
 352 is weaker than convexity in Assumption 1. Assumption (ii) induces the following type of smoothness
 353 commonly observed in standard optimization: (ii)' There exists $S_F \geq 0$ such that $F(q) \leq F(q') +$
 354 $\int \frac{\delta F}{\delta q}(q') d(q - q') + \frac{S_F}{2} D_{\text{KL}}(q \| q')$. When the inner-loop error is ignored, it is possible to prove
 355 convergence using only the smoothness assumption (ii)' instead of assumption (ii). For details,
 356 please refer to Appendix A.1.1.

357 Under this assumption, we can show the following convergence guarantee with respect to the se-
 358 quence $(\hat{q}^{(k)})_{k=1}^K$ even in a non-convex setting.

360 **Theorem 2.** Suppose that $\beta' > \beta + L_{\text{TV}}$ and $\text{TV}(\hat{q}^{(k)}, q^{(k)}) \leq \epsilon_{\text{TV}}$ for all k , then under Assumption
 361 2, both Option 1 and 2 yield the following convergence:

- 362 (i) $\lim_{k \rightarrow \infty} D_{\text{KL}}(\hat{q}^{(k+1)} \| \hat{q}^{(k)}) = 0$.
 363
 364 (ii) For all K , it holds that

$$365 \min_{k=1, \dots, K} \left\{ c_k D_{\text{KL}}(\hat{q}^{(k+1)} \| \hat{q}^{(k)}) \right\} \leq \frac{(\tilde{L}_1(\hat{q}^{(1)} - L(\hat{q}_{\text{opt}})) + (L_{\text{TV}} + B_F)K\epsilon_{\text{TV}})}{K\beta'} =: \Psi_K,$$

366 where $c_k = \frac{\beta k + 2\beta'}{2}$ for Option 1 and $c_k = 1$ for Option 2.
 367
 368

369 See Appendix A.1.1 for the proof. The proof utilizes an analogous argument with Liu et al. (2023a)
 370 that analyzed convergence of a DA method in a finite dimensional non-convex optimization problem.
 371 However, we need to reconstruct a proof because we should work on the probability measure space,
 372 which is not a vector space, and carefully make use of the property of the KL-divergence. We
 373 see that $\Psi_K = \mathcal{O}(1/K)$ if ϵ_{TV} is sufficiently small as $\epsilon_{\text{TV}} = \mathcal{O}(1/K)$, and thus the discrepancy
 374 between $\hat{q}^{(k+1)}$ and $\hat{q}^{(k)}$ converges. Especially, the convergence of $D_{\text{KL}}(\hat{q}^{(k+1)} \| \hat{q}^{(k)})$ yields the
 375 convergence of the ‘‘dual variable’’ for Option 2 as in the following corollary. For that purpose, we
 376 define $\tilde{L}_k(q) := L(q) + \frac{\beta'}{k} D_{\text{KL}}(q \| p_{\text{ref}})$ (see its similarity to the inner objective of the DA update (3)
 377 and (4)), and define $\psi_q(g) = \log(\mathbb{E}_q[\exp(-g + \mathbb{E}_q[g])])$ which is a ‘‘moment generating function’’
 of a dual variable g .

Corollary 1 (Convergence in Option 2). *Under the same condition as Theorem 2, we have that*

$$\min_{1 \leq k \leq K} \psi_{\hat{q}^{(k)}} \left(\frac{k}{\beta^{k+1}} \frac{\delta \bar{L}_k}{\delta q}(\hat{q}^{(k)}) \right) \leq \Psi_K.$$

Roughly speaking, this corollary indicates that the variance of the gradient $\frac{\delta \bar{L}_k}{\delta q}(\hat{q}^{(k)})$ converges as $\text{Var}_{\hat{q}^{(k)}} \left(\frac{\delta \bar{L}_k}{\delta q}(\hat{q}^{(k)}) \right) = \mathcal{O}(1/K)$ because we may approximate $\psi_q(g) \simeq \frac{1}{2} \text{Var}_q(g)$ when $|g - \mathbb{E}_q[g]|$ is sufficiently small. Therefore, we have a convergence guarantee of the dual variable (gradient) $\frac{\delta \bar{L}_k}{\delta q}(\hat{q}^{(k)}, x) \rightarrow 0$ (up to a constant w.r.t. x) even in a non-convex setting, which justifies usage of our method for general objective functions.

5.2 DISCRETIZATION ERROR OF DOOB’S H-TTRANSFORM

We now provide the sampling error analysis after obtaining the approximate solution f_K . In the analysis of Dual Averaging, p_{ref} was assumed to be known, and the goal was to obtain the optimal solution of (1) that corresponds to $\hat{q}_{\text{opt}} = \exp(-\hat{f}_{\text{opt}})p_{\text{ref}}$. From here, considering that p_{ref} estimates p_* , we shift our focus to sample from the optimal alignment $q_* \propto \rho_* p_*$, while the dynamics we implement involves several approximations: (i) time discretization approximation, (ii) approximation of the score $\nabla_x \log p_t$ by $s(x, T-t)$, (iii) approximation of ρ^* by $\rho = \exp(-f_K)$, (iv) approximation of u_* by u .

To evaluate how such approximation affects the final quality of our generative model, we will give a bound of the TV-distance between q_* and $\hat{q} = \rho p_{\text{ref}}$ by putting all those errors together. To do so, we put the following assumption.

- Assumption 3.**
1. $\nabla \log p_t$ is L_p -smooth at every time t and it has finite second moment $\mathbb{E}[\|\bar{X}_t\|_2^2] \leq m < \infty$ for all $t \in \mathbb{R}_+$ and $x \in \mathbb{R}^d$.
 2. $\nabla \log \rho_*$ is L_ρ -smooth and bounded as $C_\rho^{-1} \leq \rho_* \leq C_\rho$ for a constant C_ρ .
 3. The score estimation error is bounded by $\mathbb{E}_{\bar{X}_t^\leftarrow} [\|s(\bar{X}_t^\leftarrow, t) - \nabla \log p_{T-t}(\bar{X}_t^\leftarrow)\|_2^2] \leq \varepsilon$ at each time t .
 4. $\mathbb{E}_{\bar{X}_t^\leftarrow} [\|u_*(\bar{X}_t^\leftarrow, t) - u(\bar{X}_{lh}^\leftarrow, lh)\|_2^2] \leq \varepsilon_{\rho,l}^2$ for any $1 \leq l \leq T/h$ and $t \in [lh, (l+1)h)$.

This assumption is rather standard, for example, Chen et al. (2023c) employed these conditions except the last condition on u and u_* . The fourth assumption in Assumption 3 is imposed to mathematically formulate the situation: $\hat{q}_{\text{opt}}/p_{\text{ref}} \simeq q_*/p_*$. Then, we obtain the following error bound:

Theorem 3. *Suppose that Assumption 3 is satisfied. Then, we have the following bound on the distribution \hat{q} of Y_T^\leftarrow :*

$$\text{TV}(q_*, \hat{q})^2 \lesssim T\varepsilon^2 + \sum_{l=1}^{T/h} h\varepsilon_{\rho,l}^2 + T(L_p C_\rho^2 + L_\rho)^2 (dh + mh^2) + \exp(-2T) D_{\text{KL}}(q_* \| N(0, I)).$$

The proof is given in Appendix C.1. It basically follows Chen et al. (2023c;b), but we have derived the smoothness of $\nabla \log(q_{*,t})$ from that of $\nabla \log(p_t)$. In this bound, we did not give any evaluation on $\varepsilon_{\rho,l}^2$, however, this error term can be bounded as follows with additional conditions.

Assumption 4. (i) $\nabla_x s(\cdot, \cdot)$ is H_s -Lipschitz continuous in a sense that $\|\nabla_x s(x, t) - \nabla_y s(y, t)\|_{\text{op}} \leq H_s \|x - y\|$ for any $x, y \in \mathbb{R}^d$ and $0 \leq t \leq T$ and $\mathbb{E}[\|s(\bar{X}_{kh}^\leftarrow, kh)\|_2^2] \leq Q^2$ for any k , (ii) There exists $R > 0$ such that $\sup_{t,x} \{\|\nabla_x^2 \log p_t(x)\|_{\text{op}}, \|\nabla_x^2 \log s(x, t)\|_{\text{op}}\} \leq R$.

Theorem 4. *Suppose that Assumptions 3 and 4 hold and $\|\rho_* - \rho\|_\infty \leq \varepsilon'$ and $\|\rho\|_\infty \leq C_\rho$. We also assume $\nabla \rho^*$ is bounded and Lipschitz continuous. Then, for any choice of $0 \leq h \leq \delta \leq 1/(1+2R)$, we have that*

$$\varepsilon_{\rho,l}^2 \lesssim C_\rho^3 \left\{ \Xi_{\delta,\varepsilon} + R_\varphi^2 (\varepsilon^2 + L_p^2 d(\delta + m\delta^2)) + [L_\varphi^2 (m + Q^2 + dh) + R_\varphi^2 (1 + 2R)^2] h^2 \right\} + \min\{T - lh, 1/(2 + 2R)\}^{-1} \varepsilon'^2,$$

where $\Xi_{\delta,\varepsilon} := C_\rho^2 (1 + 2R)^2 \delta + C_\rho^2 \frac{1 + \delta R_\varphi^2}{\delta} [\varepsilon^2 + L_p^2 d(h + mh^2)]$, and R_φ and L_φ are constants introduced in Lemma 10.

The proof is given in Appendix C.3. We applied the so-called *Bismut-Elworthy-Li* integration-by-parts formula (Bismut, 1984; Elworthy & Li, 1994) to obtain the discretization error. By substituting

$\delta \leftarrow \sqrt{h}$ to balance the terms related to h and δ , we obtain a simplified upper bound of $\sum_{l=1}^{T/h} h \varepsilon_{\rho,l}^2$ as $\sum_{l=1}^{T/h} h \varepsilon_{\rho,l}^2 \lesssim \left(1 + \frac{1}{\sqrt{h}}\right) \varepsilon^2 T + T\sqrt{h} + (T + \log(1/h))\varepsilon'^2$. These results can be seen as h -Transform extension of the approximation error analysis given in Chen et al. (2023c). However, the approximation error corresponding to u has worse dependency on h . This is because the computation of u uses the discretized process p_{ref} and is affected by its error while the ordinary diffusion model does not require sampling to obtain the score.

6 NUMERICAL EXPERIMENTS

We conducted numerical experiments to confirm the effectiveness of minimizing nonlinear objectives. We used Option 1 and β was set to be 0.04. We also compared the DPO objective (Rafailov et al., 2023) we minimized with the upper-bound (Wallace et al., 2024) using a toy case, Gaussian Mixture Model (GMM). For detailed experimental setting, please refer to Appendix D.

Alignment for Gaussian Mixture Model. We aligned a score-based diffusion model to sample from a 2-dimensional GMM using the DPO objective. The reference density was defined as $\frac{1}{2}(\mathcal{N}(\mu_1, \Sigma) + \mathcal{N}(\mu_2, \Sigma))$, $\mu_1 = [-2.5, 0]$, $\mu_2 = [2.5, 0]$, $\Sigma = [[1, 0], [0, 5]]$. The target point was $\mu_w := \mu_2$. The preference of points x_w and x_l was determined by the Euclidean distance $d(\cdot, \mu_w)$ from μ_w . $x_w \succ x_l$ if and only if $d(x_w, \mu_w) < d(x_l, \mu_w)$. We describe the implementation details below:

Dual Averaging. We set the hyperparameter β' in $[0.04, 0.2]$, which controls the learning speed illustrated at the middle in Figure 2. In k th DA iteration ($k = 1, \dots, K$), using empirical samples $\{x_i = (x_{1,i}, x_{2,i})\}_{i=1}^{1000}$ from p_{ref} and the previous potential f_{k-1} ($q^{(k-1)} \propto e^{-f_{k-1} p_{\text{ref}}}$) implemented by neural networks, we prepare $\{(x_i, \frac{\delta F}{\delta q}(q^{(k-1)}, x_i))\}_{i=1}^{1000}$ to construct $f_k \simeq \bar{g}^{(k-1)}$ with the recurrence formula (47) in Appendix D. Please note that, to calculate $\frac{\delta F}{\delta q}$ for DPO, we only need the f_k and empirical samples from p_{ref} to calculate the expectation $\mathbb{E}_{x \sim p_{\text{ref}}}[\cdot]$ as described in Eq. (2). The convergence of the true DPO loss is depicted in Figure 2, compared to Diffusion-DPO (Wallace et al., 2024). The true DPO loss, upperbound, and metric loss (mean of the Euclidean distance of the particles from μ_w) attained by Diffusion-DPO and our method, with optimization time and GPU memory consumption, are summarized in Table 1. Diffusion-DPO optimizes the approximate upperbound instead of the true loss, and therefore it failed to completely control the true loss. Compared to Diffusion-DPO, our algorithm allowed us to optimize the loss to a smaller value within an acceptable computational budget.

Doob’s h -transform. We constructed the aligned model by calculating the correction terms. The conditional expectations were calculated using naive Monte Carlo method with 30000 samples. The number of the diffusion steps was 50. The histograms of aligned samples are shown at the right of Figure 2. In the simplest phase 2 that we present (Algorithm D.2), we used significant computational resources, with $\mathcal{O}(L^2)$ time complexity. To estimate the correction term u for each sample simultaneously by Monte Carlo with N samples, $\mathcal{O}(N)$ memory space is required. However, this Doob’s h -transform technique itself has been used in image generation (Uehara et al., 2024a;b), Bayesian sampling (Heng et al., 2024), and filtering (Chopin et al., 2023). In particular, computational resources can be saved by approximating the correction term using a neural ODE (Uehara et al., 2024b).

Table 1: The quantitative comparison between Diffusion-DPO and our method.

	Ref.	Diffusion-DPO (50 iter., w/o reg.)	Diffusion-DPO (200 iter., w/ reg.)	Ours ($\beta' = 0.04$)
True DPO loss	0.346	0.340	0.343	0.328
(Approx.) Upperbound	-	0.342	0.337	-
Metric loss	3.226	2.828	3.283	2.098
Opt. time (s)	-	509.99	2039.99	1166.00
GPU memory (%)	-	6.540	6.540	8.710

Image Generation Alignment based on a Target Color. We aligned the image generation of the basic pre-trained model available Diffusion Models Course (source: HuggingFace (2022)) to simulate specific generations for data augmentation. The pre-trained model generates RGB-colored 32×32 pixel images of butterflies. In this experiment, the model was aligned based on a target color,

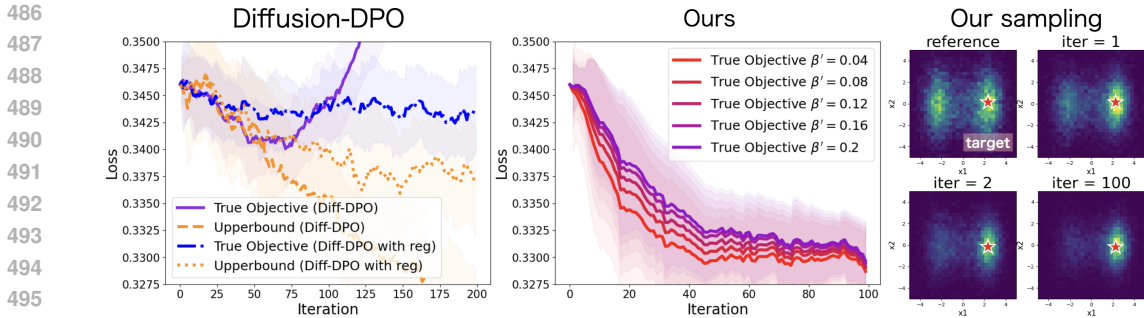


Figure 2: **Left and Middle.** The loss during optimization for Gaussian Mixture Model in Diffusion-DPO with/without regularization (left) and ours (middle). “True Objective”: the true DPO loss (Rafailov et al., 2023) whose target point was $\mu_w = [2.5, 0]$. “Upperbound”: An upperbound of “Objective” optimized by Diffusion-DPO (Wallace et al., 2024). **Right.** Aligned samples by Doob’s h-transform. “Ref.” represents the empirical density of p_{ref} .

which is (R,G,B)= (0.9, 0.9, 0.9) while (1,1,1) corresponds to white, using the DPO objective. Please refer to Figure 6 for an illustration of the preference indicated by DPO. We leveraged 1024 images generated by the pre-trained model to train f_k in each DA iteration. We see that the (regularized) objective went down during DA and the generated images reflected the target density more, on the right side of Figure 3. Please refer to Figure 7 in Appendix for the convergence results.

Tilt Correction for Image Generation. The goal of this experiment is data augmentation of images facing the same direction, given only a dataset of rotated images. We used 10000 images of Head CT in Medical MNIST (Lozano, 2017) and augmented it by rotating images up to 40000. Data augmentation of brain images is useful for tumor analysis and anomaly detection (Shen et al., 2024; Fontanella et al., 2024). In each DA iteration, 6400 images were generated to train f_k . The results are in Figure 3. For the convergence results, please refer to Figure 11 in Appendix. From the results, we see that the (regularized) objective decreased during DA and the generated images became more preferred.

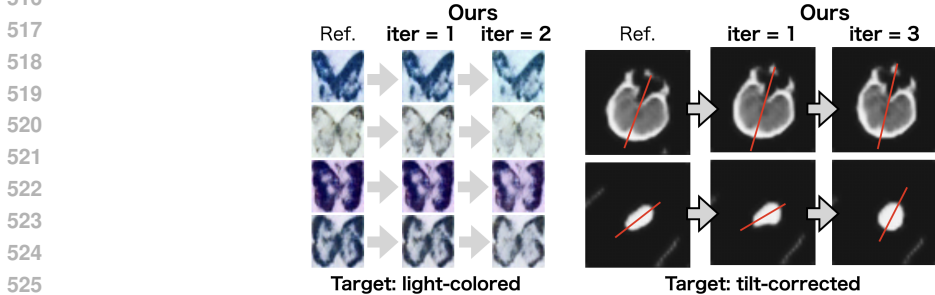


Figure 3: **Left.** Examples of aligned image generation. Our goal was to generate light-colored butterflies. “iter=2”: ours with $k = 2$ DA iterations, “iter=1”: ours with $k = 1$ DA iteration. “Ref.”: samples from p_{ref} . **Right.** Tilt-corrected Head CT image generation. “iter=3”: ours with $k = 3$ DA iterations, “iter=1”: ours with $k = 1$ DA iteration. “Ref.”: samples from p_{ref} .

7 CONCLUSION

We proved that the distributional optimization can be solved even if p_{ref} and \hat{q}_{opt} are multimodal and we only have access to the score, not the density. This setting includes important fine-tuning methodologies for diffusion models: Reinforcement Learning, DPO, and KTO. Our algorithms are based on the DA algorithm and Doob’s h-transform technique and it can solve them more directly than previous works. They are guaranteed to be useful for general objective functions, the dual variable converges even in a non-convex setting. While our framework has potential applications in general distributional optimization problems, such as density ratio estimation under covariate shift and climate change tracking, further exploration of these applications is left for future work.

REFERENCES

- 540
541
542 Dominique Bakry, Ivan Gentil, Michel Ledoux, et al. *Analysis and geometry of Markov diffusion*
543 *operators*, volume 348 of *Grundlehren der mathematischen Wissenschaften*. Springer, 2014.
- 544
545 Jean-Michel Bismut. *Large deviations and the Malliavin calculus*, volume 45 of *Progress in Math-*
546 *ematics*. Birkhäuser Boston, Inc., Boston, MA, 1984.
- 547
548 Kevin Black, Michael Janner, Yilun Du, Ilya Kostrikov, and Sergey Levine. Training diffusion
549 models with reinforcement learning, 2024. URL <https://arxiv.org/abs/2305.13301>.
- 550
551 Fan Chen, Zhenjie Ren, and Songbo Wang. Entropic fictitious play for mean field optimization
552 problem. *Journal of Machine Learning Research*, 24(211):1–36, 2023a.
- 553
554 Hongrui Chen, Holden Lee, and Jianfeng Lu. Improved analysis of score-based generative modeling:
555 User-friendly bounds under minimal smoothness assumptions. In *International Conference on*
556 *Machine Learning*, pp. 4735–4763. PMLR, 2023b.
- 557
558 Sitan Chen, Sinho Chewi, Jerry Li, Yuanzhi Li, Adil Salim, and Anru Zhang. Sampling is as easy as
559 learning the score: theory for diffusion models with minimal data assumptions. In *The Eleventh*
560 *International Conference on Learning Representations*, 2023c. URL [https://openreview.](https://openreview.net/forum?id=zyLVMgsZ0U_)
561 [net/forum?id=zyLVMgsZ0U_](https://openreview.net/forum?id=zyLVMgsZ0U_).
- 562
563 Lénaïc Chizat. Mean-field langevin dynamics : Exponential convergence and annealing. *Transac-*
564 *tions on Machine Learning Research*, 2022. ISSN 2835-8856. URL [https://openreview.](https://openreview.net/forum?id=BDqzLHlgEm)
565 [net/forum?id=BDqzLHlgEm](https://openreview.net/forum?id=BDqzLHlgEm).
- 566
567 Lénaïc Chizat and Francis Bach. On the global convergence of gradient descent
568 for over-parameterized models using optimal transport. In S. Bengio, H. Wal-
569 lach, H. Larochelle, K. Grauman, N. Cesa-Bianchi, and R. Garnett (eds.), *Ad-*
570 *vances in Neural Information Processing Systems*, volume 31. Curran Associates, Inc.,
571 2018. URL [https://proceedings.neurips.cc/paper_files/paper/2018/](https://proceedings.neurips.cc/paper_files/paper/2018/file/alafc58c6ca9540d057299ec3016d726-Paper.pdf)
572 [file/alafc58c6ca9540d057299ec3016d726-Paper.pdf](https://proceedings.neurips.cc/paper_files/paper/2018/file/alafc58c6ca9540d057299ec3016d726-Paper.pdf).
- 573
574 Nicolas Chopin, Andras Fulop, Jeremy Heng, and Alexandre H. Thiery. Computational doob h-
575 transforms for online filtering of discretely observed diffusions. In Andreas Krause, Emma
576 Brunskill, Kyunghyun Cho, Barbara Engelhardt, Sivan Sabato, and Jonathan Scarlett (eds.), *Pro-*
577 *ceedings of the 40th International Conference on Machine Learning*, volume 202 of *Proce-*
578 *edings of Machine Learning Research*, pp. 5904–5923. PMLR, 23–29 Jul 2023. URL [https:](https://proceedings.mlr.press/v202/chopin23a.html)
579 [/proceedings.mlr.press/v202/chopin23a.html](https://proceedings.mlr.press/v202/chopin23a.html).
- 580
581 Kevin Clark, Paul Vicol, Kevin Swersky, and David J Fleet. Directly fine-tuning diffusion models
582 on differentiable rewards, 2024. URL <https://arxiv.org/abs/2309.17400>.
- 583
584 K.D. Elworthy and X.M. Li. Formulae for the derivatives of heat semigroups. *Journal of Functional*
585 *Analysis*, 125(1):252–286, 1994.
- 586
587 Kawin Ethayarajh, Winnie Xu, Niklas Muennighoff, Dan Jurafsky, and Douwe Kiela. Kto:
588 Model alignment as prospect theoretic optimization, 2024. URL [https://arxiv.org/abs/](https://arxiv.org/abs/2402.01306)
589 [2402.01306](https://arxiv.org/abs/2402.01306).
- 590
591 Ying Fan, Olivia Watkins, Yuqing Du, Hao Liu, Moonkyung Ryu, Craig Boutilier, Pieter
592 Abbeel, Mohammad Ghavamzadeh, Kangwook Lee, and Kimin Lee. Dpok: Rein-
593 forcement learning for fine-tuning text-to-image diffusion models. In A. Oh, T. Nau-
mann, A. Globerson, K. Saenko, M. Hardt, and S. Levine (eds.), *Advances in Neural*
Information Processing Systems, volume 36, pp. 79858–79885. Curran Associates, Inc.,
2023. URL [https://proceedings.neurips.cc/paper_files/paper/2023/](https://proceedings.neurips.cc/paper_files/paper/2023/file/fc65fab891d83433bd3c8d966edde311-Paper-Conference.pdf)
[file/fc65fab891d83433bd3c8d966edde311-Paper-Conference.pdf](https://proceedings.neurips.cc/paper_files/paper/2023/file/fc65fab891d83433bd3c8d966edde311-Paper-Conference.pdf).
- Alessandro Fontanella, Grant Mair, Joanna Wardlaw, Emanuele Trucco, and Amos Storkey. Diffu-
sion models for counterfactual generation and anomaly detection in brain images. *IEEE Transac-*
tions on Medical Imaging, pp. 1–1, 2024. doi: 10.1109/TMI.2024.3460391.

- 594 Jeremy Heng, Valentin De Bortoli, and Arnaud Doucet. Diffusion Schrödinger Bridges for Bayesian
595 Computation. *Statistical Science*, 39(1):90–99, 2024. doi: 10.1214/23-STS908. URL <https://doi.org/10.1214/23-STS908>.
596
597
- 598 Jonathan Ho, Ajay Jain, and Pieter Abbeel. Denoising diffusion probabilistic models. In
599 H. Larochelle, M. Ranzato, R. Hadsell, M.F. Balcan, and H. Lin (eds.), *Advances in Neural
600 Information Processing Systems*, volume 33, pp. 6840–6851. Curran Associates, Inc.,
601 2020. URL [https://proceedings.neurips.cc/paper_files/paper/2020/
602 file/4c5bcfec8584af0d967f1ab10179ca4b-Paper.pdf](https://proceedings.neurips.cc/paper_files/paper/2020/file/4c5bcfec8584af0d967f1ab10179ca4b-Paper.pdf).
- 603 Richard Holley and Daniel Stroock. Logarithmic sobolev inequalities and stochastic ising models.
604 *Journal of statistical physics*, 46(5-6):1159–1194, 1987.
605
- 606 Kaitong Hu, Zhenjie Ren, David Šiška, and Łukasz Szpruch. Mean-field langevin dynamics and
607 energy landscape of neural networks. In *Annales de l’Institut Henri Poincaré (B) Probabilités et
608 statistiques*, volume 57, pp. 2043–2065. Institut Henri Poincaré, 2021.
- 609 HuggingFace. The hugging face diffusion models course, 2022. [https://huggingface.co/
610 course,2022](https://huggingface.co/course,2022).
611
- 612 Shufan Li, Konstantinos Kallidromitis, Akash Gokul, Yusuke Kato, and Kazuki Kozuka. Align-
613 ing diffusion models by optimizing human utility, 2024. URL [https://arxiv.org/abs/
614 2404.04465](https://arxiv.org/abs/2404.04465).
- 615 Fenghua Ling, Zeyu Lu, Jing-Jia Luo, Lei Bai, Swadhin K Behera, Dachao Jin, Baoxiang Pan,
616 Huidong Jiang, and Toshio Yamagata. Diffusion model-based probabilistic downscaling for 180-
617 year east asian climate reconstruction. *npj Climate and Atmospheric Science*, 7(1):131, 2024.
618
- 619 Changxin Liu, Xuyang Wu, Xinlei Yi, Yang Shi, and Karl H. Johansson. Rate analysis of dual aver-
620 aging for nonconvex distributed optimization. *IFAC-PapersOnLine*, 56(2):5209–5214, 2023a.
621 ISSN 2405-8963. doi: <https://doi.org/10.1016/j.ifacol.2023.10.117>. URL [https://www.
622 sciencedirect.com/science/article/pii/S2405896323004639](https://www.sciencedirect.com/science/article/pii/S2405896323004639). 22nd IFAC
623 World Congress.
- 624 Linshan Liu, Mateusz B Majka, and Łukasz Szpruch. Polyak–Łojasiewicz inequality on the space
625 of measures and convergence of mean-field birth-death processes. *Applied Mathematics & Opti-
626 mization*, 87(3):48, 2023b.
627
- 628 Arturo Polanco Lozano. Medical mnist classification, 2017. URL [https://github.com/
629 apolanco3225/Medical-MNIST-Classification](https://github.com/apolanco3225/Medical-MNIST-Classification).
- 630 Pierre Marion, Anna Korba, Peter Bartlett, Mathieu Blondel, Valentin De Bortoli, Arnaud Doucet,
631 Felipe Llinares-López, Courtney Paquette, and Quentin Berthet. Implicit diffusion: Efficient
632 optimization through stochastic sampling, 2024. URL [https://arxiv.org/abs/2402.
633 05468](https://arxiv.org/abs/2402.05468).
- 634 Song Mei, Andrea Montanari, and PhanMinh Nguyen. A mean field view of the landscape of two-
635 layer neural networks. In *Proceedings of the National Academy of Sciences of the United States
636 of America*, volume 33, pp. E7665–E7671, 2018.
637
- 638 Stéphane Mischler. An introduction to evolution PDEs, Chapter 0: On the Gron-
639 wall lemma, 2019. URL [https://www.ceremade.dauphine.fr/~mischler/
640 Enseignements/M2evol2018/chap0.pdf](https://www.ceremade.dauphine.fr/~mischler/Enseignements/M2evol2018/chap0.pdf).
- 641 Yurii Nesterov. Primal-dual subgradient methods for convex problems. *Mathematical Programming*,
642 120(1):221–259, Aug 2009.
643
- 644 Naoki Nishikawa, Taiji Suzuki, Atsushi Nitanda, and Denny Wu. Two-layer neural network
645 on infinite dimensional data: global optimization guarantee in the mean-field regime. In Al-
646 lice H. Oh, Alekh Agarwal, Danielle Belgrave, and Kyunghyun Cho (eds.), *Advances in Neural
647 Information Processing Systems*, 2022. URL [https://openreview.net/forum?id=
Hr8475tQGKE](https://openreview.net/forum?id=Hr8475tQGKE).

- 648 Atsushi Nitanda. Improved particle approximation error for mean field neural networks. *arXiv*
649 *preprint 2405.15767*, 2024.
- 650
- 651 Atsushi Nitanda, Denny Wu, and Taiji Suzuki. Particle dual averaging: Optimization
652 of mean field neural network with global convergence rate analysis. In M. Ranzato,
653 A. Beygelzimer, Y. Dauphin, P.S. Liang, and J. Wortman Vaughan (eds.), *Advances in Neu-*
654 *ral Information Processing Systems*, volume 34, pp. 19608–19621. Curran Associates, Inc.,
655 2021. URL [https://proceedings.neurips.cc/paper_files/paper/2021/](https://proceedings.neurips.cc/paper_files/paper/2021/file/a34e1ddbb4d329167f50992ba59fe45a-Paper.pdf)
656 [file/a34e1ddbb4d329167f50992ba59fe45a-Paper.pdf](https://proceedings.neurips.cc/paper_files/paper/2021/file/a34e1ddbb4d329167f50992ba59fe45a-Paper.pdf).
- 657 Atsushi Nitanda, Denny Wu, and Taiji Suzuki. Convex analysis of the mean field langevin dynamics.
658 In Gustau Camps-Valls, Francisco J. R. Ruiz, and Isabel Valera (eds.), *Proceedings of The 25th*
659 *International Conference on Artificial Intelligence and Statistics*, volume 151 of *Proceedings*
660 *of Machine Learning Research*, pp. 9741–9757. PMLR, 28–30 Mar 2022. URL [https://](https://proceedings.mlr.press/v151/nitanda22a.html)
661 proceedings.mlr.press/v151/nitanda22a.html.
- 662 Atsushi Nitanda, Kazusato Oko, Denny Wu, Nobuhito Takenouchi, and Taiji Suzuki. Primal and
663 dual analysis of entropic fictitious play for finite-sum problems. In Andreas Krause, Emma
664 Brunskill, Kyunghyun Cho, Barbara Engelhardt, Sivan Sabato, and Jonathan Scarlett (eds.),
665 *Proceedings of the 40th International Conference on Machine Learning*, volume 202 of *Pro-*
666 *ceedings of Machine Learning Research*, pp. 26266–26282. PMLR, 23–29 Jul 2023. URL
667 <https://proceedings.mlr.press/v202/nitanda23a.html>.
- 668 Kazusato Oko, Taiji Suzuki, Atsushi Nitanda, and Denny Wu. Particle stochastic dual coordinate
669 ascent: Exponential convergent algorithm for mean field neural network optimization. In *Intern-*
670 *ational Conference on Learning Representations, 2022*. URL [https://openreview.net/](https://openreview.net/forum?id=PQQp7AJwz3)
671 [forum?id=PQQp7AJwz3](https://openreview.net/forum?id=PQQp7AJwz3).
- 672
- 673 Long Ouyang, Jeffrey Wu, Xu Jiang, Diogo Almeida, Carroll Wainwright, Pamela Mishkin, Chong
674 Zhang, Sandhini Agarwal, Katarina Slama, Alex Ray, John Schulman, Jacob Hilton, Fraser Kel-
- 675 ton, Luke Miller, Maddie Simens, Amanda Askell, Peter Welinder, Paul F Christiano, Jan Leike,
676 and Ryan Lowe. Training language models to follow instructions with human feedback. In
677 S. Koyejo, S. Mohamed, A. Agarwal, D. Belgrave, K. Cho, and A. Oh (eds.), *Advances in*
678 *Neural Information Processing Systems*, volume 35, pp. 27730–27744. Curran Associates, Inc.,
679 2022. URL [https://proceedings.neurips.cc/paper_files/paper/2022/](https://proceedings.neurips.cc/paper_files/paper/2022/file/b1efde53be364a73914f58805a001731-Paper-Conference.pdf)
680 [file/b1efde53be364a73914f58805a001731-Paper-Conference.pdf](https://proceedings.neurips.cc/paper_files/paper/2022/file/b1efde53be364a73914f58805a001731-Paper-Conference.pdf).
- 681 Rafael Rafailov, Archit Sharma, Eric Mitchell, Christopher D Manning, Stefano Ermon, and Chelsea
682 Finn. Direct preference optimization: Your language model is secretly a reward model. In
683 A. Oh, T. Naumann, A. Globerson, K. Saenko, M. Hardt, and S. Levine (eds.), *Advances in*
684 *Neural Information Processing Systems*, volume 36, pp. 53728–53741. Curran Associates, Inc.,
685 2023. URL [https://proceedings.neurips.cc/paper_files/paper/2023/](https://proceedings.neurips.cc/paper_files/paper/2023/file/a85b405ed65c6477a4fe8302b5e06ce7-Paper-Conference.pdf)
686 [file/a85b405ed65c6477a4fe8302b5e06ce7-Paper-Conference.pdf](https://proceedings.neurips.cc/paper_files/paper/2023/file/a85b405ed65c6477a4fe8302b5e06ce7-Paper-Conference.pdf).
- 687 L. C. G. Rogers and David Williams. *Diffusions, Markov Processes and Martingales*. Cambridge
688 Mathematical Library. Cambridge University Press, 2 edition, 2000.
- 689
- 690 Shai Shalev-Shwartz and Tong Zhang. Stochastic dual coordinate ascent methods for regularized
691 loss minimization. *Journal of Machine Learning Research*, 14(1), 2013.
- 692 Yiqing Shen, Guannan He, and Mathias Unberath. Promptable counterfactual diffusion model for
693 unified brain tumor segmentation and generation with mris, 2024. URL [https://arxiv.](https://arxiv.org/abs/2407.12678)
694 [org/abs/2407.12678](https://arxiv.org/abs/2407.12678).
- 695
- 696 Jascha Sohl-Dickstein, Eric Weiss, Niru Maheswaranathan, and Surya Ganguli. Deep unsupervised
697 learning using nonequilibrium thermodynamics. In Francis Bach and David Blei (eds.), *Pro-*
698 *ceedings of the 32nd International Conference on Machine Learning*, volume 37 of *Proceedings*
699 *of Machine Learning Research*, pp. 2256–2265, Lille, France, 07–09 Jul 2015. PMLR. URL
700 <https://proceedings.mlr.press/v37/sohl-dickstein15.html>.
- 701 Yang Song and Stefano Ermon. Generative modeling by estimating gradients of the data dis-

- 702 R. Garnett (eds.), *Advances in Neural Information Processing Systems*, volume 32. Curran
703 Associates, Inc., 2019. URL [https://proceedings.neurips.cc/paper_files/
704 paper/2019/file/3001ef257407d5a371a96dcd947c7d93-Paper.pdf](https://proceedings.neurips.cc/paper_files/paper/2019/file/3001ef257407d5a371a96dcd947c7d93-Paper.pdf).
705
- 706 Yang Song, Jascha Sohl-Dickstein, Diederik P Kingma, Abhishek Kumar, Stefano Ermon, and Ben
707 Poole. Score-based generative modeling through stochastic differential equations. In *International
708 Conference on Learning Representations*, 2021. URL [https://openreview.net/
709 forum?id=PXTIG12RRHS](https://openreview.net/forum?id=PXTIG12RRHS).
- 710 Masashi Sugiyama, Taiji Suzuki, Shinichi Nakajima, Hisashi Kashima, Paul Von Bünau, and Mo-
711 toaki Kawanabe. Direct importance estimation for covariate shift adaptation. *Annals of the Insti-
712 tute of Statistical Mathematics*, 60:699–746, 2008.
- 713 Taiji Suzuki, Denny Wu, and Atsushi Nitanda. Convergence of mean-field langevin dy-
714 namics: time-space discretization, stochastic gradient, and variance reduction. In A. Oh,
715 T. Naumann, A. Globerson, K. Saenko, M. Hardt, and S. Levine (eds.), *Advances in Neu-
716 ral Information Processing Systems*, volume 36, pp. 15545–15577. Curran Associates, Inc.,
717 2023. URL [https://proceedings.neurips.cc/paper_files/paper/2023/
718 file/32133a6a24d6554263d3584e3ac10faa-Paper-Conference.pdf](https://proceedings.neurips.cc/paper_files/paper/2023/file/32133a6a24d6554263d3584e3ac10faa-Paper-Conference.pdf).
- 719 Yuta Tsuboi, Hisashi Kashima, Shohei Hido, Steffen Bickel, and Masashi Sugiyama. Direct density
720 ratio estimation for large-scale covariate shift adaptation. *Journal of Information Processing*, 17:
721 138–155, 2009.
- 722 Masatoshi Uehara, Yulai Zhao, Tommaso Biancalani, and Sergey Levine. Understanding rein-
723 forcement learning-based fine-tuning of diffusion models: A tutorial and review, 2024a. URL
724 <https://arxiv.org/abs/2407.13734>.
- 725 Masatoshi Uehara, Yulai Zhao, Kevin Black, Ehsan Hajiramezanali, Gabriele Scalia, Nathaniel Lee
726 Diamant, Alex M Tseng, Tommaso Biancalani, and Sergey Levine. Fine-tuning of continuous-
727 time diffusion models as entropy-regularized control, 2024b. URL [https://arxiv.org/
728 abs/2402.15194](https://arxiv.org/abs/2402.15194).
- 729 Arash Vahdat, Karsten Kreis, and Jan Kautz. Score-based generative modeling in latent space.
730 In M. Ranzato, A. Beygelzimer, Y. Dauphin, P.S. Liang, and J. Wortman Vaughan (eds.),
731 *Advances in Neural Information Processing Systems*, volume 34, pp. 11287–11302. Curran
732 Associates, Inc., 2021. URL [https://proceedings.neurips.cc/paper_files/
733 paper/2021/file/5dca4c6b9e244d24a30b4c45601d9720-Paper.pdf](https://proceedings.neurips.cc/paper_files/paper/2021/file/5dca4c6b9e244d24a30b4c45601d9720-Paper.pdf).
- 734 Patrick von Platen, Suraj Patil, Anton Lozhkov, Pedro Cuenca, Nathan Lambert, Kashif Ra-
735 sul, Mishig Davaadorj, Dhruv Nair, Sayak Paul, William Berman, Yiyi Xu, Steven Liu, and
736 Thomas Wolf. Diffusers: State-of-the-art diffusion models. [https://github.com/
737 huggingface/diffusers](https://github.com/huggingface/diffusers), 2022.
- 738 Bram Wallace, Meihua Dang, Rafael Rafailov, Linqi Zhou, Aaron Lou, Senthil Purushwalkam,
739 Stefano Ermon, Caiming Xiong, Shafiq Joty, and Nikhil Naik. Diffusion model alignment using
740 direct preference optimization. In *Proceedings of the IEEE/CVF Conference on Computer Vision
741 and Pattern Recognition (CVPR)*, pp. 8228–8238, June 2024.
- 742 Rentian Yao, Linjun Huang, and Yun Yang. Minimizing convex functionals over space of probability
743 measures via KL divergence gradient flow. In Sanjoy Dasgupta, Stephan Mandt, and Yingzhen Li
744 (eds.), *Proceedings of The 27th International Conference on Artificial Intelligence and Statistics*,
745 volume 238 of *Proceedings of Machine Learning Research*, pp. 2530–2538. PMLR, 02–04 May
746 2024. URL <https://proceedings.mlr.press/v238/yao24a.html>.
- 747 Daniel M. Ziegler, Nisan Stiennon, Jeffrey Wu, Tom B. Brown, Alec Radford, Dario Amodei, Paul
748 Christiano, and Geoffrey Irving. Fine-tuning language models from human preferences, 2020.
749 URL <https://arxiv.org/abs/1909.08593>.

750
751
752
753
754
755

NOTATIONS

Table 2: List of commonly used symbols

Symbol	Description
d	dimension of the sample space \mathbb{R}^d .
$\mathcal{B}(\mathbb{R}^d)$	Borel set on \mathbb{R}^d .
\mathcal{P}	The space of probability density functions to the Lebesgue measure on $(\mathbb{R}^d, \mathcal{B}(\mathbb{R}^d))$.
$F : \mathbb{R}^d : \mathcal{P} \rightarrow \mathbb{R}$	A functional.
$\frac{\delta F}{\delta q}(q, x)$	The functional derivative of F . We often abbreviate this as $\frac{\delta F}{\delta q}(q)$.
$D_{\text{KL}}(q\ p)$	Kullback-Leibler divergence between q and p .
$\text{TV}(q, p)$	Total Variation between q and p .
$L(q)$	The regularized loss $F(q) + \beta D_{\text{KL}}(q\ p_{\text{ref}})$.
β	The regularization coefficient of $L(q)$.
$p_* \in \mathcal{P}$	The target distribution of pre-training.
$p_{\text{ref}} \in \mathcal{P}$	The output distribution at the final denoising step of the pre-trained model.
$q_* = \rho_* p_* \propto \exp(-f_*) p_* \in \mathcal{P}$	The target distribution of alignment.
$\hat{q}_{\text{opt}} = \hat{\rho}_{\text{opt}} p_{\text{ref}} \propto \exp(-\hat{f}_{\text{opt}}) p_{\text{ref}} \in \mathcal{P}$	The unique minimizer of $L(q)$, that corresponds to q_* when $p_{\text{ref}} = p_*$. We assume that $\rho_* \propto \exp(-f_*)$ can be estimated by minimizing $L(q)$, i.e. $\hat{\rho}_{\text{opt}} \simeq \rho_*$.
$\hat{q}^{(k)} \propto \exp(-\bar{g}^{(k)}) p_{\text{ref}}$	The optimal solution of the subproblem solved iteratively during Dual Averaging.
$q^{(k)} \propto \exp(-f_k) p_{\text{ref}}$	The implemented density that estimates $\hat{q}^{(k)}$.
β'	The hyperparameter of Dual Averaging that controls the optimization speed.
u_*	The optimal correction term to sample from q_* .
u	The implemented correction term using the estimated output density ratio $\rho \simeq \hat{\rho}_{\text{opt}}$.
$\mathcal{N}(\mu, \sigma)$	Gaussian with mean = μ and variance = σ^2
$T > 0$	The diffusion time.
$\{B_t\}_{t \in [0, T]}$	Brownian motion on \mathbb{R}^d .
$\{\bar{X}_t\}_{t \in [0, T]}$	The Ornstein-Uhlenbeck (OU) process starts from p_* .

810	$\{\bar{X}_t^{\leftarrow}\}_{t \in [0, T]}$	The reversed Ornstein-Uhlenbeck (ROU) process of
811		$\{\bar{X}_t\}_{t \in [0, T]}$, initialized at p_T .
812		
813	$\{X_t^{\leftarrow}\}_{t \in [0, T]}$	The time-discretized, and score-estimated ROU process of
814		$\{\bar{X}_t\}_{t \in [0, T]}$, initialized as $X_0^{\leftarrow} \sim \mathcal{N}(0, I_d)$.
815		
816	$\{\bar{Y}_t\}_{t \in [0, T]}$	The Ornstein-Uhlenbeck (OU) process starts from q_* .
817		
818	$\{\bar{Y}_t^{\leftarrow}\}_{t \in [0, T]}$	The reversed Ornstein-Uhlenbeck (ROU) process starts from
819		q_T .
820		
821	$\{Y_t^{\leftarrow}\}_{t \in [0, T]}$	The time-discretized dynamics using s and u .
822		
823	p_t	The law of \bar{X}_t , and the law of $\bar{X}_{T-t}^{\leftarrow}$.
824		
825	q_t	The law of the OU process \bar{Y}_t corresponding to $q_* = \rho_* p_*$.
826		
827	$h > 0$	The discretized time step of $\{X_t^{\leftarrow}\}_{t \in [0, T]}$.
828		
829	L	The number of steps of $\{X_t^{\leftarrow}\}_{t \in [0, T]}$.
830		
831	$s : \mathbb{R}^d \times \mathbb{R} \rightarrow \mathbb{R}^d$	A score network to implement $\{X_t^{\leftarrow}\}_{t \in [0, T]}$
832		
833	B_F	A constant that bounds $\frac{\delta F}{\delta q}$.
834		
835	L_{TV}	Lipschitz constant of $\frac{\delta F}{\delta q}$.
836		
837	S_F	Smoothness constant of the weaker smoothness of F .
838		
839	$\nabla_x f(x)$	Gradient of f with respect to x
840		
841	$\nabla_x^2 f(x)$	Hessian matrix of f
842		
843	$\ \cdot\ $	Euclid norm
844		
845	$\ \cdot\ _\infty$	L^∞ norm
846		
847	$\ \cdot\ _{\text{op}}$	The operator norm
848		
849	$\mathbb{E}[\cdot X]$	the conditional expectation given a random variable X .
850		
851	$\mathbb{E}[\cdot X = x]$	the conditional expectation given a random variable X ,
852		evaluated at $X = x$.
853		
854	\mathcal{O}	Big-O notation
855		
856	\lesssim, \gtrsim	inequalities ignoring constants.
857		
858		
859		
860		
861		
862		
863		

A CONVERGENCE ANALYSIS OF DUAL AVERAGING

Overview for convex loss

In Section A.1, we are interested in the convergence of Option 1 when the objective functional F is convex in a distributional sense:

$$F(q) \geq F(q') + \int \frac{\delta F}{\delta q}(q') d(q - q'), \quad \text{for any } q, q' \in \mathcal{P}.$$

Then, the regularized objective $L(q) = F(q) + \beta D_{\text{KL}}(q \| p_{\text{ref}})$ becomes strongly convex with $\beta > 0$. Formally, we assume that

- (i) $\frac{\delta F}{\delta q}$ is bounded: There exists $B_F > 0$ such that $\|\frac{\delta F}{\delta q}(q)\|_\infty \leq B_F$ for any $q \in \mathcal{P}$,
- (ii) $\frac{\delta F}{\delta q}$ is Lipschitz continuous with respect to the TV distance: There exists $L_{\text{TV}} > 0$ such that $\|\frac{\delta F}{\delta q}(q) - \frac{\delta F}{\delta q}(q')\|_\infty \leq L_{\text{TV}} \text{TV}(q, q')$ for any $q, q' \in \mathcal{P}$.
- (iii) F is convex: $F(q) \geq F(q') + \int \frac{\delta F}{\delta q}(q') d(q - q')$ for any $q, q' \in \mathcal{P}$,

In the update of Option 1, we iteratively use the distributional proximal operator. We minimize

$$\mathbb{E}_q \left[\sum_{j=1}^k \frac{2j}{k(k+1)} g^{(j)} \right] + \beta D_{\text{KL}}(q \| p_{\text{ref}}) + \beta' \frac{2}{k} D_{\text{KL}}(q \| p_{\text{ref}}) \quad (5)$$

by the minimizer $\hat{q}^{(k)}$, where $g^{(k)}$ denotes $\frac{\delta F}{\delta q}(q^{(k)})$ with $q^{(k)} \simeq \hat{q}^{(k)}$ ($q^{(k)}$ is constructed by neural networks and samples from p_{ref} , while we do not directly compute $q^{(k)}$). Intuitively, with $k \rightarrow \infty$, we hope that q is almost converged around the minimizer \hat{q}_{opt} , i.e. $q \simeq \hat{q}_{\text{opt}}$. Then, from the differentiability of F , each $\mathbb{E}_q[g^{(j)}]$ in the first term would be a linear functional that well approximates $F(q^{(j)})$, with sufficiently large j . In addition, $\beta' \frac{2}{k} D_{\text{KL}}(q \| p_{\text{ref}})$ vanishes, so the equation (5) is roughly written as

$$\begin{aligned} & \sum_{j=1}^k \frac{2j}{k(k+1)} \left[\mathbb{E}_q [g^{(j)}] + \beta D_{\text{KL}}(q \| p_{\text{ref}}) \right] + \beta' \frac{2}{k} D_{\text{KL}}(q \| p_{\text{ref}}) \\ & \simeq \sum_{j=1}^k \frac{2j}{k(k+1)} (F(q^{(j)}) + \beta D_{\text{KL}}(q \| p_{\text{ref}})) + \beta' \frac{2}{k} D_{\text{KL}}(q \| p_{\text{ref}}) \\ & \simeq \sum_{j=1}^k \frac{2j}{k(k+1)} (F(\hat{q}^{(j)}) + \beta D_{\text{KL}}(\hat{q}^{(j)} \| p_{\text{ref}})). \end{aligned}$$

This is the weighted average of the regularized losses $L(q) = F(q) + \beta D_{\text{KL}}(q \| p_{\text{ref}})$. From this concept, we will show that the convergence represented as

$$\left[\text{Weighted average of } L(\hat{q}^{(k)}) \right] = \left[\text{Weighted average of } L(\hat{q}_{\text{opt}}) \right] + \mathcal{O}\left(\frac{1}{k}\right).$$

Overview for nonconvex loss

In Section A.2, we are interested in the case that F is not necessarily convex (mainly) in Option 2. Alternatively, we use the assumption that F is smooth in terms of KL-divergence:

- (ii)' (The weaker smoothness derived from (ii)). There exists $S_F \geq 0$ such that

$$F(q) \leq F(q') + \int \frac{\delta F}{\delta q}(q') d(q - q') + \frac{S_F}{2} D_{\text{KL}}(q \| q') \quad \text{for any } q, q' \in \mathcal{P}, \quad (6)$$

This is induced by Lipschitz continuity of $\frac{\delta F}{\delta q}$ ((ii) of Assumption 1 and 2) and Pinsker's inequality. When the inner-loop error is ignored, it is possible to prove convergence using only the smoothness (6) instead of Lipschitz continuity of $\frac{\delta F}{\delta q}$. Please note that KL-divergence would be the "quadratic

term” in the ordinary definition of smoothness. Following the theoretical analysis of standard non-convex optimization, our goal is to show that the “derivative” of the (regularized) objective $L(q)$ goes to zero in the form of functional derivative:

$$\frac{\delta L}{\delta q}(\hat{q}^{(k)}, x) \rightarrow 0 \quad (\text{up to constant w.r.t. } x.)$$

Please note that we can ignore $\frac{\delta L}{\delta q}(\hat{q}^{(k)}, x)$ if it is a constant because of the definition of the functional derivatives.

At the first step, both in Option 1 and 2, the regularized objective $L(q)$ (roughly) monotonically decrease during the Dual Averaging. Ignoring some terms, we want to show that

$$L(\hat{q}^{(k+1)}) - L(\hat{q}^{(k)}) \lesssim -D_{\text{KL}}(\hat{q}^{(k)} \parallel \hat{q}^{(k+1)}) < 0.$$

Next, by taking a telescoping sum, we obtain that

$$\frac{1}{K} \sum_{k=1}^K (\text{weight})_k D_{\text{KL}}(\hat{q}^{(k)} \parallel \hat{q}^{(k+1)}) = \mathcal{O}\left(\frac{1}{K}\right).$$

From the above equation, it is immediately shown that

$$\min_{k=1, \dots, K} (\text{weight})_k D_{\text{KL}}(\hat{q}^{(k)} \parallel \hat{q}^{(k+1)}) = \mathcal{O}\left(\frac{1}{K}\right),$$

where $(\text{weight})_k \simeq k$ in the Option 1, while $(\text{weight})_k \simeq 1$ in the Option 2. Therefore, when we choose the Option 2, it holds that

$$\min_{k=1, \dots, K} D_{\text{KL}}(\hat{q}^{(k)} \parallel \hat{q}^{(k+1)}) = \mathcal{O}\left(\frac{1}{K}\right)$$

Finally, we get the conclusion $\frac{\delta L(\hat{q}^{(k)})}{\delta q} \rightarrow 0$ (up to constant w.r.t. x) because $D_{\text{KL}}(\hat{q}^{(k)} \parallel \hat{q}^{(k+1)})$ is the approximate “moment generation function” of $\frac{\delta L(\hat{q}^{(k)})}{\delta q}$; when $k \rightarrow \infty$,

$$\min_{k=1, \dots, K} \left(\text{“Variance” of } \frac{\delta L(\hat{q}^{(k)})}{\delta q} \right) \simeq \min_{k=1, \dots, K} D_{\text{KL}}(\hat{q}^{(k)} \parallel \hat{q}^{(k+1)}) = \mathcal{O}\left(\frac{1}{K}\right).$$

This result aligns with the result for standard, non-distributional Dual Averaging (Liu et al., 2023a), $\min_{k=1, \dots, K} \|(\text{gradient of the objective})_k\|^2 = \mathcal{O}(1/K)$ because the variance is the second moment.

A.1 WHEN F IS CONVEX

We will show that, when F is convex in the distributional sense, the convergence of the Option 1 can be written as

$$\left[\text{Weighted average of } L(\hat{q}^{(k)}) \right] - \left[\text{Weighted average of } L(\hat{q}_{\text{opt}}) \right] = \mathcal{O}\left(\frac{1}{K}\right).$$

We require β to be positive to make the regularized objective $F(q) + \beta D_{\text{KL}}(q \parallel p_{\text{ref}})$ strongly convex. In addition, one of the necessary conditions $\beta' \geq \beta$ implies that the “learning rate” should be controlled to converge.

Theorem (restated - Theorem 1). *Assume that F is convex, $|\frac{\delta F}{\delta q}| \leq B_F$, $\frac{\delta F}{\delta q}$ is L_{TV} -Lipshitz with respect to q in TV distance, $\text{TV}(\hat{q}^{(k)}, q^{(k)}) \leq \epsilon_{\text{TV}}$, and $\beta' \geq \beta$. Then,*

$$\begin{aligned} & \frac{2}{K(K+1)} \sum_{k=1}^K k \left[F(\hat{q}^{(k)}) + \beta D_{\text{KL}}(\hat{q}^{(k)} \parallel p_{\text{ref}}) - F(\hat{q}_{\text{opt}}) - \beta D_{\text{KL}}(\hat{q}_{\text{opt}} \parallel p_{\text{ref}}) \right] \\ & \leq \frac{2}{K(K+1)} \sum_{k=1}^K k \left[2L_{\text{TV}}\epsilon_{\text{TV}} + \mathbb{E}_{\hat{q}^{(k)}}[g^{(k)}] - \mathbb{E}_{\hat{q}_{\text{opt}}}[g^{(k)}] + \beta(D_{\text{KL}}(\hat{q}^{(k)} \parallel p_{\text{ref}}) - D_{\text{KL}}(\hat{q}_{\text{opt}} \parallel p_{\text{ref}})) \right] \\ & \leq 2L_{\text{TV}}\epsilon_{\text{FD}} + \frac{2}{K(K+1)} \left[B_F + \beta(K+3)D_{\text{KL}}(\hat{q}_{\text{opt}} \parallel p_{\text{ref}}) + \mathbb{E}_{\hat{q}_{\text{opt}}}[g^{(1)}] + \frac{B_F^2 K}{\beta} \right]. \end{aligned}$$

First, we want to show that the D_{KL} regularization term plays a role of the “quadratic” regularization, which makes the regularized objective $F(q) + \beta D_{\text{KL}}(q\|p_{\text{ref}})$ strongly convex. We observe that the sum of the linear (convex and concave) objective and the D_{KL} regularization term

$$\tilde{F}(q) = \mathbb{E}_q[r(x)] + \beta D_{\text{KL}}(q\|p)$$

is strongly convex in the distributional sense. In particular, if q is the minimizer of \tilde{F} , then

$$\tilde{F}(q) + \frac{\beta}{2} \text{TV}(q, q')^2 \leq \tilde{F}(q') \text{ for all } q' \in \mathcal{P}.$$

This result is useful to prove Lemma 2, which controls the regularized and linearized objective $\mathbb{E}_q[\frac{\delta F}{\delta q}] + \beta D_{\text{KL}}(q\|p_{\text{ref}})$:

Lemma 1 (Nitanda et al. (2021)). $\tilde{F} : \mathcal{P} \rightarrow \mathbb{R}$, $\tilde{F}(q) = \mathbb{E}_q[r(x)] + \beta D_{\text{KL}}(q\|p)$. Assume that r is bounded. We put $r_1 := \frac{dq}{dp}$, $r_2 := \frac{dq'}{dp}$,

$$\tilde{F}(q) \leq \tilde{F}(q') + \mathbb{E}_q[(r_1 - r_2)(r(x) + \beta \log r_1)] - \frac{\beta}{2} \|r_1 - r_2\|_{L^1(p)}^2.$$

Especially, if $q \propto \exp(-\frac{r}{\beta})p$,

$$\tilde{F}(q) \leq \tilde{F}(q') - \frac{\beta}{2} \|r_1 - r_2\|_{L^1(p)}^2.$$

Proof. Omitted. See Nitanda et al. (2021). We use Pinsker’s inequality $\text{TV}(q, q')^2 \lesssim D_{\text{KL}}(q\|q')$. \square

Given that $F(q) + \beta D_{\text{KL}}(q\|p_{\text{ref}})$ is strongly convex, let us prove Theorem 1:

Proof. The main parts of the proof follow existing papers (Nitanda et al., 2021; Nishikawa et al., 2022). The key difference lies in that we are not using Langevin sampler in the inner loop, which slightly changes how the error of $q^{(k)}$ is handled.

We begin by linearizing the weighted sum of the losses. $g^{(k)}$ denotes $\frac{\delta F}{\delta q}(q^{(k)})$, and \hat{q}_{opt} denotes the minimizer of F . From the convexity of F ,

$$\begin{aligned} & \frac{2}{K(K+1)} \sum_{k=1}^K k \left[F(\hat{q}^{(k)}) + \beta D_{\text{KL}}(\hat{q}^{(k)}\|p_{\text{ref}}) - F(\hat{q}_{\text{opt}}) - \beta D_{\text{KL}}(\hat{q}_{\text{opt}}\|p_{\text{ref}}) \right] \\ & \leq \frac{2}{K(K+1)} \sum_{k=1}^K k \left[\int \frac{\delta F}{\delta q}(\hat{q}^{(k)}) d(\hat{q}^{(k)} - \hat{q}_{\text{opt}}) + \beta (D_{\text{KL}}(\hat{q}^{(k)}\|p_{\text{ref}}) - D_{\text{KL}}(\hat{q}_{\text{opt}}\|p_{\text{ref}})) \right] \\ & \leq \frac{2}{K(K+1)} \sum_{k=1}^K k \left[\left| \int \frac{\delta F}{\delta q}(\hat{q}^{(k)}) - \frac{\delta F}{\delta q}(q^{(k)}) d(\hat{q}^{(k)} - \hat{q}_{\text{opt}}) \right| + \mathbb{E}_{\hat{q}^{(k)}}[g^{(k)}] - \mathbb{E}_{\hat{q}_{\text{opt}}}[g^{(k)}] \right. \\ & \quad \left. + \beta (D_{\text{KL}}(\hat{q}^{(k)}\|p_{\text{ref}}) - D_{\text{KL}}(\hat{q}_{\text{opt}}\|p_{\text{ref}})) \right]. \end{aligned}$$

Here, we bound the estimation error of $g^{(k)} = \frac{\delta F}{\delta q}(q^{(k)})$ using the Lipschitz continuity of $\frac{\delta F}{\delta q}$ with respect to q :

$$\begin{aligned} & \left| \int \frac{\delta F}{\delta q}(\hat{q}^{(k)}) - g^{(k)} d(\hat{q}^{(k)} - \hat{q}_{\text{opt}}) \right| \\ & \leq \text{TV}(\hat{q}^{(k)}, \hat{q}_{\text{opt}}) \sup_x \left| \frac{\delta F}{\delta q}(\hat{q}^{(k)}, x) - g^{(k)}(x) \right| \\ & \leq 2L_q \epsilon_{\text{TV}}. \end{aligned}$$

Then we obtain

$$\begin{aligned} & \frac{2}{K(K+1)} \sum_{k=1}^K k \left[F(\hat{q}^{(k)}) + \beta D_{\text{KL}}(\hat{q}^{(k)} \| p_{\text{ref}}) - F(\hat{q}_{\text{opt}}) - \beta D_{\text{KL}}(\hat{q}_{\text{opt}} \| p_{\text{ref}}) \right] \\ & \leq \frac{2}{K(K+1)} \sum_{k=1}^K k \left[2L_q \epsilon_{\text{TV}} + \mathbb{E}_{\hat{q}^{(k)}}[g^{(k)}] - \mathbb{E}_{\hat{q}_{\text{opt}}}[g^{(k)}] \right. \\ & \quad \left. + \beta(D_{\text{KL}}(\hat{q}^{(k)} \| p_{\text{ref}}) - D_{\text{KL}}(\hat{q}_{\text{opt}} \| p_{\text{ref}})) \right]. \end{aligned} \quad (7)$$

This implies that it is sufficient to bound the weighted sum of the (regularized) linearized objectives $\mathbb{E}_{\hat{q}^{(k)}}[g^{(k)}] + \beta(D_{\text{KL}}(\hat{q}^{(k)} \| p_{\text{ref}}))$, $k = 1, \dots, K$.

In each update of Option 1, $\hat{q}^{(k+1)}$ is obtained by maximizing

$$V_{k+1}(q) = -\mathbb{E}_q \left[\sum_{j=1}^k j g^{(j)} \right] - \frac{\beta k(k+1)}{2} D_{\text{KL}}(q \| p_{\text{ref}}) - \beta'(k+1) D_{\text{KL}}(q \| p_{\text{ref}}).$$

We also define

$$r_*^{(k+1)} = \frac{d\hat{q}^{(k+1)}}{dp_{\text{ref}}}, \quad V_{k+1}^* = V_{k+1}(\hat{q}^{(k+1)}).$$

Then, we can show that V_k^* has the following recursive relation. Lemma 2 approximately implies

$$k \mathbb{E}_{\hat{q}^{(k)}}[g^{(k)}] + k \beta D_{\text{KL}}(\hat{q}^{(k+1)} \| p_{\text{ref}}) \lesssim V_k^* - V_{k+1}^* + \mathcal{O}(1),$$

then, summing from $k = 1$ to K , we roughly obtain,

$$\frac{2}{K(K+1)} \left[\sum_{k=1}^K k (\mathbb{E}_{\hat{q}^{(k)}}[g^{(k)}] + \beta D_{\text{KL}}(\hat{q}^{(k)} \| p_{\text{ref}})) + V_{K+1}^* \right] \lesssim \mathcal{O}\left(\frac{1}{K}\right). \quad (8)$$

So, as long as we prove Lemma 2, we can connect this inequality (8) to the inequality (7) because $V_{K+1}^* \gtrsim -\sum_{k=1}^K k (\mathbb{E}_{\hat{q}_{\text{opt}}}[g^{(k)}] + \beta D_{\text{KL}}(\hat{q}_{\text{opt}} \| p_{\text{ref}}))$:

Lemma 2. For $k \geq 1$,

$$V_{k+1}^* \leq V_k^* - k \mathbb{E}_{\hat{q}^{(k)}}[g^{(k)}] - (\beta k + \beta') D_{\text{KL}}(\hat{q}^{(k+1)} \| p_{\text{ref}}) + \frac{B_F^2 k}{\beta(k-1) + 2\beta'}. \quad (9)$$

For the proof of Lemma 2, please refer to Section A.1.1, in which we use Lemma 1.

From here, we will rigorously explain the result derived from Lemma 2. When $k = 1$, because $\|g^{(k)}\|_\infty \leq B_F$,

$$V_1^* \leq B_F - \beta D_{\text{KL}}(\hat{q}^{(1)} \| p_{\text{ref}}).$$

By taking a telescoping sum of (9),

$$\begin{aligned} V_{K+1}^* & \leq B_F - \sum_{k=1}^K k \left(\mathbb{E}_{\hat{q}^{(k)}}[g^{(k)}] + \beta D_{\text{KL}}(\hat{q}^{(k)} \| p_{\text{ref}}) \right) - [\beta(K+1) + \beta'] D_{\text{KL}}(\hat{q}^{(K+2)} \| p_{\text{ref}}) \\ & \quad + \sum_{k=1}^K \frac{B_F^2 k}{\beta(k-1) + 2\beta'} \\ & \leq B_F - \sum_{k=1}^K k \left(\mathbb{E}_{\hat{q}^{(k)}}[g^{(k)}] + \beta D_{\text{KL}}(\hat{q}^{(k)} \| p_{\text{ref}}) \right) + \frac{B_F^2 K}{\beta}, \end{aligned} \quad (10)$$

where we used $\beta' \geq \beta$ in the last inequality. On the other hand, we see that

$$\begin{aligned} V_{K+1}^* & \geq -\mathbb{E}_{\hat{q}_{\text{opt}}} \left[\sum_{k=1}^K k g^{(k)} \right] - \frac{\beta K(K+1) + 2\beta'(K+1)}{2} D_{\text{KL}}(\hat{q}_{\text{opt}} \| p_{\text{ref}}) \\ & = -\mathbb{E}_{\hat{q}_{\text{opt}}} \left[\sum_{k=1}^K k (g^{(k)} + \beta D_{\text{KL}}(\hat{q}_{\text{opt}} \| p_{\text{ref}})) \right] - \beta'(K+1) D_{\text{KL}}(\hat{q}_{\text{opt}} \| p_{\text{ref}}) \end{aligned} \quad (11)$$

because V_{K+2}^* is the maximal value. Combining the upper bound (Eq. 10) and the lower bound (Eq. 11),

$$\begin{aligned} & \sum_{k=1}^K k \left(\mathbb{E}_{\hat{q}^{(k)}}[g^{(k)}] - \mathbb{E}_{\hat{q}_{\text{opt}}} [g^{(k)}] + \beta(D_{\text{KL}}(\hat{q}^{(k)} \| p_{\text{ref}}) - D_{\text{KL}}(\hat{q}_{\text{opt}} \| p_{\text{ref}})) \right) \\ & \leq B_F + \beta'(K+1)D_{\text{KL}}(\hat{q}_{\text{opt}} \| p_{\text{ref}}) + \frac{B_F^2 K}{\beta}. \end{aligned}$$

Finally we get the convergence rate:

$$\begin{aligned} & \frac{2}{K(K+1)} \sum_{k=1}^K k \left[F(\hat{q}^{(k)}) + \beta D_{\text{KL}}(\hat{q}^{(k)} \| p_{\text{ref}}) - F(\hat{q}_{\text{opt}}) - \beta D_{\text{KL}}(\hat{q}_{\text{opt}} \| p_{\text{ref}}) \right] \\ & \leq \frac{2}{K(K+1)} \sum_{k=1}^K k \left[2L_{\text{TV}}\epsilon_{\text{TV}} + \mathbb{E}_{\hat{q}^{(k)}}[g^{(k)}] - \mathbb{E}_{\hat{q}_{\text{opt}}}[g^{(k)}] + \beta(D_{\text{KL}}(\hat{q}^{(k)} \| p_{\text{ref}}) - D_{\text{KL}}(\hat{q}_{\text{opt}} \| p_{\text{ref}})) \right] \\ & \leq 2L_{\text{TV}}\epsilon_{\text{FD}} + \frac{2}{K(K+1)} \left[B_F + \beta'(K+1)D_{\text{KL}}(\hat{q}_{\text{opt}} \| p_{\text{ref}}) + \frac{B_F^2 K}{\beta} \right]. \end{aligned}$$

This concludes the assertion. \square

A.1.1 PROOF OF LEMMA 2

Proof. We can calculate the relation between $V_{k+1}^* = V_{k+1}(\hat{q}^{(k+1)})$ and $V_k(\hat{q}^{(k+1)})$ as

$$\begin{aligned} V_{k+1}^* &= -\mathbb{E}_{\hat{q}^{(k+1)}} \left[\sum_{j=1}^k j g^{(j)} \right] - \frac{(k+1)(\beta k + 2\beta')}{2} D_{\text{KL}}(\hat{q}^{(k+1)} \| p_{\text{ref}}) \\ &= -\mathbb{E}_{\hat{q}^{(k+1)}} \left[\sum_{j=1}^{k-1} j g^{(j)} \right] - \frac{\beta k(k-1)}{2} D_{\text{KL}}(\hat{q}^{(k+1)} \| p_{\text{ref}}) - \beta' k D_{\text{KL}}(\hat{q}^{(k+1)} \| p_{\text{ref}}) \\ &\quad - k \mathbb{E}_{\hat{q}^{(k+1)}}[g^{(k)}] - (\beta k + \beta') D_{\text{KL}}(\hat{q}^{(k+1)} \| p_{\text{ref}}) \\ &= V_k(\hat{q}^{(k+1)}) - k \mathbb{E}_{\hat{q}^{(k)}}[g^{(k)}] + k(\mathbb{E}_{\hat{q}^{(k)}}[g^{(k)}] - \mathbb{E}_{\hat{q}^{(k+1)}}[g^{(k)}]) - (\beta k + \beta') D_{\text{KL}}(\hat{q}^{(k+1)} \| p_{\text{ref}}), \end{aligned} \tag{12}$$

where we used the definitions of V_k and V_{k+1} . Next, we upper bound the RHS of Eq. (12) using Lemma 1 about the convexity of D_{KL} :

$$\begin{aligned} & \text{(RHS of Eq. (12))} \\ & \leq V_k^* - \frac{\beta k(k-1) + 2\beta' k}{4} \|r_*^{(k+1)} - r_*^{(k)}\|_{L^1(p_{\text{ref}})}^2 - k \mathbb{E}_{\hat{q}^{(k)}}[g^{(k)}] + k(\mathbb{E}_{\hat{q}^{(k)}}[g^{(k)}] - \mathbb{E}_{\hat{q}^{(k+1)}}[g^{(k)}]) \\ &\quad - (\beta k + \beta') D_{\text{KL}}(\hat{q}^{(k+1)} \| p_{\text{ref}}) \quad (\because \text{the second equation in Lemma 1 and the optimality of } V_k^*) \\ & \leq V_k^* - \frac{\beta k(k-1) + 2\beta' k}{4} \|r_*^{(k+1)} - r_*^{(k)}\|_{L^1(p_{\text{ref}})}^2 - k \mathbb{E}_{\hat{q}^{(k)}}[g^{(k)}] + k \left| \mathbb{E}_{\hat{q}^{(k)}}[g^{(k)}] - \mathbb{E}_{\hat{q}^{(k+1)}}[g^{(k)}] \right| \\ &\quad - \beta(k+1) D_{\text{KL}}(\hat{q}^{(k+1)} \| p_{\text{ref}}) \\ & \leq V_k^* - \frac{\beta k(k-1) + 2\beta' k}{4} \|r_*^{(k+1)} - r_*^{(k)}\|_{L^1(p_{\text{ref}})}^2 - k \mathbb{E}_{\hat{q}^{(k)}}[g^{(k)}] + B_F k \|r_*^{(k+1)} - r_*^{(k)}\|_{L^1(p_{\text{ref}})} \\ &\quad - \beta(k+1) D_{\text{KL}}(p_*^{(t+1)} \| q) \quad (\because \|g^{(k)}\|_{\infty} \leq B_F) \\ & \leq V_k^* - k \mathbb{E}_{\hat{q}^{(k)}}[g^{(k)}] - \beta(k+1) D_{\text{KL}}(\hat{q}^{(k+1)} \| p_{\text{ref}}) + \frac{B_F^2 k}{\beta(k-1) + 2\beta'}, \end{aligned}$$

where we used the arithmetic-geometric mean inequality in the last inequality. This concludes the proof. \square

1134 A.2 CONVERGENCE PROOF FOR NON-CONVEX LOSS F

1135 Here, we give the proof of Theorem 2 and Corollary 1. In this section, we always assume Assump-
1137 tion 2 holds. We are mainly interested in the property that F is smooth with respect to KL-divergence
1138 instead of convexity:

1139 (ii)' (A weaker version of (ii)). There exists $S_F \geq 0$ such that

$$1140 F(q) \leq F(q') + \int \frac{\delta F}{\delta q}(q')d(q - q') + \frac{S_F}{2} D_{\text{KL}}(q||q') \quad \text{for any } q, q' \in \mathcal{P}. \quad (13)$$

1141 This property can be derived from (ii) in Assumption 2 that is Lipschitz continuity of $\frac{\delta F}{\delta q}$:

1142 **Lemma 3.** Assume that $\frac{\delta F}{\delta q}$ is Lipschitz continuous with respect to the TV distance: There exists
1143 $L_{\text{TV}} > 0$ such that $\|\frac{\delta F}{\delta q}(q) - \frac{\delta F}{\delta q}(q')\|_\infty \leq L_{\text{TV}} \text{TV}(q, q')$ for any $q, q' \in \mathcal{P}$. Then,

$$1144 F(q) \leq F(q') + \int \frac{\delta F}{\delta q}(q')d(q - q') + \frac{L_{\text{TV}}}{2} \text{TV}(q, q')^2 \quad \text{for any } q, q' \in \mathcal{P}.$$

1145 From Pinsker's inequality,

$$1146 F(q) \leq F(q') + \int \frac{\delta F}{\delta q}(q')d(q - q') + L_{\text{TV}} D_{\text{KL}}(q||q') \quad \text{for any } q, q' \in \mathcal{P}.$$

1147 *Proof.* The proof is almost identical to the proof of L_{TV} -smoothness commonly discussed in the
1148 context of standard optimization. For $q, q' \in \mathcal{P}$, we define $q_t = q' + t(q - q') \in \mathcal{P}$. Then,

$$\begin{aligned} 1149 & F(q) - F(q') - \int \frac{\delta F}{\delta q}(q')d(q - q') \\ 1150 &= \int_{t=0}^{t=1} \int \frac{\delta F}{\delta q}(q_t)d(q - q')dt - \int \frac{\delta F}{\delta q}(q')d(q - q') \\ 1151 &= \int_{t=0}^{t=1} \int \left[\frac{\delta F}{\delta q}(q_t) - \frac{\delta F}{\delta q}(q') \right] d(q - q')dt \\ 1152 &\leq \int_{t=0}^{t=1} t L_{\text{TV}} \text{TV}(q, q')^2 dt \quad (L_{\text{TV}}\text{-Lipshitz continuity of } \frac{\delta F}{\delta q}) \\ 1153 &= \frac{L_{\text{TV}}}{2} \text{TV}(q, q')^2, \end{aligned}$$

1154 while we used the fundamental theorem of calculus in the first equation and the assumption in the
1155 inequality. \square

1156 We emphasize that when the inner-loop error is ignored, it is possible to prove convergence using
1157 only the smoothness (13) instead of (ii) in Assumption 2. Therefore, we will use the notation S_F for
1158 the parts that can be derived using Assumption (ii)' instead of Assumption (ii).

1159 Under the assumptions, our goal is to show that the functional derivative of $L(q) = F(q) +$
1160 $\beta D_{\text{KL}}(q||p_{\text{ref}})$ goes to a constant:

$$1161 \frac{\delta L}{\delta q} \rightarrow 0 \quad (\text{up to constant w.r.t. } x)$$

1162 We prepare the following Lemma about the convexity of D_{KL} :

1163 **Lemma 4.** The following equations hold:

$$1164 (i) D_{\text{KL}}(q||p) = D_{\text{KL}}(q'||p) + \int \frac{\delta}{\delta q} D_{\text{KL}}(q'||p)d(q - q') + D_{\text{KL}}(q||q'),$$

1165 (ii) Let $r : \mathbb{R}^d \rightarrow \mathbb{R}$ be a smooth function. For $\tilde{F}(q) = \mathbb{E}_q[r(x)] + D_{\text{KL}}(q||p)$, $q' = \exp(-r)q$,
1166 it holds that

$$1167 \tilde{F}(q) = \tilde{F}(q') + D_{\text{KL}}(q||q').$$

1168 $\tilde{F}(q)$ is uniquely minimized at $q = q'$.

We omit its proof because it is straight forward. Lemma 4 implies that D_{KL} also plays a important role as a “quadratic” penalty term of the proximal operator whose output is

$$\operatorname{argmin}_{q \in \mathcal{P}} \{H(q) + D_{\text{KL}}(q \| p_{\text{ref}})\}, \text{ for any functional } H.$$

This property allows for the use of standard nonconvex convergence analysis of Dual Averaging based on the proximal operator (Liu et al., 2023a).

Roughly speaking, the intermediate goal is to show that $L(q)$ monotonically decreases in each k th iteration:

$$L(\hat{q}^{(k+1)}) - L(\hat{q}^{(k)}) \lesssim 0.$$

By the weaker smoothness of F (Eq.(13)), the left hand side is approximately bounded as

$$\begin{aligned} L(\hat{q}^{(k+1)}) - L(\hat{q}^{(k)}) &\lesssim \int \frac{\delta F}{\delta q}(\hat{q}^{(k)}) d(\hat{q}^{(k+1)} - \hat{q}^{(k)}) + D_{\text{KL}}(\hat{q}^{(k+1)} \| \hat{q}^{(k)}) \\ &\lesssim \int \frac{\delta L}{\delta q}(\hat{q}^{(k)}) d(\hat{q}^{(k+1)} - \hat{q}^{(k)}) + D_{\text{KL}}(\hat{q}^{(k+1)} \| \hat{q}^{(k)}), \end{aligned} \quad (14)$$

ignoring various minor terms and constants. To bound the right hand side in (14), we show the following inequality regarding the Option 2 using Lemma 4.

Lemma 5. *Assume that $\text{TV}(\hat{q}^{(k)}, q^{(k)}) \leq \epsilon_{\text{TV}}/2$ for all k . Then, the Option 2 achieves*

$$\begin{aligned} &\int \frac{\delta L}{\delta q}(q^{(k)}) d(\hat{q}^{(k+1)} - \hat{q}^{(k)}) \\ &\leq B_F \epsilon_{\text{TV}} + \frac{\beta'}{k} \left(D_{\text{KL}}(\hat{q}^{(k)} \| p_{\text{ref}}) - D_{\text{KL}}(\hat{q}^{(k+1)} \| p_{\text{ref}}) - k D_{\text{KL}}(\hat{q}^{(k+1)} \| \hat{q}^{(k)}) - (k+1) D_{\text{KL}}(\hat{q}^{(k)} \| \hat{q}^{(k+1)}) \right) \end{aligned}$$

Proof. In the Option 2, $\hat{q}^{(k+1)}$ minimizes

$$r_{k+1}(q) := \sum_{j=1}^k \int j \frac{\delta L}{\delta q}(q^{(j)}) d(q - \hat{q}^{(j)}) + \beta'(k+1) D_{\text{KL}}(q \| p_{\text{ref}}).$$

We interpret that Option 2 computes the proximal operator of the weighted sum of $\frac{\delta L}{\delta q}$ and this concept is justified by Lemma 4. By the definition of r_k and r_{k+1} , it holds that

$$r_{k+1}(q) = r_k(q) + \int k \frac{\delta L}{\delta q}(q^{(k)}) d(q - \hat{q}^{(k)}) + \beta' D_{\text{KL}}(q \| p_{\text{ref}}). \quad (15)$$

From Lemma 4, we also have

$$r_k(q) - r_k(\hat{q}^{(k)}) = \beta' k D_{\text{KL}}(q \| \hat{q}^{(k)}), \text{ for all } q \in \mathcal{P} \quad (16)$$

because $r_k(q)$ is just the sum of the linear functional of q and the KL-divergence ignoring the constant. Letting $q = \hat{q}^{(k+1)}$ and we obtain

$$\begin{aligned} 0 &\leq r_k(\hat{q}^{(k+1)}) - r_k(\hat{q}^{(k)}) - \beta' k D_{\text{KL}}(\hat{q}^{(k+1)} \| \hat{q}^{(k)}) \\ &= r_{k+1}(\hat{q}^{(k+1)}) - \int k \frac{\delta L}{\delta q}(q^{(k)}) d(\hat{q}^{(k+1)} - \hat{q}^{(k)}) - \beta' D_{\text{KL}}(\hat{q}^{(k+1)} \| p_{\text{ref}}) \\ &\quad - r_k(\hat{q}^{(k)}) - \beta' k D_{\text{KL}}(\hat{q}^{(k+1)} \| \hat{q}^{(k)}). \end{aligned} \quad (17)$$

In the last equality, we decomposed the sum using the equation (15). Thus,

$$\begin{aligned} &\int k \frac{\delta L}{\delta q}(q^{(k)}) d(\hat{q}^{(k+1)} - \hat{q}^{(k)}) \\ &\leq r_{k+1}(\hat{q}^{(k+1)}) - r_k(\hat{q}^{(k)}) - \beta' D_{\text{KL}}(\hat{q}^{(k+1)} \| p_{\text{ref}}) - \beta' k D_{\text{KL}}(\hat{q}^{(k+1)} \| \hat{q}^{(k)}). \end{aligned}$$

By using the same argument as Eq. (16) for $k \leftarrow k+1$, we have

$$\begin{aligned} r_{k+1}(\hat{q}^{(k+1)}) + \beta'(k+1) D_{\text{KL}}(\hat{q}^{(k)} \| \hat{q}^{(k+1)}) &= r_{k+1}(\hat{q}^{(k)}) \\ &= r_k(\hat{q}^{(k)}) + \beta' D_{\text{KL}}(\hat{q}^{(k)} \| p_{\text{ref}}). \end{aligned}$$

Substituting this relation to Eq. (17) and noticing $|\frac{\delta F}{\delta q}| \leq B_F$, we obtain the assertion. \square

We also show the result for Option 1 that is similar to Lemma 5:

Lemma 6. Assume that $\text{TV}(\hat{q}^{(k)}, q^{(k)}) \leq \epsilon_{\text{TV}}/2$ for all k . Then, Algorithm 1 achieves

$$\begin{aligned} & \int \frac{\delta F}{\delta q}(q^{(k)}) d(\hat{q}^{(k+1)} - \hat{q}^{(k)}) \\ & \leq B_F \epsilon_{\text{TV}} + \frac{\beta k + \beta'}{k} \left(D_{\text{KL}}(\hat{q}^{(k)} \| p_{\text{ref}}) - D_{\text{KL}}(\hat{q}^{(k+1)} \| p_{\text{ref}}) \right) \\ & \quad - \left(\frac{\beta(k-1) + 2\beta'}{2} \right) D_{\text{KL}}(\hat{q}^{(k+1)} \| \hat{q}^{(k)}) - \left(\frac{\beta(k+1) + 2\beta'(1+1/k)}{2} \right) D_{\text{KL}}(\hat{q}^{(k)} \| \hat{q}^{(k+1)}) \end{aligned}$$

Proof. Please refer to Appendix A.2.1. The proof is almost identical to the proof of Lemma 5. \square

We mentioned that our rough intermediate goal was to show that $L(q)$ monotonically decreases in each k th iteration:

$$L(\hat{q}^{(k+1)}) - L(\hat{q}^{(k)}) \lesssim 0.$$

Rigorously, we will show that

$$\tilde{L}_k(q) := L(q) + \frac{\beta'}{k} D_{\text{KL}}(q \| p_{\text{ref}})$$

decreases. This is an objective function with additional regularization imposed by the hyperparameter β' . From Lemma 5, we prove that $\tilde{L}_k(\hat{q}^{(k)})$ decreases as in the following lemma.

Lemma 7. Assume that $\text{TV}(\hat{q}^{(k)}, q^{(k)}) \leq \epsilon_{\text{TV}}/2$ for all k and $2\beta + S_F \leq 2\beta'$. Then, Option 2 satisfies

$$\tilde{L}_{k+1}(\hat{q}^{(k+1)}) - \tilde{L}_k(\hat{q}^{(k)}) \leq (L_{\text{TV}} + B_F) \epsilon_{\text{TV}} - \frac{\beta'(k+1)}{k} D_{\text{KL}}(\hat{q}^{(k)} \| \hat{q}^{(k+1)}), \quad (18)$$

and Option 1 satisfies

$$\tilde{L}_{k+1}(\hat{q}^{(k+1)}) - \tilde{L}_k(\hat{q}^{(k)}) \leq (L_{\text{TV}} + B_F) \epsilon_{\text{TV}} - \frac{\beta k(k+1) + 2\beta'(k+1)}{2k} D_{\text{KL}}(\hat{q}^{(k)} \| \hat{q}^{(k+1)}), \quad (19)$$

By this lemma, it can be shown that the sum of the KL divergences $D_{\text{KL}}(\hat{q}^{(k)} \| \hat{q}^{(k+1)})$ converges to 0 at a rate of $\mathcal{O}(1/K)$ through a telescoping sum: we obtain that

$$\frac{1}{K} \sum_{k=1}^K (\text{weight})_k D_{\text{KL}}(\hat{q}^{(k)} \| \hat{q}^{(k+1)}) = \mathcal{O}\left(\frac{1}{K}\right).$$

From the above equation, it is immediately shown that

$$\min_{k=1, \dots, K} (\text{weight})_k D_{\text{KL}}(\hat{q}^{(k)} \| \hat{q}^{(k+1)}) = \mathcal{O}\left(\frac{1}{K}\right),$$

where $(\text{weight})_k \simeq k$ in Option 1, while $(\text{weight})_k \simeq 1$ in Option 2. In Option 2, we will be able to show that $\min_k D_{\text{KL}}(\hat{q}^{(k)} \| \hat{q}^{(k+1)}) \rightarrow 0$, which implies that $\hat{q}^{(k)}$ converges to some point (in fact, this is the stationary point).

Now let us prove Lemma 7:

Proof. We only prove the inequality for Option 2. By the smoothness of F (the weaker smoothness (ii)' in Eq.(13)), the Lipschitz continuity of $\frac{\delta F}{\delta q}$ and the property of the KL-divergence (Lemma 4), we have

$$\begin{aligned} L(\hat{q}^{(k+1)}) - L(\hat{q}^{(k)}) & \leq \int \frac{\delta F}{\delta q}(\hat{q}^{(k)}) d(\hat{q}^{(k+1)} - \hat{q}^{(k)}) + \frac{S_F}{2} D_{\text{KL}}(\hat{q}^{(k+1)} \| \hat{q}^{(k)}) \\ & \quad + \beta D_{\text{KL}}(\hat{q}^{(k+1)} \| \hat{q}^{(k)}) + \int (-\beta \bar{g}^{(k-1)}) d(\hat{q}^{(k+1)} - \hat{q}^{(k)}) \\ & \leq \int \left(\frac{\delta F}{\delta q}(q^{(k)}) - \beta \bar{g}^{(k-1)} \right) d(\hat{q}^{(k+1)} - \hat{q}^{(k)}) \\ & \quad + \frac{S_F}{2} D_{\text{KL}}(\hat{q}^{(k+1)} \| \hat{q}^{(k)}) + \beta D_{\text{KL}}(\hat{q}^{(k+1)} \| \hat{q}^{(k)}) + L_{\text{TV}} \epsilon_{\text{TV}}. \quad (20) \end{aligned}$$

We have used the induced smoothness of F (Eq.(13)) in the first inequality, and used the Lipschitz continuity in the second inequality. By Lemma 5, we can bound $\int \left(\frac{\delta F}{\delta q}(q^{(k)}) - \beta \bar{g}^{(k-1)} \right) d(\hat{q}^{(k+1)} - \hat{q}^{(k)}) = \int \frac{\delta \tilde{L}}{\delta q}(\hat{q}^{(k)}) d(\hat{q}^{(k+1)} - \hat{q}^{(k)})$. Thus the RHS of Eq. (20) can be bounded as

$$\begin{aligned} \text{(RHS)} &\leq \frac{\beta'}{k} \left(D_{\text{KL}}(\hat{q}^{(k)} \| p_{\text{ref}}) - D_{\text{KL}}(\hat{q}^{(k+1)} \| p_{\text{ref}}) - k D_{\text{KL}}(\hat{q}^{(k+1)} \| \hat{q}^{(k)}) - (k+1) D_{\text{KL}}(\hat{q}^{(k)} \| \hat{q}^{(k+1)}) \right) \\ &\quad + \frac{2\beta + S_F}{2} D_{\text{KL}}(\hat{q}^{(k+1)} \| \hat{q}^{(k)}) + (L_{\text{TV}} + B_F) \epsilon_{\text{TV}} \\ &\leq \frac{\beta'}{k} \left(D_{\text{KL}}(\hat{q}^{(k)} \| p_{\text{ref}}) - D_{\text{KL}}(\hat{q}^{(k+1)} \| p_{\text{ref}}) - (k+1) D_{\text{KL}}(\hat{q}^{(k)} \| \hat{q}^{(k+1)}) \right) \\ &\quad + \frac{(2\beta + S_F - 2\beta')}{2} D_{\text{KL}}(\hat{q}^{(k+1)} \| \hat{q}^{(k)}) + (L_{\text{TV}} + B_F) \epsilon_{\text{TV}}, \end{aligned}$$

which gives the assertion in Option 2 by noting $\frac{\beta'}{k} D_{\text{KL}}(\hat{q}^{(k+1)} \| p_{\text{ref}}) \geq \frac{\beta'}{k+1} D_{\text{KL}}(\hat{q}^{(k+1)} \| p_{\text{ref}})$. As for Option 1, we repeat the same argument to show the desired result. \square

Combining Lemma 5 and Lemma 7, we will prove that

$$\frac{1}{K} \sum_{k=1}^K (\text{weight})_k D_{\text{KL}}(\hat{q}^{(k)} \| \hat{q}^{(k+1)}) = \mathcal{O}\left(\frac{1}{K}\right)$$

where $(\text{weight})_k \simeq k$ in Option 1 and $(\text{weight})_k \simeq 1$ in Option 2. When we take Option 2, it holds that $\min_k D_{\text{KL}}(\hat{q}^{(k)} \| \hat{q}^{(k+1)}) = \mathcal{O}(1/K)$. It is important that $D_{\text{KL}}(\hat{q}^{(k)} \| \hat{q}^{(k+1)})$ is also the approximate ‘‘moment generation function’’ $\psi_q(g) = \log(\mathbb{E}_q[\exp(-g + \mathbb{E}_q[g])])$ of $\frac{\delta \tilde{L}_k(\hat{q}^{(k)})}{\delta q}$; when $k \rightarrow \infty$,

$$\min_{k=1, \dots, K} \left(\text{‘‘Variance’’ of } \frac{\delta \tilde{L}_k}{\delta q} \right) (\hat{q}^{(k)}, x) \simeq \min_{k=1, \dots, K} D_{\text{KL}}(\hat{q}^{(k)} \| \hat{q}^{(k+1)}) = \mathcal{O}\left(\frac{1}{K}\right).$$

This can be interpreted as $\frac{\delta \tilde{L}_k}{\delta q}(\hat{q}^{(k)}, x) \rightarrow 0$ (up to constant w.r.t. x).

This result is consistent with the findings for standard, non-distributional Dual Averaging (Liu et al., 2023a), where $\min_{k=1, \dots, K} \|(\text{gradient of the objective})_k\|^2 = \mathcal{O}(1/K)$ as the variance corresponds to the second moment.

We rigorously formulate the above discussion as the following proposition.

Proposition 1. *Let*

$$\Psi_K := \frac{1}{K\beta'} (\tilde{L}_1(\hat{q}^{(1)}) - L^*) + \frac{(L_{\text{TV}} + B_F)}{K\beta'} \sum_{k=1}^K \epsilon_{\text{TV}}.$$

Then, Algorithm 1 satisfies

$$\frac{1}{K} \sum_{k=1}^K \frac{\beta k + 2\beta'}{2} D_{\text{KL}}(\hat{q}^{(k)} \| \hat{q}^{(k+1)}) \leq \Psi_K$$

and Algorithm 2 satisfies

$$\frac{1}{K} \sum_{k=1}^K D_{\text{KL}}(\hat{q}^{(k)} \| \hat{q}^{(k+1)}) \leq \Psi_K.$$

This also yields that the following bound holds for Algorithm 2:

$$\begin{aligned} \min_{1 \leq k \leq K} \psi_{\hat{q}^{(k)}} \left(\frac{k}{\beta'(k+1)} \frac{\delta \tilde{L}_k}{\delta q}(\hat{q}^{(k)}) \right) &\leq \mathbb{E}_{k \sim \text{Univ}([K])} \left[\psi_{\hat{q}^{(k)}} \left(\frac{k}{\beta'(k+1)} \frac{\delta \tilde{L}_k}{\delta q}(\hat{q}^{(k)}) \right) \right] \\ &\leq \Psi_K, \end{aligned}$$

where the expectation in the middle term is taken over a random index k uniformly chosen from $[K] = \{1, \dots, K\}$.

1350 *Proof.* Summing up (19) for $k = 1, \dots, K$, we have that

$$1351 \tilde{L}_{K+1}(\hat{q}^{(K+1)}) - \tilde{L}_1(\hat{q}^{(1)}) \leq (L_{\text{TV}} + B_F) \sum_{k=1}^K \epsilon_{\text{TV}} - \beta' \sum_{k=1}^K \frac{k+1}{k} D_{\text{KL}}(\hat{q}^{(k)} \parallel \hat{q}^{(k+1)}).$$

1352 This yields that

$$1353 \frac{\beta'}{K} \sum_{k=1}^K \frac{k+1}{k} D_{\text{KL}}(\hat{q}^{(k)} \parallel \hat{q}^{(k+1)}) + \frac{1}{K} (\tilde{L}_{K+1}(\hat{q}^{(K+1)}) - L^*)$$

$$1354 \leq \frac{1}{K} (\tilde{L}_1(\hat{q}^{(1)}) - L^*) + \frac{(L_{\text{TV}} + B_F)}{K} \sum_{k=1}^K \epsilon_{\text{TV}}. \quad (21)$$

1355 Please note that

$$1356 \frac{\beta'}{K} \sum_{k=1}^K D_{\text{KL}}(\hat{q}^{(k)} \parallel \hat{q}^{(k+1)}) \leq \frac{\beta'}{K} \sum_{k=1}^K \frac{k+1}{k} D_{\text{KL}}(\hat{q}^{(k)} \parallel \hat{q}^{(k+1)}) + \frac{1}{K} (\tilde{L}_{K+1}(\hat{q}^{(K+1)}) - L^*)$$

1357 by the optimality of L^* and that the RHS in (21) is $\mathcal{O}(1/K)$. Here, we see that

$$1358 D_{\text{KL}}(\hat{q}^{(k)} \parallel \hat{q}^{(k+1)})$$

$$1359 = \mathbb{E}_{\hat{q}^{(k)}} [-\bar{g}^{(k-1)} + \bar{g}^{(k)}] - \log(\mathbb{E}_{p_{\text{ref}}}[\exp(-\bar{g}^{(k-1)})]) + \log(\mathbb{E}_{p_{\text{ref}}}[\exp(-\bar{g}^{(k)})])$$

$$1360 = \mathbb{E}_{\hat{q}^{(k)}} [-\bar{g}^{(k-1)} + \bar{g}^{(k)}] + \log(\mathbb{E}_{\hat{q}^{(k)}}[\exp(-\bar{g}^{(k)} + \bar{g}^{(k-1)})])$$

$$1361 = \log \left\{ \mathbb{E}_{\hat{q}^{(k)}} \left[\exp \left(-\bar{g}^{(k)} + \bar{g}^{(k-1)} \right) - \mathbb{E}_{\hat{q}^{(k)}} \left[-\bar{g}^{(k)} + \bar{g}^{(k-1)} \right] \right] \right\},$$

1362 Now, the term $\bar{g}^{(k)} - \bar{g}^{(k-1)}$ can be evaluated as

$$1363 \bar{g}^{(k)} - \bar{g}^{(k-1)} = \frac{k}{\beta'(k+1)} \frac{\delta L}{\delta q}(\hat{q}^{(k)}) - \frac{1}{k+1} \bar{g}^{(k-1)} = \frac{k}{\beta'(k+1)} \frac{\delta \tilde{L}_k}{\delta q}(\hat{q}^{(k)}),$$

1364 which yields the assertion because

$$1365 D_{\text{KL}}(\hat{q}^{(k)} \parallel \hat{q}^{(k+1)})$$

$$1366 = \log \left\{ \mathbb{E}_{\hat{q}^{(k)}} \left[\exp \left(\frac{k}{\beta'(k+1)} \frac{\delta \tilde{L}_k}{\delta q}(\hat{q}^{(k)}) - \mathbb{E}_{\hat{q}^{(k)}} \left[\frac{k}{\beta'(k+1)} \frac{\delta \tilde{L}_k}{\delta q}(\hat{q}^{(k)}) \right] \right) \right] \right\},$$

1367 which is the ‘‘moment generating function’’ $\psi_{\hat{q}^{(k)}}$ of $\frac{k}{\beta'(k+1)} \frac{\delta \tilde{L}_k}{\delta q}(\hat{q}^{(k)})$. \square

1368 A.2.1 PROOF OF LEMMA 6

1369 *Proof.* The proof is almost identical to Lemma 5. In Algorithm 1, $\hat{q}^{(k+1)}$ is defined as the minimizer

1370 of the following quantity:

$$1371 r_{k+1}(q) := \sum_{j=1}^k j \left(\int \frac{\delta F}{\delta q}(q^{(j)}) d(q - \hat{q}^{(j)}) + \beta D_{\text{KL}}(q \parallel p_{\text{ref}}) \right) + \beta'(k+1) D_{\text{KL}}(q \parallel p_{\text{ref}}).$$

1372 Hence, we have

$$1373 r_{k+1}(q) = r_k(q) + \int k \frac{\delta F}{\delta q}(q^{(k)}) d(q - \hat{q}^{(k)}) + (\beta k + \beta') D_{\text{KL}}(q \parallel p_{\text{ref}}) \quad (22)$$

1374 by the definition of r_k . Moreover, Lemma 4 and the optimality of $\hat{q}^{(k)}$ gives that

$$1375 r_k(q) - r_k(\hat{q}^{(k)}) = \left(\frac{\beta k(k-1)}{2} + \beta' k \right) D_{\text{KL}}(q \parallel \hat{q}^{(k)}), \quad \text{for all } q \in \mathcal{P}. \quad (23)$$

Substituting $q \leftarrow \hat{q}^{(k+1)}$, we obtain

$$\begin{aligned}
0 &\leq r_k(\hat{q}^{(k+1)}) - r_k(\hat{q}^{(k)}) - \left(\frac{\beta k(k-1)}{2} + \beta' k \right) D_{\text{KL}}(\hat{q}^{(k+1)} \parallel \hat{q}^{(k)}) \\
&= r_{k+1}(\hat{q}^{(k+1)}) - \int k \frac{\delta F}{\delta q}(q^{(k)}) d(\hat{q}^{(k+1)} - \hat{q}^{(k)}) - (\beta k + \beta') D_{\text{KL}}(\hat{q}^{(k+1)} \parallel p_{\text{ref}}) \quad (\text{used (22)}) \\
&\quad - r_k(\hat{q}^{(k)}) - \left(\frac{\beta k(k-1)}{2} + \beta' k \right) D_{\text{KL}}(\hat{q}^{(k+1)} \parallel \hat{q}^{(k)}). \tag{24}
\end{aligned}$$

This is equivalent to

$$\begin{aligned}
&\int k \frac{\delta F}{\delta q}(q^{(k)}) d(\hat{q}^{(k+1)} - \hat{q}^{(k)}) \\
&\leq r_{k+1}(\hat{q}^{(k+1)}) - r_k(\hat{q}^{(k)}) - (\beta k + \beta') D_{\text{KL}}(\hat{q}^{(k+1)} \parallel p_{\text{ref}}) - \left(\frac{\beta k(k-1)}{2} + \beta' k \right) D_{\text{KL}}(\hat{q}^{(k+1)} \parallel \hat{q}^{(k)}).
\end{aligned}$$

By using the same argument as Eq. (23) for $k \leftarrow k+1$, we have

$$\begin{aligned}
&r_{k+1}(\hat{q}^{(k+1)}) + \left(\frac{\beta k(k+1)}{2} + \beta'(k+1) \right) D_{\text{KL}}(\hat{q}^{(k)} \parallel \hat{q}^{(k+1)}) \\
&= r_{k+1}(\hat{q}^{(k)}) \\
&= r_k(\hat{q}^{(k)}) + (\beta k + \beta') D_{\text{KL}}(\hat{q}^{(k)} \parallel p_{\text{ref}}).
\end{aligned}$$

Substituting this relation to Eq. (24) and noticing $|\frac{\delta F}{\delta q}| \leq B_F$, we obtain the assertion. \square

B DERIVATIONS OF FUNCTIONAL DERIVATIVES

B.1 DIRECT PREFERENCE OPTIMIZATION

We can apply the proposed algorithm to the (populational) objective of Direct Preference Optimization (DPO) (Rafailov et al., 2023). DPO is an effective approach for learning from human preference for not only language models but also diffusion models.

Original DPO objective Let x_w, x_l be “winning” and “losing” outputs independently sampled from the reference model p_{ref} . The event $\{x_w \succ x_l\}$ is determined by the human preference. The original DPO objective is formulated as

$$L_{\text{DPO,original}}(q) = -\mathbb{E}_{x_w, x_l} \left[\log \sigma \left(\gamma \log \frac{q(x_w)}{p_{\text{ref}}(x_w)} - \gamma \log \frac{q(x_l)}{p_{\text{ref}}(x_l)} \right) \right],$$

where $\gamma > 0$ is a hyperparameter. The expectation is taken by x_w, x_l , that are “winning” and “losing” samples from p_{ref} . Wallace et al. (2024) derived a new objective that is the upper bound of $L_{\text{DPO,original}}(q)$, but it is a specialized derivation of the optimization method for DPO.

Reformulating of the DPO Objective The goal is to directly minimize $L_{\text{DPO,original}}(q)$, however, in the above expression, we cannot apply DPO to diffusion models directly because the expectation with tuple (x_w, x_l) is not formulated well. We start with another expression of the objective of DPO:

$$L_{\text{DPO}}(q) := -\mathbb{E}_{x_w \sim p_{\text{ref}}} \mathbb{E}_{x_l \sim p_{\text{ref}}} \left[\log \sigma \left(\gamma \log \frac{q(x_w)}{p_{\text{ref}}(x_w)} - \gamma \log \frac{q(x_l)}{p_{\text{ref}}(x_l)} \right) \mathbb{1}_{x_w \succ x_l}(x_w, x_l) \right],$$

$\mathbb{1}_{x \succ y}(x, y)$ is 1 if $x \succ y$, 0 otherwise. This L_{DPO} is in the regime of our algorithm and the functional derivative can be derived:

Proposition 2. *The functional derivative of $L_{\text{DPO}}(q)$ is calculated as*

$$\begin{aligned}
&\frac{\delta L_{\text{DPO}}}{\delta q}(q, x) \\
&= -\gamma \mathbb{E}_{x_l \sim p_{\text{ref}}} \left[(1 - \sigma(-\gamma f(x) + \gamma f(x_l))) \frac{\int e^{-f} dp_{\text{ref}}}{e^{-f(x)}} \mathbb{1}_{x \succ x_l}(x, x_l) \right] \\
&\quad + \gamma \mathbb{E}_{x_w \sim p_{\text{ref}}} \left[(1 - \sigma(-\gamma f(x_w) + \gamma f(x))) \frac{\int e^{-f} dp_{\text{ref}}}{e^{-f(x)}} \mathbb{1}_{x_w \succ x}(x_w, x) \right],
\end{aligned}$$

where $q = e^{-f} p_{\text{ref}} / \int e^{-f} dp_{\text{ref}}$. This functional derivative is tractable in our settings.

1458 *Proof.* In this proof, we use the following notations:

- 1461 • p_{ref} : the output distribution of a pre-trained model,
- 1462
- 1463 • $q := e^{-f} p_{\text{ref}} / \int e^{-f} dp_{\text{ref}}$: the output distribution of an aligned model,
- 1464
- 1465 • $\text{LSL}(q_1, q_2) := \log \sigma(\gamma \log q_1 / p_{\text{ref}} - \gamma \log q_2 / p_{\text{ref}})$,
- 1466
- 1467 • $\partial_1 \text{LSL}(q_1, q_2) = \gamma(1 - \sigma(\gamma \log q_1 / p_{\text{ref}} - \gamma \log q_2 / p_{\text{ref}})) \frac{1}{q_1}$,
- 1468
- 1469 • $\partial_2 \text{LSL}(q_1, q_2) = -(1 - \sigma(\gamma \log q_1 / p_{\text{ref}} - \gamma \log q_2 / p_{\text{ref}})) \frac{1}{q_2}$,
- 1470
- 1471 • $\psi(r_1, r_2) := \gamma(\log r_1 - \log r_2)$,
- 1472
- 1473 • $\text{Inv}(f, x) = \frac{\int e^{-f} dp_{\text{ref}}}{e^{-f(x)}}$.
- 1474

1475 The objective of DPO is written as

$$1476 L_{\text{DPO}}(q) := -\mathbb{E}_{x_w \sim p_{\text{ref}}} \mathbb{E}_{x_l \sim p_{\text{ref}}} [\text{LSL}(q(x_w), qp(x_l)) \mathbb{1}_{x_w \succ x_l}(x_w, x_l)].$$

1477 We obtain the first variation of the objective as follows:

$$1478 \begin{aligned} 1479 & L_{\text{DPO}}(q + \epsilon(\tilde{q} - q)) \\ 1480 &= L_{\text{DPO}}(q) - \epsilon \mathbb{E}_{x_w \sim p_{\text{ref}}} \mathbb{E}_{x_l \sim p_{\text{ref}}} [(\partial_1 \text{LSL}(q(x_w), q(x_l))(\tilde{q} - q)(x_w) \\ 1481 &\quad + \partial_2 \text{LSL}(q(x_w), q(x_l))(\tilde{q} - q)(x_l)) \mathbb{1}_{x_w \succ x_l}(x_w, x_l)] + \mathcal{O}(\epsilon^2) \\ 1482 &= L_{\text{DPO}}(p) \\ 1483 &\quad - \epsilon \left[\mathbb{E}_{x_l \sim p_{\text{ref}}} \left[\int \gamma(1 - \sigma(\psi(\frac{q(x_w)}{p_{\text{ref}}(x_w)}, \frac{q(x_l)}{p_{\text{ref}}(x_l)}))) (\tilde{q} - q)(x_w) \text{Inv}(f, x_w) dx_w \mathbb{1}_{x_w \succ x_l} \right] \right. \\ 1484 &\quad \left. + \mathbb{E}_{x_w \sim p_{\text{ref}}} \left[\int \gamma(1 - \sigma(\psi(\frac{q(x_w)}{p_{\text{ref}}(x_w)}, \frac{q(x_l)}{p_{\text{ref}}(x_l)}))) (\tilde{q} - q)(x_l) \text{Inv}(f, x_l) dx_l \mathbb{1}_{x_w \succ x_l} \right] \right] \\ 1485 &\quad + \mathcal{O}(\epsilon^2). \end{aligned}$$

1486 Then, the first derivative of F is

$$1487 \begin{aligned} 1488 \frac{\delta L_{\text{DPO}}}{\delta p}(p, x) &= -\mathbb{E}_{x_l \sim p_{\text{ref}}} \left[\gamma \left(1 - \sigma \left(\psi \left(\frac{q(x)}{p_{\text{ref}}(x)}, \frac{q(x_l)}{p_{\text{ref}}(x_l)} \right) \right) \right) \mathbb{1}_{x \succ x_l}(x, x_l) \right] \text{Inv}(f, x) \\ 1489 &\quad + \mathbb{E}_{x_w \sim p_{\text{ref}}} \left[\gamma \left(1 - \sigma \left(\psi \left(\frac{q(x_w)}{p_{\text{ref}}(x_w)}, \frac{q(x)}{p_{\text{ref}}(x)} \right) \right) \right) \mathbb{1}_{x_w \succ x}(x_w, x) \right] \text{Inv}(f, x). \end{aligned}$$

1490 □

1501 B.2 KAHNEMAN-TVERSKY OPTIMIZATION

1502 Assume that the whole data space \mathbb{R}^d is split into a desirable domain \mathcal{D}_D and an undesirable domain \mathcal{D}_U . The objective of original KTO (Ethayarajh et al., 2024) is formulated as

$$1503 \begin{aligned} 1504 L_{\text{KTO}}(q) &= \mathbb{E}_{x \sim p_{\text{ref}}} \left[\gamma_D \left(1 - \sigma \left(\kappa \log \frac{q}{p_{\text{ref}}} - D_{\text{KL}}(q \| p_{\text{ref}}) \right) \right) \mathbb{1}_{\{x \in \mathcal{D}_D\}} \right. \\ 1505 &\quad \left. + \gamma_U \left(1 - \sigma \left(D_{\text{KL}}(q \| p_{\text{ref}}) - \kappa \log \frac{q}{p_{\text{ref}}} \right) \right) \mathbb{1}_{\{x \in \mathcal{D}_U\}} \right], \end{aligned}$$

1506 where γ_D , γ_U , κ are hyper parameters, and σ is a sigmoid function.

Proposition 3. *The functional derivative of L_{KTO} is calculated as*

$$\begin{aligned} & \frac{\delta L_{\text{KTO}}}{\delta q}(q, x) \\ &= -\kappa\gamma_D \sigma_{\text{deriv}}(\phi(x)) \frac{\int e^{-f} dp_{\text{ref}}}{e^{-f(x)}} \mathbb{1}_{\{x \in \mathcal{D}_D\}} \\ & \quad + (-f(x) - \log \int e^{-f(x)} dp_{\text{ref}}) \mathbb{E}_{y \sim p_{\text{ref}}} [\gamma_D \sigma_{\text{deriv}}(\phi(y)) \mathbb{1}_{\{y \in \mathcal{D}_D\}}] \\ & \quad + \kappa\gamma_U \sigma_{\text{deriv}}(-\phi(x)) \frac{\int e^{-f} dp_{\text{ref}}}{e^{-f(x)}} \mathbb{1}_{\{x \in \mathcal{D}_U\}} \\ & \quad - (-f(x) - \log \int e^{-f(x)} dp_{\text{ref}}) \mathbb{E}_{y \sim p_{\text{ref}}} [\gamma_U \sigma_{\text{deriv}}(-\phi(y)) \mathbb{1}_{\{y \in \mathcal{D}_U\}}] \end{aligned}$$

where $\sigma_{\text{deriv}}(\cdot) := \sigma(\cdot)(1 - \sigma(\cdot))$, $\phi(x) := \kappa \log \frac{q(x)}{p_{\text{ref}}(x)} - D_{\text{KL}}(q \| p_{\text{ref}})$, $q = \frac{e^{-f} p_{\text{ref}}}{\int e^{-f} dp_{\text{ref}}}$.

The functional derivative of KTO can be calculated if you have $f(x)$ and the samples from p_{ref} . Note that $\log q(x)/p_{\text{ref}}(x) = -f(x) - \log \int e^{-f(x)} dp_{\text{ref}}$.

Proof. The first variation of L_{KTO} is

$$\begin{aligned} & L_{\text{KTO}}(q + \epsilon(\tilde{q} - q)) - L_{\text{KTO}}(q) \\ & \simeq \epsilon \mathbb{E}_{x \sim p_{\text{ref}}} \left[-\kappa\gamma_D \sigma_{\text{deriv}}(\phi(x)) \left(\frac{\tilde{q}(x) - q(x)}{q(x)} + \int \log \frac{q(y)}{p_{\text{ref}}(y)} d(\tilde{q} - q)(y) \right) \mathbb{1}_{\{x \in \mathcal{D}_D\}} \right] \\ & \quad + \epsilon \mathbb{E}_{x \sim p_{\text{ref}}} \left[\kappa\gamma_U \sigma_{\text{deriv}}(-\phi(x)) \left(\frac{\tilde{q}(x) - q(x)}{q(x)} - \int \log \frac{q(y)}{p_{\text{ref}}(y)} d(\tilde{q} - q)(y) \right) \mathbb{1}_{\{x \in \mathcal{D}_U\}} \right] \\ & = \epsilon \int \left\{ -\kappa\gamma_D \sigma_{\text{deriv}}(\phi(x)) \text{Inv}(f, x) \mathbb{1}_{\{x \in \mathcal{D}_D\}} \right. \\ & \quad \left. + \log \frac{q(x)}{p_{\text{ref}}(x)} \mathbb{E} [\kappa\gamma_D \sigma_{\text{deriv}}(\phi(y)) \mathbb{1}_{\{y \in \mathcal{D}_D\}}] \right\} d(\tilde{q} - q)(y) \\ & \quad + \epsilon \int \left\{ \kappa\gamma_U \sigma_{\text{deriv}}(-\phi(x)) \text{Inv}(f, x) \mathbb{1}_{\{x \in \mathcal{D}_U\}} \right. \\ & \quad \left. - \log \frac{q(x)}{p_{\text{ref}}(x)} \mathbb{E} [\kappa\gamma_U \sigma_{\text{deriv}}(-\phi(y)) \mathbb{1}_{\{y \in \mathcal{D}_U\}}] \right\} d(\tilde{q} - q)(y), \end{aligned}$$

where $\text{Inv}(f, x) = \frac{\int e^{-f} dp_{\text{ref}}}{e^{-f(x)}}$. Now the desired result immediately follows. \square

C ERROR ANALYSIS OF DIFFUSION MODEL

C.1 OVERVIEW

Here, we analyze the sampling error caused by the diffusion model. Let us organize the settings and notations used in this section.

Target distribution. The target distribution is $q_* = q_0$, which is decomposed as $q_*(x) = \rho_*(x)p_*(x)$ with $p_* = p_0$ and ρ_* . Here p_* and ρ_* represent the distribution of the original model and the density ratio obtained by fine-tuning, respectively.

Sampling with score-based diffusion model. In the score-based diffusion model, we start with the forward process, which is written as a stochastic differential equation (SDE). Choosing the Ornstein-Uhlenbeck (OU) process, $\{\bar{X}_t\}_{t \geq 0}$ follows the following SDE:

$$\bar{X}_0 \sim p_*, \quad d\bar{X}_t = -\bar{X}_t dt + \sqrt{2} dB_t, \quad (25)$$

where $\{B_t\}_{t \geq 0}$ is the standard Brownian motion. At each time t , the law of X_t is written as

$$p_t(x) = \int p_*(y) \exp\left(-\frac{1}{2\sigma_t^2} \|m_t y - x\|^2\right) dx,$$

where $m_t = e^{-t}$ and $\sigma_t^2 = 1 - e^{-2t}$. In the same way, define $\{\bar{Y}_t\}_{t \geq 0}$ by replacing p_* by q_* in (25) and let q_t be the law of \bar{Y}_t .

Then, for some $T \geq 0$, we can define the reverse process for $\{\bar{X}_t^{\leftarrow}\}_{0 \leq t \leq T}$. (Let B_t below be distinct from the one in (25).)

$$\bar{X}_0^{\leftarrow} \sim p_T, \quad d\bar{X}_t^{\leftarrow} = \{\bar{X}_t^{\leftarrow} + 2\nabla \log p_{T-t}(\bar{X}_t^{\leftarrow})\}dt + \sqrt{2}dB_t. \quad (26)$$

Then, the law of \bar{X}_t^{\leftarrow} equals p_{T-t} , which is why we call (26) as the reverse process. In the same way, we define $\{\bar{Y}_t^{\leftarrow}\}_{0 \leq t \leq T}$ as the reverse process of $\{\bar{Y}_t\}_{t \geq 0}$.

Doob's h-transform. By applying Doob's h-transform to $\nabla \log q_{T-t}$, it can be decomposed into the original score $\nabla \log p_{T-t}$ and a correction term.

$$\nabla \log q_{T-t}(\bar{Y}_t^{\leftarrow}) = \nabla \log p_{T-t}(\bar{Y}_t^{\leftarrow}) + \nabla_x \log(\mathbb{E}[\rho_*(\bar{X}_0) | \bar{X}_{T-t} = x])|_{x=\bar{Y}_t^{\leftarrow}}. \quad (27)$$

See Lemma 12 for derivation.

Approximation of the score and correction term. Because we do not have access to the exact value of p_t and ρ_* and therefore cannot implement (27) exactly, we consider approximating them by, e.g., neural networks. We approximate $\nabla \log p_{T-t}(x)$ by $s(x, t): \mathbb{R}^{d+1} \rightarrow \mathbb{R}^d$. Also, we approximate $u_*(x, t) = \nabla_x \log(\mathbb{E}[\rho_*(\bar{X}_0) | \bar{X}_{T-t} = x])$ by $u(x, t): \mathbb{R}^{d+1} \rightarrow \mathbb{R}^d$.

Discretization. Also, we need to discretize the stochastic differential equation. We finally obtain the approximation of (26), denoted by $\{Y_t^{\leftarrow}\}_{0 \leq t \leq T}$, as

$$Y_0^{\leftarrow} \sim \mathcal{N}(0, I_d), \quad dY_t^{\leftarrow} = \{Y_t^{\leftarrow} + 2s(Y_{kh}^{\leftarrow}, kh) + 2u(Y_{kh}^{\leftarrow}, kh)\}dt + \sqrt{2}dB_t, \quad t \in [kh, (k+1)h].$$

Obtaining the correction term (approximately). Given the score network $s(x, t)$ approximating $\nabla \log p_t(x)$ and the function \bar{h} that approximates h_* , we can approximate the correction term $u(x, t)$. Remind that, for fixed $x \in \mathbb{R}^d$, $t = kh$, $s = k(h+1) \in \mathbb{R}$, the correction term is calculated as

$$\nabla_x \log(\mathbb{E}[\rho_*(\bar{X}_0) | \bar{X}_{T-t} = x]) = \frac{\int \mathbb{E}[\rho_*(\bar{X}_0) | \bar{X}_{T-s} = x'] \frac{\partial}{\partial x} \mathbb{P}[\bar{X}_{T-s} = x' | \bar{X}_{T-t} = x] dx'}{\mathbb{E}[\rho_*(\bar{X}_0) | \bar{X}_{T-t} = x]}. \quad (28)$$

One way to approximate (28) starts from approximating $\mathbb{E}[\rho_*(\bar{X}_0) | \bar{X}_{T-t} = x]$. If we run the reverse diffusion process

$$\tilde{X}_t^{\leftarrow} = x, \quad d\tilde{X}_\tau^{\leftarrow} = \{\tilde{X}_\tau^{\leftarrow} + 2\nabla \log p_{T-\tau}(\tilde{X}_\tau^{\leftarrow})\}d\tau + \sqrt{2}dB_\tau,$$

we obtain that the law of \tilde{X}_T^{\leftarrow} is equal to that of $\bar{X}_0 | \bar{X}_{T-t} = x$. Therefore, by running the approximated reverse process (with a slight abuse of notation)

$$\tilde{X}_t = x, \quad d\tilde{X}_\tau = \{\tilde{X}_\tau + 2s(\tilde{X}_{lh}, lh)\}dt + \sqrt{2}dB_\tau, \quad \tau \in [lh, (l+1)h],$$

multiple times, the sample of \tilde{X}_T , denoted by $\{\tilde{x}_{T,i}\}_{i=1}^n$, can approximate $\mathbb{E}[\rho_*(\bar{X}_0) | \bar{X}_{T-t} = x]$ as

$$\mathbb{E}[\rho_*(\bar{X}_0) | \bar{X}_{T-t} = x] \approx \frac{1}{n} \sum_{i=1}^n \rho'(\tilde{x}_{T,i}), \quad (29)$$

where ρ' is the approximation of ρ_* .

On the other hand, we approximate $\frac{\partial}{\partial x} \mathbb{P}[\bar{X}_{T-s} = x' | \bar{X}_{T-t} = x]$ by approximating $\mathbb{P}[\bar{X}_{T-s} = x' | \bar{X}_{T-t} = x]$ with a Gaussian distribution. Specifically, because $\bar{X}_{T-s} = x' | \bar{X}_{T-t} = x$ is obtained by the following reverse diffusion process

$$\tilde{X}_t^{\leftarrow} = x, \quad d\tilde{X}_\tau^{\leftarrow} = \{\tilde{X}_\tau^{\leftarrow} + 2\nabla \log p_{T-\tau}(\tilde{X}_\tau^{\leftarrow})\}d\tau + \sqrt{2}dB_\tau,$$

we approximate $\nabla \log p_{T-\tau}(\tilde{X}_\tau^{\leftarrow})$ by $s(x_{kh}, kh)$ to obtain

$$\dot{X}_t^{\leftarrow} = x_{kh}, \quad d\dot{X}_\tau^{\leftarrow} = \{\dot{X}_\tau^{\leftarrow} + 2s(x_{kh}, kh)\}d\tau + \sqrt{2}dB_\tau.$$

The distribution of \tilde{X}_s^{\leftarrow} is denoted by

$$\mathcal{N}(e^h x_{kh} + 2(e^h - 1)s(x_{kh}, kh), e^{2h} - 1). \quad (30)$$

Using this, our approximation is

$$\begin{aligned} & \frac{\partial}{\partial x} \mathbb{P}[\bar{X}_{T-s} = x' | \bar{X}_{T-t} = x] \\ & \approx \frac{\partial}{\partial x} \frac{1}{(2\pi(e^{2h} - 1))^{\frac{d}{2}}} \exp\left(-\frac{(x' - (e^h x + 2(e^h - 1)s(x_{kh}, kh)))^2}{2(e^{2h} - 1)}\right) \\ & = \frac{e^h(x' - (e^h x + 2(e^h - 1)s(x_{kh}, kh)))}{(e^{2h} - 1)(2\pi(e^{2h} - 1))^{\frac{d}{2}}} \exp\left(-\frac{(x' - (e^h x + 2(e^h - 1)s(x_{kh}, kh)))^2}{2(e^{2h} - 1)}\right). \end{aligned}$$

This implies that, if we sample $\{x'_j\}_{j=1}^m$ from (30),

$$\begin{aligned} & \int \mathbb{E}[\rho_*(\bar{X}_0) | \bar{X}_{T-s} = x'] \frac{\partial}{\partial x} \mathbb{P}[\bar{X}_{T-s} = x' | \bar{X}_{T-t} = x] dx' \\ & \approx \frac{e^h}{(e^{2h} - 1)} \frac{1}{m} \sum_{j=1}^m \mathbb{E}[\rho_*(\bar{X}_0) | \bar{X}_{T-s} = x'_j] (x'_j - (e^h x + 2(e^h - 1)s(x_t, t))), \end{aligned}$$

and approximate each $\mathbb{E}[\rho_*(\bar{X}_0) | \bar{X}_{T-s} = x'_j]$ in the same way as (29), we can approximate the correction term (28).

Now, our goal is to bound the error of the whole pipeline under the following assumptions of p_* and ρ_* and the score approximation error.

Assumption 5 (Assumption 3, restated). 1. $\nabla \log p_t$ is L_p -smooth at every time t and it has finite second moment $\mathbb{E}[\|\bar{X}_t\|_2^2] \leq m < \infty$ for all $t \in \mathbb{R}_+$ and $x \in \mathbb{R}^d$.

2. $\nabla \log \rho_*$ is L_ρ -smooth and bounded as $C_\rho^{-1} \leq \rho_* \leq C_\rho$ for a constant C_ρ .

3. The score estimation error is bounded by $\mathbb{E}_{\bar{X}_t^{\leftarrow}}[\|s(\bar{X}_t^{\leftarrow}, t) - \nabla \log p_{T-t}(\bar{X}_{T-t}^{\leftarrow})\|^2] \leq \varepsilon$ at each time t .

4. $\mathbb{E}_{p_t}[\|u_*(x, lh) - u(x, lh)\|^2] \leq \varepsilon_{\rho, l}^2$ for any $1 \leq l \leq T/h$.

Theorem 5 (Theorem 3, restated). Suppose that Assumption 5 is satisfied. Then, we have the following bound on the distribution \hat{q} of Y_T^{\leftarrow} :

$$\text{TV}(q_*, \hat{q})^2 \lesssim T\varepsilon^2 + \sum_{l=1}^{T/h} h\varepsilon_{\rho, l}^2 + T(L_p C_\rho^2 + L_\rho)^2(dh + m^2 h^2) + \exp(-2T) D_{\text{KL}}(\hat{q}_{\text{opt}} \| N(0, I)).$$

Proof. Suppose that $\|s(\cdot, t) + u(\cdot, t) - \nabla \log q_{T-t}\|_{L^\infty} \leq \varepsilon'$ and $\nabla \log q_{T-t}$ is L_q -smooth at every time t . According to Chen et al. (2023c) and Pinsker's inequality, the distribution \hat{q} of Y_T satisfies

$$\text{KL}(\hat{q} \| q_*)^2 \lesssim T\varepsilon^2 + \sum_{l=1}^{T/h} h\varepsilon_{\rho, l}^2 + TL_p^2(dh + m^2 h^2) + \exp(-2T) D_{\text{KL}}(\hat{q}_{\text{opt}} \| N(0, I)).$$

According to Lemma 8, L_q is bounded by

$$L_q \lesssim L_p C_\rho^2 + L_\rho,$$

which yields the assertion. \square

In the bound, we assumed that the term $\varepsilon_{\rho, l}^2$ can be bounded, however this approximation error can be derived as in the following theorem with additional technical conditions.

Assumption 6 (Assumption 4 restated). (i) $\nabla_x s(\cdot, \cdot)$ is H_s -Lipschitz continuous in a sense that $\|\nabla_x s(x, t) - \nabla_y s(y, t)\|_{\text{op}} \leq H_s \|x - y\|$ for any $x, y \in \mathbb{R}^d$ and $0 \leq t \leq T$ and $\mathbb{E}[\|s(\bar{X}_{kh}^{\leftarrow}, kh)\|^2] \leq Q^2$ for any k , (ii) There exists $R > 0$ such that $\sup_{t, x} \{\|\nabla_x^2 \log p_t(x)\|_{\text{op}}, \|\nabla_x^2 \log s(x, t)\|_{\text{op}}\} \leq R$.

Theorem 6 (Theorem 4 restated). Suppose that Assumptions 3 and 4 hold. Assume that $\|\rho_* - \rho\|_\infty \leq \varepsilon'$, $\|\rho\|_\infty \leq C_\rho$, and $\sup_x \|\nabla \rho_*(x)\| \leq R_\rho$, $\|\nabla \rho_*(x) - \nabla \rho_*(y)\| \leq L_\rho \|x - y\|$ ($\forall x, y$). Then, for any choice of $0 \leq h \leq \delta \leq 1/(1 + 2R)$, we have that

$$\begin{aligned} \varepsilon_{\rho, l}^2 & \lesssim C_\rho^3 \{\Xi_{\delta, \varepsilon} + R_\varphi^2 (\varepsilon^2 + L_p^2 d(\delta + m\delta^2))\} + [L_\varphi^2 (m + Q^2 + dh) + R_\varphi^2 (1 + 2R)^2] h^2 \\ & + \min\{T - lh, 1/(2 + 2R)\}^{-1} \varepsilon'^2, \end{aligned}$$

where $\Xi_{\delta, \varepsilon} := C_\rho^2 (1 + 2R)^2 \delta + C_\rho^{\frac{1+\delta R_\varphi^2}{\delta}} [\varepsilon^2 + L_p^2 d(h + mh^2)]$, and R_φ and L_φ are constants introduced in Lemma 10.

1674 C.2 BOUNDING THE SMOOTHNESS

1675
1676 The proof of Theorem 3 (i.e., Theorem 5) utilizes the smoothness of the density q_t corresponding to
1677 the aligned model. The following lemma gives its bound.

1678 **Lemma 8.** *Suppose that $\nabla \log p_t$ is L_p -Lipschitz for all t and $\nabla \log \rho_*$ is L_ρ -Lipschitz, and $C_\rho^{-1} \leq$
1679 $\rho_* \leq C_\rho$. Then, $\nabla \log q_t$ is L_q -Lipschitz for all t , where L_q is bounded by*

$$1680 L_q \leq \min \left\{ \frac{4(L_p + L_\rho)^2}{2(L_p + L_\rho) - 1}, (4 + C_\rho^2)L_p + 4L_\rho \right\} \lesssim L_p C_\rho^2 + L_\rho.$$

1683 *Proof.* We divide the proof into two parts, with $\sigma_t^2 = \frac{1}{2(L_p + L_\rho)}$ as the boundary.
1684

1685 First consider the case when $\sigma_t^2 \leq \frac{1}{2(L_p + L_\rho)}$. Remind that
1686

$$1687 q_t(x) = \int q_*(y) \frac{1}{(2\pi\sigma_t^2)^{\frac{d}{2}}} \exp\left(-\frac{1}{2\sigma_t^2} \|m_t y - x\|^2\right) dy,$$

1689 with $\sigma_t^2 = 1 - e^{-2t}$ and $m_t = e^{-t}$. From this, $\nabla_x q_t(x)$ and $\nabla_x^2 q_t(x)$ are computed as
1690

$$1691 \nabla_x q_t(x) = \nabla_x \int q_*(y) \frac{1}{(2\pi\sigma_t^2)^{\frac{d}{2}}} \exp\left(-\frac{1}{2\sigma_t^2} \|m_t y - x\|^2\right) dy$$

$$1692 = m_t^{-1} \int (\nabla_y q_*(y)) \frac{1}{(2\pi\sigma_t^2)^{\frac{d}{2}}} \exp\left(-\frac{1}{2\sigma_t^2} \|m_t y - x\|^2\right) dy$$

1695 and

$$1696 \nabla_x^2 q_t(x) = m_t^{-2} \int (\nabla_y^2 q_*(y)) \frac{1}{(2\pi\sigma_t^2)^{\frac{d}{2}}} \exp\left(-\frac{1}{2\sigma_t^2} \|m_t y - x\|^2\right) dy.$$

1699 Thus, we can compute $\nabla_x^2 \log q_t(x)$ as

$$1700 \nabla_x^2 \log q_t(x)$$

$$1701 = \frac{\nabla_x^2 q_t(x)}{q_t(x)} - \frac{\nabla_x q_t(x) (\nabla_x q_t(x))^\top}{(q_t(x))^2}$$

$$1702 = \frac{m_t^{-2} \int \left(\frac{\nabla_y^2 q_*(y)}{q_*(y)} - \frac{\nabla_y q_*(y) \nabla_y q_*(y)^\top}{q_*(y)^2} \right) q_*(y) \exp\left(-\frac{1}{2\sigma_t^2} \|m_t y - x\|^2\right) dy}{\int q_*(y) \exp\left(-\frac{1}{2\sigma_t^2} \|m_t y - x\|^2\right) dy} \quad (31)$$

$$1707 + \frac{m_t^{-2} \int \frac{\nabla_y q_*(y) \nabla_y q_*(y)^\top}{q_*(y)^2} q_*(y) \exp\left(-\frac{1}{2\sigma_t^2} \|m_t y - x\|^2\right) dy}{\int q_*(y) \exp\left(-\frac{1}{2\sigma_t^2} \|m_t y - x\|^2\right) dy} \quad (32)$$

$$1710 - \frac{m_t^{-2} \int \frac{\nabla_y q_*(y)}{q_*(y)} q_*(y) \exp\left(-\frac{1}{2\sigma_t^2} \|m_t y - x\|^2\right) dy \int \frac{\nabla_y q_*(y)}{q_*(y)} q_*(y) \exp\left(-\frac{1}{2\sigma_t^2} \|m_t y - x\|^2\right) dy}{\left(\int q_*(y) \exp\left(-\frac{1}{2\sigma_t^2} \|m_t y - x\|^2\right) dy\right)^2} \quad (33)$$

1715 Eq. (31) is an expectation of $\nabla_y^2 \log q_*(y) = \frac{\nabla_y^2 q_*(y)}{q_*(y)} - \frac{\nabla_y q_*(y) \nabla_y q_*(y)^\top}{q_*(y)^2}$ with respect to a distribution
1716

$$1717 A(y|x) \propto q_*(y) \exp\left(-\frac{1}{2\sigma_t^2} \|m_t y - x\|^2\right).$$

1718 Therefore, (31) is bounded by $m_t^{-2}(L_p + L_\rho)$ from the assumption. On the other hand, the other two
1720 terms are regarded as the covariance of $\nabla \log q_*(y)$ with respect to that distribution. Because $\sigma_t^2 \leq$
1721 $\frac{1}{2(L_p + L_\rho)}$, $A(y|x)$ is $(L_p + L_\rho)$ -strongly concave, and therefore satisfies the Poincaré inequality with
1722 a constant $\frac{1}{L_p + L_\rho}$. Therefore, for any $a \in \mathbb{R}^d$, we have

$$1723 a^\top ((32) + (33)) a$$

$$1724 = m_t^{-2} a^\top (\mathbb{E}_{A(y|x)} [(\nabla \log q_*(y)) (\nabla \log q_*(y))^\top] - \mathbb{E}_{A(y|x)} [\nabla \log q_*(y)] \mathbb{E}_{A(y|x)} [\nabla \log q_*(y)]^\top) a$$

$$1725 \leq \frac{m_t^{-2}}{L_p + L_\rho} \cdot \mathbb{E}[\|a \nabla^2 \log q_*(y)\|^2] \leq \frac{m_t^{-2}}{L_p + L_\rho} (L_p + L_\rho)^2 = m_t^{-2} L_p + L_\rho.$$

This implies that (32)+(33) is $m_t^{-2}(L_p + L_\rho)$ -smooth and $\nabla_x^2 \log q_t(x)$ is $2m_t^{-2}(L_p + L_\rho)$ -smooth. Because $m_t = \sqrt{1 - \sigma_t^2}$, we have $m_t \geq \sqrt{1 - \frac{1}{2(L_p + L_\rho)}}$. By applying this, we have $2m_t^{-2}(L_p + L_\rho) \leq \frac{4(L_p + L_\rho)^2}{2(L_p + L_\rho) - 1}$.

Next, let us consider the case when $\sigma_t^2 \geq \frac{2}{(L_p + L_\rho)}$. Note that $\nabla_x q_t(x)$ and $\nabla_x^2 q_t(x)$ are also written as

$$\nabla_x q_t(x) = - \int q_*(y) \frac{1}{(2\pi\sigma_t^2)^{\frac{d}{2}}} \exp\left(-\frac{1}{2\sigma_t^2} \|m_t y - x\|^2\right) \frac{x - m_t y}{\sigma_t^2} dy$$

and

$$\begin{aligned} \nabla_x^2 q_t(x) &= - \int q_*(y) \frac{1}{(2\pi\sigma_t^2)^{\frac{d}{2}}} \exp\left(-\frac{1}{2\sigma_t^2} \|m_t y - x\|^2\right) \frac{I}{\sigma_t^2} dy \\ &\quad + \int q_*(y) \frac{1}{(2\pi\sigma_t^2)^{\frac{d}{2}}} \exp\left(-\frac{1}{2\sigma_t^2} \|m_t y - x\|^2\right) \frac{(x - m_t y)(x - m_t y)^\top}{\sigma_t^4} dy. \end{aligned}$$

Thus, we can compute $\nabla_x^2 \log q_t(x)$ as

$$\begin{aligned} \nabla_x^2 \log q_t(x) &= \frac{\nabla_x^2 q_t(x)}{q_t(x)} - \frac{\nabla_x q_t(x)(\nabla_x q_t(x))^\top}{(q_t(x))^2} \\ &= - \frac{\int q_*(y) \exp\left(-\frac{1}{2\sigma_t^2} \|m_t y - x\|^2\right) \frac{I}{\sigma_t^2} dy}{\int q_*(y) \exp\left(-\frac{1}{2\sigma_t^2} \|m_t y - x\|^2\right) dy} \end{aligned} \quad (34)$$

$$+ \frac{\int q_*(y) \exp\left(-\frac{1}{2\sigma_t^2} \|m_t y - x\|^2\right) \frac{(x - m_t y)(x - m_t y)^\top}{\sigma_t^4} dy}{\int q_*(y) \exp\left(-\frac{1}{2\sigma_t^2} \|m_t y - x\|^2\right) dy} \quad (35)$$

$$- \frac{\left(\int q_*(y) \exp\left(-\frac{1}{2\sigma_t^2} \|m_t y - x\|^2\right) \frac{(x - m_t y)}{\sigma_t^2} dy\right) \left(\int q_*(y) \exp\left(-\frac{1}{2\sigma_t^2} \|m_t y - x\|^2\right) \frac{(x - m_t y)}{\sigma_t^2} dy\right)^\top}{\left(\int q_*(y) \exp\left(-\frac{1}{2\sigma_t^2} \|m_t y - x\|^2\right) dy\right)^2}. \quad (36)$$

Eq. (34) is bounded by $\sigma_t^{-2} \leq 2(L_p + L_\rho)$. On the other hand, (35)+(36) are transformed into

(35)+(36)

$$\begin{aligned} &= \frac{m_t^2 \int q_*(y) \exp\left(-\frac{1}{2\sigma_t^2} \|m_t y - x\|^2\right) y y^\top dy}{\sigma_t^4 \int q_*(y) \exp\left(-\frac{1}{2\sigma_t^2} \|m_t y - x\|^2\right) dy} \\ &\quad - \frac{m_t^2 \left(\int q_*(y) \exp\left(-\frac{1}{2\sigma_t^2} \|m_t y - x\|^2\right) y dy\right) \left(\int q_*(y) \exp\left(-\frac{1}{2\sigma_t^2} \|m_t y - x\|^2\right) y dy\right)^\top}{\sigma_t^4 \left(\int q_*(y) \exp\left(-\frac{1}{2\sigma_t^2} \|m_t y - x\|^2\right) dy\right)^2} \\ &= \frac{m_t^2}{\sigma_t^4} \text{Var}_{q_{0|t}(y|x)}(y), \end{aligned}$$

where $\text{Var}_{q_{0|t}(y|x)}(y)$ means the variance of X_0 conditioned on $X_t = x$, with respect to q_t .

Thus, bounding $\text{Var}_{q_{0|t}(y|x)}(x)$ yields the conclusion. Lemma 9 implies that

$$\text{Var}_{q_{0|t}(y|x)}(y) \leq C_\rho^2 \text{Var}_{p_{0|t}(y|x)}(y). \quad (37)$$

Similarly to $\nabla_x^2 \log q_t(x)$, $\nabla_x^2 \log p_t(x)$ satisfies

$$\nabla_x^2 \log p_t(x) = -\sigma_t^{-2} I_d + \frac{m_t^2}{\sigma_t^4} \text{Var}_{p_{0|t}(y|x)}(y). \quad (38)$$

By combining (37) and (38), we have

$$\frac{m_t^2}{\sigma_t^4} \text{Var}_{q_{0|t}(y|x)}(y) \leq C_\rho^2 \sigma_t^{-2} I_d + C_\rho^2 \nabla_x^2 \log p_t(x).$$

Therefore, from the assumption that $\nabla_x \log p_t(x)$ is L_p -Lipschitz and $\sigma_t^{-2} \geq 2(L_p + L_\rho)$, we obtain that $\|\frac{m_t^2}{\sigma_t^4} \text{Var}_{q_{0|t}(y|x)}(y)\| \leq (2 + C_\rho^2)L_p + 2L_\rho$.

By putting it all together, $\nabla \log q_t$ is $((4 + C_\rho^2)L_p + 4L_\rho)$ -Lipschitz. \square

Lemma 9. When $C_\rho^{-1} \leq h_*(x) \leq C_\rho$, we have

$$\frac{q_{0|t}(x|x')}{p_{0|t}(x|x')} \leq C_\rho^2$$

for all x, x' and t .

Proof. We can write $q_{0|t}(x|x')$ as

$$q_{0|t}(x|x') = \frac{q_{0,t}(x, x')}{\int q_0(x'')q_{t|0}(x|x'')dx''} = \frac{p_*(x)\rho_*(x)q_{t|0}(x'|x)}{\int p_*(x'')\rho_*(x'')q_{t|0}(x|x'')dx''}.$$

Because $C_\rho^{-1} \leq \rho_*(x) \leq C_\rho$ and $q_{t|0}(x'|x) = p_{t|0}(x'|x)$, we have

$$q_{0|t}(x|x') \leq C_\rho^2 \frac{p_*(x)p_{t|0}(x'|x)}{\int p_*(x'')p_{t|0}(x|x'')dx''} = C_\rho^2 p_{0|t}(x|x'),$$

which concludes the proof. \square

C.3 ESTIMATION ERROR OF THE CORRECTION TERM

Since we have shown the time discretization error in the previous section, what we remain to show is just an upper bound of $\varepsilon_{\rho,l}^2$. For that purpose, we put an additional assumption which is almost same as Assumption 4 except the condition (iii). A bound of $\varepsilon_{\text{TV}}^2$ in the third condition (iii) will be given as $\varepsilon_{\text{TV}}^2 = \mathcal{O}(\varepsilon^2 + h)$ by Chen et al. (2023c).

Assumption 7. (i) $\nabla_x s(\cdot, \cdot)$ is H_s -Lipschitz continuous in a sense that $\|\nabla_x s(x, t) - \nabla_y s(y, t)\|_{\text{op}} \leq H_s \|x - y\|$ for any $x, y \in \mathbb{R}^d$ and $0 \leq t \leq T$ and $\mathbb{E}[\|s(\bar{X}_{kh}^{\leftarrow}, kh)\|^2] \leq Q^2$ for any k .

(ii) There exists $R > 0$ such that $\sup_{t,x} \{\|\nabla_x^2 \log p_t(x)\|_{\text{op}}, \|\nabla_x^2 \log s(x, t)\|_{\text{op}}\} \leq R$.

(iii) $\mathbb{E}_{\bar{X}_t}[\text{TV}(\bar{X}_T^{\leftarrow}, X_T^{\leftarrow} | \bar{X}_{T-t}^{\leftarrow} = X_{T-t}^{\leftarrow} = \bar{X}_t)] \leq \varepsilon_{\text{TV}}^2$ for any $t \in [0, T]$.

Theorem 7. Suppose that $0 \leq h \leq \delta \leq 1/(1 + 2R)$ and Assumptions 7 and 5 hold. Let L_φ and R_φ be as given in Lemma 10. Then, it holds that

$$\begin{aligned} & \mathbb{E}_{\bar{X}_t^{\leftarrow}} [\|\nabla_x \mathbb{E}[\rho_*(\bar{X}_T^{\leftarrow}) | \bar{X}_t] - \nabla_x \mathbb{E}[\rho_*(X_T^{\leftarrow}) | X_{kh}^{\leftarrow}]\|^2] \\ & \lesssim R_\varphi^2 (\varepsilon^2 + L_p^2 d(\delta + m\delta^2)) + \Xi_{\delta,\varepsilon} + [L_\varphi^2 (m + 4Q^2 + dh) + R_\varphi^2 (1 + 2R)^2] h^2 \\ & = \mathcal{O}\left(\varepsilon^2 + \delta + \frac{\varepsilon_{\text{TV}}^2}{\delta}\right), \end{aligned}$$

where

$$\Xi_{\delta,\varepsilon} := \frac{4c_\eta^2 C_\rho^2 (1 + 2R)^2}{3} \delta + 2 \exp(2) \left\{ C_\rho^2 \frac{\varepsilon_{\text{TV}}^2}{\delta} + C R_\varphi^2 [\varepsilon^2 + L_p^2 d(\delta + m\delta^2)] \right\},$$

and $c_\eta > 0$ is a universal constant.

By Chen et al. (2023c), $\varepsilon_{\text{TV}}^2 = \mathcal{O}(\varepsilon^2 + h)$, and thus by substituting $\delta \leftarrow \sqrt{h}$, we finally obtain an error estimate as

$$\left(1 + \frac{1}{\sqrt{h}}\right) \varepsilon^2 + \sqrt{h}.$$

Proof. Let $t \in [kh, (k+1)h)$ and $t^* = kh + \delta$ where δ is larger than or equal to h : $\delta \geq h$. We only consider a situation where $T - t \geq \delta$. The situation where $\delta < T - t$ can be treated in the same manner by noticing a trivial relation $\nabla_x \mathbb{E}[\rho_*(\bar{X}_T^\leftarrow) | \bar{X}_T^\leftarrow = x] = \nabla \rho_*(x)$. Then, for a given initial state $x \in \mathbb{R}^d$, we define the stochastic processes as

$$\bar{X}_t^\leftarrow = x, \quad d\bar{X}_\tau^\leftarrow = \{\bar{X}_\tau^\leftarrow + 2\nabla \log p_{T-\tau}(\bar{X}_\tau^\leftarrow)\}d\tau + \sqrt{2}dB_\tau, \quad (t \leq \tau \leq T),$$

and its numerical approximation as

$$X_t^\leftarrow = x, \quad dX_\tau^\leftarrow = \{X_\tau^\leftarrow + 2s(X_{k_\tau h}^\leftarrow, k_\tau h)\}d\tau + \sqrt{2}dB_\tau. \quad (t \leq \tau \leq T),$$

where k_τ is the integer such that $\tau \in [k_\tau h, (k_\tau + 1)h)$.

Note that

$$\begin{aligned} & \nabla_x \mathbb{E}[\rho_*(\bar{X}_T^\leftarrow) | \bar{X}_t^\leftarrow] - \nabla_x \mathbb{E}[\rho_*(X_T^\leftarrow) | X_{k_h}^\leftarrow] \\ &= \underbrace{(\nabla_x \mathbb{E}[\rho_*(\bar{X}_T^\leftarrow) | \bar{X}_t^\leftarrow] - \nabla_x \mathbb{E}[\rho_*(X_T^\leftarrow) | X_t^\leftarrow])}_{(a)} + \underbrace{(\nabla_x \mathbb{E}[\rho_*(X_T^\leftarrow) | X_t^\leftarrow] - \nabla_x \mathbb{E}[\rho_*(X_T^\leftarrow) | X_{k_h}^\leftarrow])}_{(b)}. \end{aligned} \quad (39)$$

We first evaluate the term (a):

$$\nabla_x \mathbb{E}[\rho_*(\bar{X}_T^\leftarrow) | \bar{X}_t^\leftarrow = x] - \nabla_x \mathbb{E}[\rho_*(X_T^\leftarrow) | X_t^\leftarrow = x].$$

As we have seen above, the derivative can be expressed by the following recursive formula of the conditional expectation:

$$\nabla_x \mathbb{E}[\mathbb{E}[\rho_*(\bar{X}_T^\leftarrow) | \bar{X}_{t^*}^\leftarrow] | \bar{X}_t^\leftarrow = x].$$

For a notation simplicity, we let $\varphi_X(x) := \mathbb{E}[\rho_*(\bar{X}_T^\leftarrow) | \bar{X}_{t^*}^\leftarrow = x]$ and $\varphi_Y(x) := \mathbb{E}[\rho_*(X_T^\leftarrow) | X_{t^*}^\leftarrow = x]$. Then, the Bismut-Elworthy-Li formula (Bismut, 1984; Elworthy & Li, 1994) yields that, for any $v \in \mathbb{R}^d$,

$$v^\top \nabla_x \mathbb{E}[\rho_*(\bar{X}_0^\leftarrow) | \bar{X}_t^\leftarrow = x] = \mathbb{E} \left[\frac{1}{\delta} \int_0^\delta \langle \eta_{\bar{X}, \tau}, dB_\tau \rangle \varphi_X(\bar{X}_{t^*}^\leftarrow) \mid \bar{X}_t^\leftarrow = x \right],$$

where $\eta_{\bar{X}, \tau}$ is the solution of

$$\begin{aligned} d\eta_{\bar{X}, \tau} &= (I + 2\nabla^2 \log p_{T-t-\tau}(\bar{X}_{t+\tau}^\leftarrow))\eta_{\bar{X}, \tau} d\tau, \\ \eta_{\bar{X}, 0} &= v. \end{aligned}$$

Similarly, we define $\eta_{X, \tau}$ for the process X_τ^\leftarrow as

$$\begin{aligned} d\eta_{X, \tau} &= (\eta_{X, \tau} + 2\nabla_x^\top s(X_{k_\tau h}^\leftarrow, k_\tau h))\eta_{X, k_\tau h - t} d\tau, \\ \eta_{X, 0} &= v. \end{aligned}$$

Then,

$$\begin{aligned} & v^\top \nabla_x \mathbb{E}[\rho_*(\bar{X}_T^\leftarrow) | \bar{X}_t^\leftarrow = x] - v^\top \nabla_x \mathbb{E}[\rho_*(X_T^\leftarrow) | X_t^\leftarrow = x] \\ &= \mathbb{E} \left[\frac{1}{\delta} \int_0^\delta \langle \eta_{\bar{X}, \tau} - \eta_{X, \tau}, dB_\tau \rangle \varphi_Y(X_{t^*}^\leftarrow) \mid \bar{X}_t^\leftarrow = X_t^\leftarrow = x \right] \\ & \quad + \mathbb{E} \left[\frac{1}{\delta} \int_0^\delta \langle \eta_{\bar{X}, \tau}, dB_\tau \rangle (\varphi_X(\bar{X}_{t^*}^\leftarrow) - \varphi_Y(X_{t^*}^\leftarrow)) \mid \bar{X}_t^\leftarrow = X_t^\leftarrow = x \right]. \end{aligned} \quad (40)$$

By the Ito isometry, the first term of the right hand side can be bounded as

$$\begin{aligned}
& \left(\mathbb{E} \left[\frac{1}{\delta} \int_0^\delta \langle \eta_{\bar{X},\tau} - \eta_{X,\tau}, dB_\tau \rangle \varphi_Y(X_{t^*}) \mid \bar{X}_t^{\leftarrow} = X_t^{\leftarrow} = x \right] \right)^2 \\
& \leq \mathbb{E} \left[\left(\frac{1}{\delta} \int_0^\delta \langle \eta_{\bar{X},\tau} - \eta_{X,\tau}, dB_\tau \rangle \varphi_Y(X_{t^*}) \right)^2 \mid \bar{X}_t^{\leftarrow} = X_t^{\leftarrow} = x \right] \\
& \leq C_\rho^2 \mathbb{E} \left[\left(\frac{1}{\delta} \int_0^\delta \langle \eta_{\bar{X},\tau} - \eta_{X,\tau}, dB_\tau \rangle \right)^2 \mid \bar{X}_t^{\leftarrow} = X_t^{\leftarrow} = x \right] \\
& = C_\rho^2 \mathbb{E} \left[\frac{1}{h^2} \int_\tau^h \|\eta_{\bar{X},\tau} - \eta_{X,\tau}\|^2 d\tau \mid \bar{X}_t^{\leftarrow} = X_t^{\leftarrow} = x \right] \\
& \leq 2C_\rho^2 \mathbb{E} \left[\frac{1}{\delta^2} \int_0^\delta (\|\eta_{\bar{X},\tau} - v\|^2 + \|\eta_{X,\tau} - v\|^2) d\tau \mid \bar{X}_t^{\leftarrow} = X_t^{\leftarrow} = x \right].
\end{aligned}$$

Hence, we just need to bound $\|\eta_{\bar{X},\tau} - v\|^2$ in the right hand side. We note that it obeys the following differential equation:

$$\begin{aligned}
& \frac{d\|\eta_{\bar{X},\tau} - v\|^2}{d\tau} \\
& = 2(\eta_{\bar{X},\tau} - v)^\top \frac{d\eta_{\bar{X},\tau}}{d\tau} \\
& = 2(\eta_{\bar{X},\tau} - v)^\top (I + 2\nabla^2 \log p_{T-t-\tau}(\bar{X}_{T-t-\tau}^{\leftarrow})) \eta_{\bar{X},\tau} \\
& = 2(\eta_{\bar{X},\tau} - v)^\top (I + 2\nabla^2 \log p_{T-t-\tau}(\bar{X}_{T-t-\tau}^{\leftarrow})) [(\eta_{\bar{X},\tau} - v) + v] \\
& \leq 2(1 + 2R) \|\eta_{\bar{X},\tau} - v\|^2 + 2(1 + 2R) \|v\| \|\eta_{\bar{X},\tau} - v\|,
\end{aligned}$$

which also yields that

$$\begin{aligned}
& 2\|\eta_{\bar{X},\tau} - v\| \frac{d\|\eta_{\bar{X},\tau} - v\|}{d\tau} \leq 2(1 + 2R) \|\eta_{\bar{X},\tau} - v\|^2 + 2(1 + 2R) \|v\| \|\eta_{\bar{X},\tau} - v\| \\
& \Rightarrow \frac{d\|\eta_{\bar{X},\tau} - v\|}{d\tau} \leq 2(1 + 2R) (\|\eta_{\bar{X},\tau} - v\| + \|v\|) \\
& \Rightarrow \|\eta_{\bar{X},\tau} - v\| \leq [\exp(2(1 + 2R)\tau) - 1] \|v\| \\
& \Rightarrow \|\eta_{\bar{X},\tau} - v\|^2 \leq [\exp(2(1 + 2R)\tau) - 1]^2 \|v\|^2.
\end{aligned}$$

Therefore, if δ is sufficiently small (such as $\delta \leq 1/(1 + 2R)$), then we arrive at

$$\|\eta_{\bar{X},\tau} - v\|^2 \leq c_\eta (1 + 2R)^2 \tau^2 \|v\|^2,$$

with a universal constant c_η , for any $0 \leq \tau \leq \delta$. In the same vein, we also have

$$\begin{aligned}
& \|\eta_{X,\tau} - v\|^2 \leq c_\eta (1 + 2R)^2 \tau^2 \|v\|^2, \\
& \|\eta_{\bar{X},\tau}\|^2 \leq \exp(4(1 + 2R)\tau) \|v\|^2, \quad \|\eta_{X,\tau}\|^2 \leq \exp(4(1 + 2R)\tau) \|v\|^2,
\end{aligned}$$

for $0 \leq \tau \leq \delta$. These bounds yield that

$$\begin{aligned}
& 2C_\rho^2 \mathbb{E} \left[\frac{1}{\delta^2} \int_0^\delta (\|\eta_{\bar{X},\tau} - v\|^2 + \|\eta_{X,\tau} - v\|^2) d\tau \mid \bar{X}_t^{\leftarrow} = X_t^{\leftarrow} = x \right] \\
& \leq 4c_\eta^2 C_\rho^2 (1 + 2R)^2 \frac{\int_0^\delta \tau^2 d\tau}{\delta^2} = \frac{4c_\eta^2 C_\rho^2 (1 + 2R)^2}{3} \delta.
\end{aligned}$$

Next, we bound the second term of the right hand side in Eq. (40):

$$\begin{aligned}
& \mathbb{E} \left[\frac{1}{\delta} \int_0^\delta \langle \eta_{\bar{X}, \tau}, dB_\tau \rangle (\varphi_X(\bar{X}_{t^*}^\leftarrow) - \varphi_Y(X_{t^*}^\leftarrow)) \mid \bar{X}_t^\leftarrow = X_t^\leftarrow = x \right]^2 \\
& \leq \mathbb{E} \left[\frac{1}{\delta^2} \int_0^\delta \|\eta_{\bar{X}, \tau}\|^2 d\tau \mid \bar{X}_t^\leftarrow = X_t^\leftarrow = x \right] \mathbb{E} [(\varphi_X(\bar{X}_{t^*}^\leftarrow) - \varphi_Y(X_{t^*}^\leftarrow))^2 \mid \bar{X}_t^\leftarrow = X_t^\leftarrow = x] \\
& \leq \frac{\exp(2(1+2R)\delta)\|v\|^2}{\delta} \mathbb{E} [(\varphi_X(\bar{X}_{t^*}^\leftarrow) - \varphi_Y(X_{t^*}^\leftarrow))^2 \mid \bar{X}_t^\leftarrow = X_t^\leftarrow = x]. \tag{41}
\end{aligned}$$

Otherwise, we also have the following inequality:

$$\begin{aligned}
& \mathbb{E} \left[\frac{1}{\delta} \int_0^\delta \langle \eta_{\bar{X}, \tau}, dB_\tau \rangle (\varphi_X(\bar{X}_{t^*}^\leftarrow) - \varphi_Y(X_{t^*}^\leftarrow)) \mid \bar{X}_t^\leftarrow = X_t^\leftarrow = x \right]^2 \\
& \leq 2\mathbb{E} \left[\frac{1}{\delta} \int_0^\delta \langle \eta_{\bar{X}, \tau}, dB_\tau \rangle (\varphi_Y(\bar{X}_{t^*}^\leftarrow) - \varphi_Y(X_{t^*}^\leftarrow)) \mid \bar{X}_t^\leftarrow = X_t^\leftarrow = x \right]^2 \\
& \quad + 2\mathbb{E} \left[\eta_{\bar{X}, \delta}^\top \nabla (\varphi_X(\bar{X}_{t^*}^\leftarrow) - \varphi_Y(\bar{X}_{t^*}^\leftarrow)) \mid \bar{X}_t^\leftarrow = X_t^\leftarrow = x \right]^2 \\
& \leq \frac{\exp(2(1+2R)\delta)\|v\|^2}{\delta} \mathbb{E} [(\varphi_Y(\bar{X}_{t^*}^\leftarrow) - \varphi_Y(X_{t^*}^\leftarrow))^2 \mid \bar{X}_t^\leftarrow = X_t^\leftarrow = x] \\
& \quad + 2\mathbb{E} [\|\eta_{\bar{X}, \delta}\| \|\nabla (\varphi_X(\bar{X}_{t^*}^\leftarrow) - \varphi_Y(\bar{X}_{t^*}^\leftarrow))\| \mid \bar{X}_t^\leftarrow = X_t^\leftarrow = x]^2. \tag{42}
\end{aligned}$$

For bounding these quantities, we need to bound the discrepancy $\|\bar{X}_\tau^\leftarrow - X_\tau^\leftarrow\|^2$. Note that this quantity follows the following ODE:

$$\begin{aligned}
& \frac{d\|\bar{X}_\tau^\leftarrow - X_\tau^\leftarrow\|^2}{d\tau} \\
& = 2(\bar{X}_\tau^\leftarrow - X_\tau^\leftarrow)^\top [(\bar{X}_\tau^\leftarrow - 2\nabla_x \log p_{T-\tau-t}(\bar{X}_\tau^\leftarrow)) - (X_\tau^\leftarrow - 2s(x, kh))] \\
& = 2\|\bar{X}_\tau^\leftarrow - X_\tau^\leftarrow\|^2 - 4(\bar{X}_\tau^\leftarrow - X_\tau^\leftarrow)^\top (\nabla_x \log p_{T-\tau-t}(\bar{X}_\tau^\leftarrow) - s(x, kh)) \\
& \leq 4\|\bar{X}_\tau^\leftarrow - X_\tau^\leftarrow\|^2 + 2\|\nabla_x \log(p_{T-\tau-t}(\bar{X}_\tau^\leftarrow)) - s(x, kh)\|^2.
\end{aligned}$$

Therefore, it satisfies that

$$\|\bar{X}_\tau^\leftarrow - X_\tau^\leftarrow\|^2 \leq 4 \int_0^\tau \|\bar{X}_s^\leftarrow - X_s^\leftarrow\|^2 ds + 2 \int_0^\tau \|\nabla_x \log(p_{T-\tau-t}(\bar{X}_s^\leftarrow)) - s(x, kh)\|^2 ds.$$

Taking its expectation, we see that

$$\mathbb{E}[\|\bar{X}_\tau^\leftarrow - X_\tau^\leftarrow\|^2] \leq 4 \int_0^\tau \mathbb{E}[\|\bar{X}_s^\leftarrow - X_s^\leftarrow\|^2] ds + 2 \underbrace{\int_0^\tau (\varepsilon^2 + L_p^2 ds + L_p^2 m s^2) ds}_{=\mathcal{O}(\varepsilon^2 \tau + L_p^2 d(\tau^2 + m\tau^3))} =: \xi(\tau)$$

where we used Theorem 10 (and its proof) of Chen et al. (2023b) for obtaining $\xi(\tau)$. Then, Gronwall inequality yields

$$\mathbb{E}[\|\bar{X}_\tau^\leftarrow - X_\tau^\leftarrow\|^2] \leq \xi(\tau) + \int 4\xi(s)e^{4(\tau-s)} ds \lesssim \varepsilon^2 \tau + L_p^2 d(\tau^2 + m\tau^3),$$

(see Mischler (2019) for example). Then, the Lipschitz continuity of φ_Y (Lemma 10) yields that

$$\mathbb{E} [(\varphi_Y(\bar{X}_{t^*}^\leftarrow) - \varphi_Y(X_{t^*}^\leftarrow))^2 \mid \bar{X}_t^\leftarrow = X_t^\leftarrow = x] \lesssim L_\varphi^2 [\varepsilon^2 \tau + L_p^2 d(\tau^2 + m\tau^3)].$$

Bound for $t = kh$: First, we show a bound for $t = kh$. The right hand side of Eq. (41) with $\delta = h$ can be bounded by

$$\begin{aligned}
& \frac{\exp(2(1+2R)\delta)\|v\|^2}{\delta} \mathbb{E}_{\bar{X}_t^\leftarrow} [\mathbb{E} [(\varphi_X(\bar{X}_{t^*}^\leftarrow) - \varphi_Y(X_{t^*}^\leftarrow))^2 \mid \bar{X}_t^\leftarrow = X_t^\leftarrow]] \\
& \leq \frac{\exp(2(1+2R)\delta)\|v\|^2}{\delta} 2\mathbb{E}_{\bar{X}_t^\leftarrow} [\mathbb{E} [(\varphi_X(\bar{X}_{t^*}^\leftarrow) - \varphi_Y(\bar{X}_{t^*}^\leftarrow))^2 + (\varphi_Y(\bar{X}_{t^*}^\leftarrow) - \varphi_Y(X_{t^*}^\leftarrow))^2 \mid \bar{X}_t^\leftarrow = X_t^\leftarrow]] \\
& \leq \frac{\exp(2(1+2R)\delta)\|v\|^2}{\delta} 2 \left\{ C_\rho^2 \varepsilon_{\text{TV}}^2 + R_\varphi^2 \mathbb{E}_{\bar{X}_t^\leftarrow} [\mathbb{E} [(\bar{X}_{t^*}^\leftarrow - X_{t^*}^\leftarrow)^2 \mid \bar{X}_t^\leftarrow = X_t^\leftarrow]] \right\},
\end{aligned}$$

1998
1999
2000
2001
2002
2003
2004
2005
2006
2007
2008
2009
2010
2011
2012
2013
2014
2015
2016
2017
2018
2019
2020
2021
2022
2023
2024
2025
2026
2027
2028
2029
2030
2031
2032
2033
2034
2035
2036
2037
2038
2039
2040
2041
2042
2043
2044
2045
2046
2047
2048
2049
2050
2051

where we used

$$\begin{aligned} \mathbb{E} [(\varphi_X(\bar{X}_{t^*}^\leftarrow) - \varphi_Y(\bar{X}_{t^*}^\leftarrow))^2] &\leq C_\rho^2 \mathbb{E}_{\bar{X}_{T-t^*}^\leftarrow} [\text{TV}(\bar{X}_T^\leftarrow, X_T^\leftarrow | X_{t^*}^\leftarrow = \bar{X}_{t^*}^\leftarrow = \bar{X}_{T-t^*}^\leftarrow)^2] \\ &\leq C_\rho^2 \varepsilon_{\text{TV}}. \end{aligned}$$

Here, by using Theorem 10 of Chen et al. (2023c) again, the right hand side can be bounded as

$$\begin{aligned} &2 \frac{\exp(2(1+2R)\delta) \|v\|^2}{\delta} \{C_\rho^2 \varepsilon_{\text{TV}}^2 + CR_\varphi^2 [\varepsilon^2 \delta + L_p^2 d(\delta^2 + m\delta^3)]\} \\ &= 2 \exp(2(1+2R)\delta) \|v\|^2 \left\{ C_\rho^2 \frac{\varepsilon_{\text{TV}}^2}{\delta} + CR_\varphi^2 [\varepsilon^2 + L_p^2 d(\delta + m\delta^2)] \right\}. \end{aligned}$$

Then, with the constraint $h \leq 1/(1+2R)$, it can be further simplified as

$$2 \exp(2) \|v\|^2 \left\{ C_\rho^2 \frac{\varepsilon_{\text{TV}}^2}{\delta} + CR_\varphi^2 [\varepsilon^2 + L_p^2 d(\delta + m\delta^2)] \right\}.$$

Therefore, by taking maximum with respect to $v \in \mathbb{R}^d$ with a constraint $\|v\| = 1$,

$$\begin{aligned} &\mathbb{E}_{\bar{X}_t^\leftarrow} [\|\nabla_x \mathbb{E}[\rho_*(\bar{X}_T^\leftarrow) | \bar{X}_t^\leftarrow] - \nabla_x \mathbb{E}[\rho_*(X_T^\leftarrow) | X_t^\leftarrow = \bar{X}_t^\leftarrow]\|^2] \\ &\leq \frac{4c_\eta^2 C_\rho^2 (1+2R)^2}{3} \delta + 2 \exp(2) \left\{ C_\rho^2 \frac{\varepsilon_{\text{TV}}^2}{\delta} + CR_\varphi^2 [\varepsilon^2 + L_p^2 d(\delta + m\delta^2)] \right\} =: \Xi_{\delta, \varepsilon}. \quad (43) \end{aligned}$$

We see that $\Xi_{\delta, \varepsilon} = \mathcal{O}(\delta + \varepsilon^2 + \varepsilon_{\text{TV}}^2/\delta)$.

Bound for general $t \in (kh, (k+1)h)$: In this setting, we utilize the inequality (42). Using the constraint $\delta \leq 1/(1+2R)$ and $\|v\| = 1$, the right hand side of (42) can be bounded by

$$\begin{aligned} &\frac{\exp(2)}{\delta} \mathbb{E} [(\varphi_Y(\bar{X}_{t^*}^\leftarrow) - \varphi_Y(X_{t^*}^\leftarrow))^2 | \bar{X}_t^\leftarrow = X_t^\leftarrow = x] \\ &+ 2\mathbb{E} [\exp(2) \|\nabla(\varphi_X(\bar{X}_{t^*}^\leftarrow)) - \varphi_Y(\bar{X}_{t^*}^\leftarrow)\| | \bar{X}_t^\leftarrow = X_t^\leftarrow = x]^2 \\ &\leq \frac{\exp(2)}{\delta} R_\varphi^2 \mathbb{E} [(\bar{X}_{t^*}^\leftarrow - X_{t^*}^\leftarrow)^2 | \bar{X}_t^\leftarrow = X_t^\leftarrow = x] + 2 \exp(2) \Xi_{\delta, \varepsilon} \quad (\because \text{Eq. (43)}). \end{aligned}$$

By taking the expectation with respect to $x = \bar{X}_t^\leftarrow$, we arrive at

$$\begin{aligned} &\mathbb{E}_{\bar{X}_t^\leftarrow} [\|\nabla_x \mathbb{E}[\rho_*(\bar{X}_T^\leftarrow) | \bar{X}_t^\leftarrow] - \nabla_x \mathbb{E}[\rho_*(X_T^\leftarrow) | X_t^\leftarrow]\|^2] \\ &\leq C \frac{\exp(2)}{\delta} R_\varphi^2 (\varepsilon^2 \delta + L_p^2 d(\delta^2 + m\delta^3)) + 2 \exp(2) \Xi_{\delta, \varepsilon} \\ &\leq C \exp(2) R_\varphi^2 (\varepsilon^2 + L_p^2 d(\delta + m\delta^2)) + 2 \exp(2) \Xi_{\delta, \varepsilon}. \quad (44) \end{aligned}$$

This gives an upper bound of the term (a) in Eq. (39). Then, we just need to bound the remaining term (b) in Eq. (39):

$$\mathbb{E}_{\bar{X}_t^\leftarrow, \bar{X}_{kh}^\leftarrow} [\|\nabla_x \mathbb{E}[\rho_*(X_T^\leftarrow) | X_t^\leftarrow] - \nabla_x \mathbb{E}[\rho_*(X_T^\leftarrow) | X_{kh}^\leftarrow]\|^2].$$

For that purpose, we define $\varphi_{Y,t}(x) = \mathbb{E}[\rho_*(X_T^\leftarrow) | X_t^\leftarrow = x]$. Then, using the Bismut-Elworthy-Li formula again,

$$\begin{aligned} &v^\top (\nabla \varphi_{Y,t}(x) - \nabla \varphi_{Y,kh}(x)) \\ &= v^\top \nabla \varphi_{Y,t}(x) - \mathbb{E}[\eta_{X,h(k+1)-t}^\top \nabla \varphi_{Y,t}(X_t^\leftarrow) | X_{kh}^\leftarrow = x] \\ &= \mathbb{E}[v^\top (\nabla \varphi_{Y,t}(x) - \nabla \varphi_{Y,t}(X_t^\leftarrow)) + (\eta_{X,(k+1)h-t}^\top - v) \nabla \varphi_{Y,t}(X_t^\leftarrow) | X_{kh}^\leftarrow = x] \\ &\leq \mathbb{E}[L_\varphi \|x - X_t^\leftarrow\| + R_\varphi \|\eta_{X,(k+1)h-t}^\top - v\| | X_{(k+1)h-t}^\leftarrow = x] \\ &\leq \mathbb{E}[L_\varphi \|((k+1)h-t)(x - 2s(x, kh)) + \sqrt{(h-\delta)} B_{kh}\| + R_\varphi \|\eta_{X,(k+1)h-t}^\top - v\| | X_{kh}^\leftarrow = x], \end{aligned}$$

which yields that

$$\begin{aligned} &\mathbb{E}_{\bar{X}_t^\leftarrow} [\|\nabla \varphi_{Y,t}(\bar{X}_t^\leftarrow) - \nabla \varphi_{Y,kh}(\bar{X}_{(k+1)h-t}^\leftarrow)\|^2] \\ &\leq 2L_\varphi^2 ((k+1)h-t)^2 \mathbb{E}_{\bar{X}_t^\leftarrow} [\|\bar{X}_{kh}^\leftarrow\|^2 + 4\|s(\bar{X}_{kh}^\leftarrow, kh)\|^2 + d((k+1)h-t)] \\ &\quad + R_\varphi^2 c_\eta (1+2R)^2 ((k+1)h-t)^2 \\ &\leq 2L_\varphi^2 h^2 (m + 4Q^2 + dh) + R_\varphi^2 c_\eta (1+2R)^2 h^2 \\ &= [2L_\varphi^2 (m + 4Q^2 + dh) + R_\varphi^2 c_\eta (1+2R)^2] h^2. \quad (45) \end{aligned}$$

Combining (44) and (45) gives the assertion. \square

Lemma 10. Suppose that $\sup_x \|\nabla \rho_*(x)\| \leq R_\rho$, $\|\nabla \rho_*(x) - \nabla \rho_*(y)\| \leq L_\rho \|x - y\|$ ($\forall x, y$), and $\nabla_x s(\cdot, \cdot)$ is H_s -Lipschitz continuous with respect to x . Let $\varphi_{Y,t}(x) = \mathbb{E}[\rho_*(X_t^\leftarrow) | X_t^\leftarrow = x]$. Then, $\nabla_x \varphi_{Y,t}(x)$ is bounded by R_φ and L_φ -Lipschitz continuous for any $0 \leq t \leq T$, where

$$R_\varphi = \max\{C_\rho 2\sqrt{(1+2R)}e, e^{1/2}R_\rho\},$$

$$L_\varphi = \max\left\{\left(\frac{2C_\eta^2 H_s^2 C_\rho^2}{1+2R} + 2(1+2R)\exp(6)R_\varphi^2\right)^{1/2}, (2C_\eta^2 H_s^2 R^2 + e^2 L_\rho^2)^{1/2}\right\},$$

for a universal constant $C_\eta > 0$.

Proof. We show it only when $t = kh$ for a positive integer k just for simplicity. The proof for a general t can be obtained in the same manner.

(i) First, we assume that $T - t \geq 1/4(1 + 2R)$. In the following, we let $v \in \mathbb{R}^d$ be an arbitrary vector with $\|v\| = 1$. We again utilize the Bismut-Elworthy-Li formula:

$$\begin{aligned} & v^\top \nabla \varphi_{Y,t}(x) \\ &= v^\top \nabla_x \mathbb{E}[\rho_*(X_T^\leftarrow) | X_t^\leftarrow = x] \\ &= \mathbb{E}\left[\frac{1}{S} \int_0^S \langle \eta_\tau, dB_\tau \rangle \varphi_{Y,S}(X_S^\leftarrow) | X_t^\leftarrow = x\right]. \end{aligned}$$

Hence,

$$\begin{aligned} & (v^\top \nabla \varphi_{Y,t}(x))^2 \\ & \leq C_\rho^2 \mathbb{E}\left[\frac{1}{S^2} \left(\int_0^S \langle \eta_\tau, dB_\tau \rangle\right)^2 | X_t^\leftarrow = x\right] \\ & \leq C_\rho^2 \mathbb{E}\left[\frac{1}{S^2} \int_0^S \|\eta_\tau\|^2 d\tau | X_t^\leftarrow = x\right]. \end{aligned}$$

Here, we know that $\|\eta_\tau\|^2 \leq \exp(4(1+2R)\tau)\|v\|^2$, and thus

$$(v^\top \nabla \varphi_{Y,t}(x))^2 \leq C_\rho^2 \frac{1}{S} \exp(4(1+2R)S)\|v\|^2.$$

Hence, by taking $S = \frac{1}{4(1+2R)}$, we have that

$$(v^\top \nabla \varphi_{Y,t}(x))^2 \leq C_\rho^2 4(1+2R)e\|v\|^2.$$

This shows that $\|\nabla \varphi_{Y,t}(x)\|$ is bounded by $R_\varphi = C_\rho 2\sqrt{(1+2R)}e$.

Next, we show its Lipschitz continuity. For that purpose, we define two stochastic processes

$$\begin{aligned} X_t^\leftarrow &= x, \quad dX_\tau^\leftarrow = \{X_\tau^\leftarrow + 2s(X_{kh}^\leftarrow, kh)\}d\tau + \sqrt{2}dB_\tau \quad (\tau \in [kh, k(h+1)]), \\ \tilde{Z}_t^\leftarrow &= y, \quad d\tilde{Z}_\tau^\leftarrow = \{\tilde{Z}_\tau^\leftarrow + 2s(\tilde{Z}_{kh}^\leftarrow, kh)\}d\tau + \sqrt{2}dB_\tau \quad (\tau \in [kh, k(h+1)]), \end{aligned}$$

where $x, y \in \mathbb{R}^d$ with $\|x - y\| \leq \varepsilon$. Accordingly, we also define

$$\begin{aligned} \eta_{X,0} &= v, \quad \frac{d\eta_{X,\tau}}{d\tau} = (I + 2\nabla_x^\top s(X_{kh}^\leftarrow, kh))\eta_{X,\tau}, \\ \eta_{Z,0} &= v, \quad \frac{d\eta_{Z,\tau}}{d\tau} = (I + 2\nabla_x^\top s(\tilde{Z}_{kh}^\leftarrow, kh))\eta_{Z,\tau}. \end{aligned}$$

Thus,

$$X_{(k+1)h}^\leftarrow - \tilde{Z}_{(k+1)h}^\leftarrow = X_{kh}^\leftarrow - \tilde{Z}_{kh}^\leftarrow + h[X_{kh}^\leftarrow - \tilde{Z}_{kh}^\leftarrow + 2(s(X_{kh}^\leftarrow, kh) - s(\tilde{Z}_{kh}^\leftarrow, kh))],$$

which yields

$$\begin{aligned} \|X_{(k+1)h}^\leftarrow - \tilde{Z}_{(k+1)h}^\leftarrow\| &\leq (1 + h(1+R))\|X_{kh}^\leftarrow - \tilde{Z}_{kh}^\leftarrow\| \\ &\leq (1 + h(1+R))^{k+1}\|x - y\|. \end{aligned}$$

Now, we assume $k \leq S/h$ so that we have $\|X_{(k+1)h}^{\leftarrow} - \tilde{Z}_{(k+1)h}^{\leftarrow}\| \leq \exp(S(1+R))\|x - y\|$ for $k = 1, \dots, S/h$. Hence,

$$\begin{aligned} & \frac{d(\eta_{X,\tau} - \eta_{Z,\tau})}{d\tau} \\ &= (\eta_{X,\tau} - \eta_{Z,\tau}) + 2\nabla_x^\top s(X_{kh}^{\leftarrow}, kh)\eta_{X,\tau} - 2\nabla_x^\top s(\tilde{Z}_{kh}^{\leftarrow}, kh)\eta_{Z,\tau} \\ &= (\eta_{X,\tau} - \eta_{Z,\tau}) + 2(\nabla_x^\top s(X_{kh}^{\leftarrow}, kh) - \nabla_x^\top s(\tilde{Z}_{kh}^{\leftarrow}, kh))\eta_{X,\tau} - 2\nabla_x^\top s(\tilde{Z}_{kh}^{\leftarrow}, kh)(\eta_{Z,\tau} - \eta_{X,\tau}), \end{aligned}$$

which also yields that

$$\begin{aligned} & \frac{d\|\eta_{X,\tau} - \eta_{Z,\tau}\|^2}{d\tau} \\ &= 2\|\eta_{X,\tau} - \eta_{Z,\tau}\|^2 + 4(\eta_{X,\tau} - \eta_{Z,\tau})^\top (\nabla_x^\top s(X_{kh}^{\leftarrow}, kh) - \nabla_x^\top s(\tilde{Z}_{kh}^{\leftarrow}, kh))\eta_{X,\tau} \\ & \quad - 4(\eta_{X,\tau} - \eta_{Z,\tau})^\top \nabla_x^\top s(\tilde{Z}_{kh}^{\leftarrow}, kh)(\eta_{Z,\tau} - \eta_{X,\tau}) \\ & \leq 2\|\eta_{X,\tau} - \eta_{Z,\tau}\|^2 + 4\|\eta_{X,\tau} - \eta_{Z,\tau}\|H_s \exp(S(1+R))\varepsilon \exp(2(1+2R)S) \\ & \quad + 4R\|\eta_{X,\tau} - \eta_{Z,\tau}\|^2. \end{aligned}$$

Therefore,

$$\begin{aligned} & \frac{d\|\eta_{X,\tau} - \eta_{Z,\tau}\|}{d\tau} \\ & \leq (1+2R) [\|\eta_{X,\tau} - \eta_{Z,\tau}\| + 2H_s \exp(S(1+R)) \exp(2(1+2R)S)\varepsilon / (1+2R)], \end{aligned}$$

and thus by noticing $\|\eta_{X,0} - \eta_{Z,0}\| = 0$, we have

$$\|\eta_{X,\tau} - \eta_{Z,\tau}\| \leq [\exp(S(1+2R)) - 1] \frac{2H_s \exp(S(1+R)) \exp(2(1+2R)S)\varepsilon}{1+2R},$$

for any $\tau \leq S$. Then, by setting $S = 1/(1+2R)$, the right hand side can be rewritten as

$$\|\eta_{X,\tau} - \eta_{Z,\tau}\| \leq C_\eta \frac{H_s}{1+2R} \varepsilon,$$

for an absolute constant C_η . Therefore, we arrive at

$$\begin{aligned} & (v^\top (\nabla \varphi_{Y,t}(x) - \nabla \varphi_{Y,t}(y)))^2 \\ &= \mathbb{E} \left[\frac{1}{S} \int_0^S \langle \eta_{X,\tau}, dB_\tau \rangle \varphi_{Y,S}(X_S^{\leftarrow}) - \frac{1}{S} \int_0^S \langle \eta_{Z,\tau}, dB_\tau \rangle \varphi_{Y,S}(\tilde{Z}_S^{\leftarrow}) \right]^2 \\ & \leq 2\mathbb{E} \left[\frac{1}{S^2} \int_0^S (\eta_{X,\tau} - \eta_{Z,\tau})^2 d\tau \right] \mathbb{E} [\varphi_{Y,S}(X_S^{\leftarrow})^2] \\ & \quad + 2\mathbb{E} \left[\frac{1}{S^2} \int_0^S \eta_{Z,\tau}^2 d\tau \right] \mathbb{E} [(\varphi_{Y,S}(X_S^{\leftarrow}) - \varphi_{Y,S}(\tilde{Z}_S^{\leftarrow}))^2] \\ & \leq \frac{2}{S} C_\eta^2 \frac{H_s^2}{(1+2R)^2} \varepsilon^2 \cdot C_\rho^2 + \frac{2}{S} \exp(4(1+2R)S) \|v\|^2 R_\varphi^2 \exp(2S(1+R)) \varepsilon^2. \end{aligned}$$

Then, for the choice of $S = 1/(1+2R)$, the right hand side can be bounded by

$$\left(\frac{2C_\eta^2 H_s^2 C_\rho^2}{1+2R} + 2(1+2R) \exp(6) R_\varphi^2 \right) \varepsilon^2.$$

This implies that $\nabla \varphi_{Y,t}(\cdot)$ is Lipschitz continuous with a constant $L_\varphi = \left(\frac{2C_\eta^2 H_s^2 C_\rho^2}{1+2R} + 2(1+2R) \exp(6) R_\varphi^2 \right)^{1/2}$.

(ii) Next, we assume that $T - t \leq S = 1/4(1+2R)$. In this situation, we may use the following relation:

$$v^\top \nabla \varphi_{Y,t}(x) = \mathbb{E}[\eta_\tau^{T-t} \nabla \rho_*(X_T^{\leftarrow}) \mid X_t^{\leftarrow} = x].$$

And, tracing an analogous argument by replacing $\varphi_{Y,S}$ with h , we obtain the assertion with

$$R_\varphi = e^{1/2}R_\rho, \quad L_\varphi = (2C_\eta^2 H_s^2 R^2 + e^2 L_\rho^2)^{1/2}.$$

Lemma 11. *If $\|\rho_* - \rho\|_\infty \leq \varepsilon'$, then*

$$\|\nabla_x \mathbb{E}[\rho_*(X_T^\leftarrow) | X_t^\leftarrow = x] - \nabla_x \mathbb{E}[\rho(X_T^\leftarrow) | X_t^\leftarrow = x]\| \leq \frac{e}{\sqrt{\min\{T-t, 1/(2+2R)\}}} \varepsilon'.$$

Proof. It can be proved by the Bismut-Elworthy-Li formula again. We omit the details. \square

Combining all inequalities, we arrive at (the formal version of) Theorem 4.

Theorem 8 (Formal statement of Theorem 4). *Assume that Assumptions 7 and 5 hold and the conditions in Lemma 10 are satisfied. and $\|\rho_* - \rho\|_\infty \leq \varepsilon'$ and $\|\rho\|_\infty \leq C_\rho$. Let L_φ and R_φ be as given in Lemma 10. Then, for $0 \leq h \leq \delta \leq 1/(1+2R)$, we have that*

$$\begin{aligned} & \mathbb{E}_{\bar{Y}_t^\leftarrow} [\|u_*(\bar{Y}_t^\leftarrow, t) - u(\bar{Y}_{k_t h}^\leftarrow, t)\|^2] \\ & \leq C_\rho^3 \{R_\varphi^2 (\varepsilon^2 + L_p^2 d(\delta + m\delta^2)) + \Xi_{\delta, \varepsilon} + [(R_\varphi^2 + L_\varphi^2)(m + 4Q^2 + dh) + R_\varphi^2(1+2R)^2]h^2\} \\ & \quad + \frac{e^2}{\min\{T-t, 1/(2+2R)\}} \varepsilon'^2 + C_\rho(1+2R) \sqrt{\frac{\log(T/(h\delta))}{nh}}, \end{aligned}$$

where

$$\Xi_{\delta, \varepsilon} := \frac{4c_\eta^2 C_\rho^2 (1+2R)^2}{3} \delta + 2 \exp(2) \left\{ C_\rho^2 \left(R_\varphi^2 + \frac{1}{\delta} \right) \varepsilon_{\text{TV}}^2 + C R_\varphi^2 [\varepsilon^2 + L_p^2 d(\delta + m\delta^2)] \right\},$$

and $c_\eta > 0$ is a universal constant.

Proof. Define

$$\rho_{*,t}(x) = \mathbb{E}[\rho_*(\bar{X}_T^\leftarrow) | \bar{X}_t^\leftarrow = x], \quad \rho_t(x) = \mathbb{E}[\rho(X_T^\leftarrow) | X_t^\leftarrow = x].$$

First, note that

$$\begin{aligned} \|u^*(x, t) - u(x, t)\|^2 &= \left\| \frac{\nabla \rho_{*,t}(x) - \nabla \rho_t(x)}{\rho_{*,t}(x)} + \frac{\nabla \rho_t(x)(\rho_{*,t}(x) - \rho_t(x))}{\rho_{*,t}(x)\rho_t(x)} \right\|^2 \\ &\leq 2 \left\| \frac{\nabla \rho_{*,t}(x) - \nabla \rho_t(x)}{\rho_{*,t}(x)} \right\|^2 + 2 \left\| \frac{\nabla \rho_t(x)(\rho_{*,t}(x) - \rho_t(x))}{\rho_{*,t}(x)\rho_t(x)} \right\|^2 \\ &\leq 2C_\rho^2 \|\nabla \rho_{*,t}(x) - \nabla \rho_t(x)\|^2 + 2 \frac{\|\nabla \rho_t(x)\|^2 |\rho_{*,t}(x) - \rho_t(x)|^2}{(\rho_{*,t}(x)\rho_t(x))^2} \\ &\leq 2C_\rho^2 \|\nabla \rho_{*,t}(x) - \nabla \rho_t(x)\|^2 + 2R_\varphi^2 C_\rho^2 |\rho_{*,t}(x) - \rho_t(x)|^2. \end{aligned}$$

Therefore, the expectation of the right hand side with respect to \bar{X}_t^\leftarrow can be bounded by

$$\begin{aligned} & \mathbb{E}_{\bar{X}_t^\leftarrow} [\|u^*(\bar{X}_t^\leftarrow, t) - u(\bar{X}_t^\leftarrow, t)\|^2] \\ & \leq 2C_\rho^2 \mathbb{E}_{\bar{X}_t^\leftarrow} [\|\nabla \rho_{*,t}(x) - \nabla \rho_t(x)\|^2] + 2R_\varphi C_\rho^2 \mathbb{E}_{\bar{X}_t^\leftarrow} [|\rho_{*,t}(x) - \rho_t(x)|^2] \\ & \leq 2C_\rho^2 \mathbb{E}_{\bar{X}_t^\leftarrow} [\|\nabla \rho_{*,t}(x) - \nabla \rho_t(x)\|^2] + 2R_\varphi C_\rho^2 \mathbb{E}_{\bar{X}_t^\leftarrow} [\text{TV}(\bar{X}_T^\leftarrow, X_T^\leftarrow | \bar{X}_t^\leftarrow = X_t^\leftarrow = x)]_{x=\bar{X}_t^\leftarrow}^2. \end{aligned}$$

The first term of the right hand side can be bounded by Theorem 7 and Lemma 11. The second term can be bounded by $\varepsilon_{\text{TV}}^2$ by Assumption 7.

In the same vein, we can bound the difference

$$\begin{aligned} & \|u(x, t) - u(x, k_t h)\|^2 \\ & \leq 2C_\rho^2 \mathbb{E}_{\bar{X}_t^\leftarrow} [\|\nabla \rho_t(x) - \nabla \rho_{k_t h}(x)\|^2] + 2R_\varphi C_\rho^2 \mathbb{E}_{\bar{X}_t^\leftarrow} [|\rho_t(x) - \rho_{k_t h}(x)|^2] \\ & \leq [2L_\varphi^2(m + 4Q^2 + dh) + R_\varphi^2 c_\eta(1+2R)^2]h^2 \\ & \quad + 2R_\varphi^2 h^2(m + 4Q^2 + dh) \\ & \leq [2(L_\varphi^2 + R_\varphi^2)(m + 4Q^2 + dh) + R_\varphi^2 c_\eta(1+2R)^2]h^2, \end{aligned}$$

where we used (45) and the same argument as (45) in the last inequality with R_φ Lipschitz continuity of ρ_t .

Finally, we convert the expectation w.r.t. $\bar{X}_t \leftarrow$ to that w.r.t. $\bar{X}_t \leftarrow$. However, the density ratio between p_t and q_t is bounded by C_ρ , which yields the assertion. \square

C.4 DOOB’S H-TRANSFORM

Lemma 12. *For all $t \in [0, T]$, the following relationship holds.*

$$\nabla_x \log q_t(x) = \nabla_x \log p_t(x) + \nabla_x \log(\mathbb{E}[\rho_*(\bar{X}_0)|\bar{X}_t = x]).$$

Proof. Let us denote the joint distribution of \bar{X}_0 and \bar{X}_t as $p_{0,t}(\bar{X}_0, \bar{X}_t)$, the conditional distributions of \bar{X}_0 given \bar{X}_t as $p_{0|t}(\bar{X}_0|\bar{X}_t)$, and the conditional distributions of \bar{X}_t given \bar{X}_0 as $p_{t|0}(\bar{X}_t|\bar{X}_0)$. Define $q_{t|0}$ in the same way. It is straightforward to see that

$$\begin{aligned} \log p_t(x) + \log(\mathbb{E}[\rho_*(\bar{X}_0)|\bar{X}_t = x]) &= \log(p_t(x)\mathbb{E}[\rho_*(\bar{X}_0)|\bar{X}_t = x]) \\ &= \log p_t(x) \int_{x'} \rho_*(x') p_{0|t}(x'|x) dx' \\ &= \log \int_{x'} \rho_*(x') p_{0,t}(x', x) dx' \\ &= \log \int_{x'} \rho_*(x') p_0(x') p_{t|0}(x|x') dx' \\ &= \log \int_{x'} q_0(x') p_{t|0}(x|x') dx'. \end{aligned} \quad (46)$$

Note that $p_{t|0}(x|x')$ and $q_{t|0}(x|x')$ are the same in (46). Therefore,

$$\begin{aligned} \log p_t(x) + \log(\mathbb{E}[\rho_*(\bar{X}_0)|\bar{X}_t = x]) &= \log \int_{x'} q_0(x') q_{t|0}(x|x') dx' \\ &= \log q_t(x), \end{aligned}$$

which concludes the proof. \square

D DETAILS OF NUMERICAL EXPERIMENTS

D.1 ALIGNMENT FOR GAUSSIAN MIXTURE MODELS

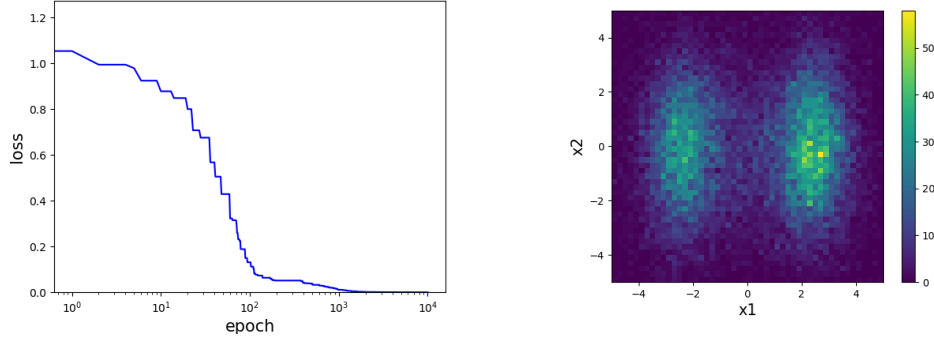
We explain how to align the pre-trained diffusion model for Gaussian Mixture Models and the technical details of our algorithm. Almost the same algorithm was used for the other experiments.

A Pre-Trained Score-Based Diffusion Model We pre-trained a score-based diffusion model to sample from the 2 dimensional mixture of Gaussian Mixture Models. The target density was $\frac{1}{2}(\mathcal{N}(\mu_1, \Sigma) + \mathcal{N}(\mu_2, \Sigma))$, $\mu_1 = [-2.5, 0]$, $\mu_2 = [2.5, 0]$, $\Sigma = [[1, 0], [0, 5]]$. The score model was implemented as simple 4 layer neural networks. The learning rate of pre-train was 0.0005, the batch size was 100, the number of epochs was 1000. The pre-train MSE loss is shown in the left side in Figure 4. The minimum losses until the current epoch were plotted. The histogram of 20000 samples from the pre-trained score-based diffusion model is the right figure in Figure 4. For sampling, T was set to be 10 and the number of sampling steps was 100.

The objective The target was the mean of the Gaussian in the right side, $\mu_w := \mu_2 = [2.5, 0]$. The preference of point x_w and x_l were determined by the Euclidean distance $d(\cdot, \mu_w)$ from $\mu_w := [2.5, 0]$. $x_w \succ x_l$ if and only if $d(x_w, \mu_w) < d(x_l, \mu_w)$. The DPO objective was used in this setting. 2000 points from p_{ref} were sampled to calculate the expectation of the functional derivative. The regularization terms β and γ were 0.04 and 0.1.

As a counter method, Diffusion-DPO (Wallace et al., 2024) was implemented with the learning rate = 0.0005, batch size = 5000. In practice, it is hardly realistic to compute the true DPO loss during Diffusion-DPO, but in this case, we forcefully carried out the computation by estimating the density ratio $q(x)/p_{\text{ref}}(x)$ with 100 samples.

2268
2269
2270
2271
2272
2273
2274
2275
2276
2277
2278
2279
2280



2281 Figure 4: **Left.** Pre-train MSE loss of denoising score matching. The minimum losses until the
2282 current epoch were plotted. **Right.** The histogram of 20000 samples from the pre-trained DDPM.

2283
2284
2285
2286
2287
2288
2289

Dual Averaging in Option 1 We implemented Option 1 for the experiment. We used 8 NVIDIA V100 GPUs with 32GB memory. We estimated the log-density ratio $\bar{g}^{(k-1)} = -\log \hat{q}^{(k)}/p_{\text{ref}} + \text{const.}$ with neural networks $f_k \simeq \bar{g}^{(k-1)}$. In each loop, the potential was trained by 1000 points in $x_1, x_2 \in [-5, 5]$, the learning rate was 0.0005, the number of epochs was 1000. We kept $\bar{g}^{(k-1)}$ as neural networks and generate the dataset for $\bar{g}^{(k)}$ from the equation ($\beta = \beta'$ for simplicity)

2290
2291
2292
2293
2294
2295
2296

$$\begin{aligned} \bar{g}^{(k)} &= \frac{2}{\beta(k+1)(k+2)} \left[\frac{\beta k(k+1)}{2} \bar{g}^{(k-1)} + k \frac{\delta F}{\delta q}(q^{(k)}) \right] \\ &= \frac{k}{k+2} \bar{g}^{(k-1)} + \frac{2k}{\beta k(k+2)} \frac{\delta F}{\delta q}(q^{(k)}). \end{aligned} \quad (47)$$

So, we only need one model to store for DA loops (we don't need $\bar{g}^{(k-2)}, \dots, \bar{g}^{(1)}$). The pseudocode for this phase is described as Algorithm D.1.

2297
2298
2299
2300
2301
2302
2303
2304
2305
2306
2307
2308
2309
2310
2311
2312

Algorithm D.1 Dual Averaging (Option 1)

Input: F : an objective, s : pre-trained score, β : Regularization scale, K : number of loops.

Output: f_K : a trained potential.

Initialize NNs f_0 randomly

Collect samples $(x_i)_i$ at the final denoising step from p_{ref} by score function s

We define $q^{(0)} \propto \exp(-f_0)p_{\text{ref}}$ (no actual computation)

Construct dataset $\{(x_i, \frac{1}{3\beta} \frac{\delta F}{\delta q}(q^{(0)}, x_i))\}_i$ with $(x_i)_i$ and f_0 using equation (2)

Train f_1 to approximate $\bar{g}^{(0)} = \frac{1}{3\beta} \frac{\delta F}{\delta q}(q^{(0)})$

for $k = 1, \dots, K - 1$ **do**

$q^{(k)} \propto \exp(-f_k)p_{\text{ref}}$ (no actual computation)

Construct dataset $\{(x_i, \frac{2k}{\beta k(k+2)} \frac{\delta F}{\delta q}(q^{(k)}, x_i))\}_i$ with $(x_i)_i$ and f_k using equation (2)

Train f_{k+1} to approximate $\frac{k}{k+2} f_k + \frac{2k}{\beta k(k+2)} \frac{\delta F}{\delta q}(q^{(k)})$ by minimizing MSE.

end for

End

2313
2314
2315
2316
2317
2318
2319
2320
2321

The heat map of the trained potential f_k is shown in Figure 5.

Doob's h-transform We sampled the aligned images with 50 diffusion steps. The guidance term of Doob's h-transform was calculated in every diffusion steps. The conditional expectation $\mathbb{E}[h_T(X_T^x) | x]$ was calculated by Monte Carlo with 30000 samples. The pseudocode for this phase is described as Algorithm D.2. In phase 2 (the sampling phase), our simplest solution (i.e., estimating the correction term at each time step using Monte Carlo) has a time complexity of $\mathcal{O}(L^2)$, where L represents the number of time steps in the denoising process. When we set N as the number of particles needed to estimate one correction term, to compute the correction term for each sample simultaneously, $\mathcal{O}(N)$ memory space is required. The sampling error for each correction term would be $\mathcal{O}(1/\sqrt{N})$. This leads to severe computational effort in phase 2. However, this Doob's

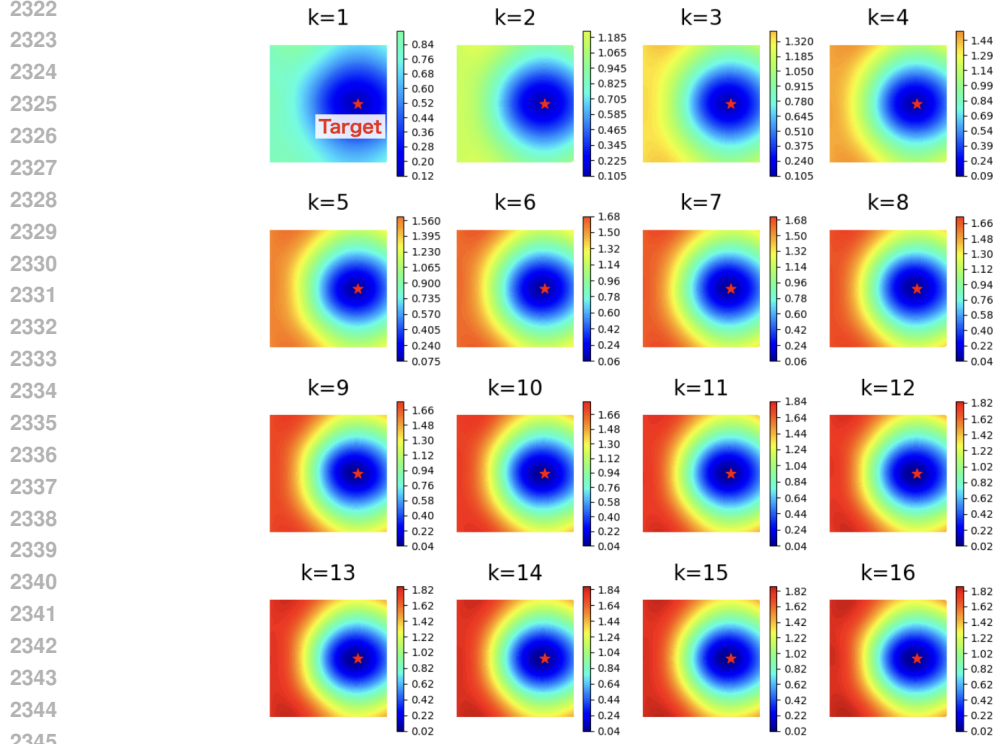


Figure 5: The heatmap of the potential f_k in the k th loop in Dual Averaging for Gaussian Mixture Model. The target point was $[2.5, 0]$. Note that f_k is the negated log-density ratio: the aligned density is $\exp(-f_k)p_{\text{ref}}$.

h-transform technique itself has been used in image generation (Uehara et al., 2024a;b), Bayesian sampling (Heng et al., 2024), and filtering (Chopin et al., 2023). As a more practical alternative of our phase 2, the idea of approximating the correction term using neural ODE solvers for faster test-time implementation has also been proposed in (Uehara et al., 2024b;a).

Algorithm D.2 Doob’s h-transform (A simplest implementation)

Input: F : an objective, f_K : a trained potential, s : pre-trained score,

Output: x_T : an output approximately from $\exp(-f_K)p_{\text{ref}}$.

Initialize x_0 as white noise

Set number of steps L and the time T .

Set the step size $h = T/L$

for $l = 0, \dots, L - 1$ **do**

 Initialize N samples $(x_{l,i})_{i \leq N}$ as x_l .

for $l' = l, \dots, L - 1$ **do**

 (denoising step of $(x_{l,i})_{i \leq N}$)

end for

 Store N samples of X_T^{\leftarrow} as $(x_{l,i})_{i \leq N}$.

 Approximate $u(x_l, lh) = \nabla \log \mathbb{E}[\exp(-f_K(X_T^{\leftarrow}) \mid X_{lh}^{\leftarrow} = x_l]$ by Monte Carlo with $(x_{l,i})_{i \leq N}$.

 Sample white noise ξ_{noise}

$x_{l+1} := x_l + \delta(x_l + 2s(x_l, T - lh) + 2u(x_l, lh) + \sqrt{2h}\xi_{\text{noise}}$

end for

End

2376 D.2 IMAGE GENERATION ALIGNMENT
2377

2378 We aligned the image generation of the basic pre-trained model in Diffusion Mod-
2379 els Course (source: HuggingFace (2022)). The pipeline path we utilized was
2380 “johnnowhitaker/ddpm-butterflies-32px”. The summarized results are show in
2381 Figure 7.

2382 **The pre-trained Model** The model samples the images of butterflies of 32×32 pixels. Number of
2383 the sampling step was 1000.

2384 **The objective** The target color was $[0.9, 0.9, 0.9]$ in RGB. The reward is visualized in Figure 6.
2385 6400 samples from p_{ref} to calculate the expectation of F and $\frac{\delta F}{\delta q}$. β and γ were 0.05 and 1. The
2386 output of the functional derivative was clipped in ± 20 to stabilize the training step. In calculation of
2387 the DPO objective, the sample that has a higher reward is the “winning” sample.
2388

2389 **Dual Averaging** In each loop, f_k was trained by 1024 images from pooled 6400 images, the learning
2390 rate was 0.0001, the batch size was 64, and the number of epochs was 5. f_k s were implemented by
2391 Unet2Dmodel in Diffusers library von Platen et al. (2022). How the potential f_k learned the reward,
2392 the distance from the target color, was shown in the right side of Figure 6. The DA algorithm
2393 succeeded to extract the target images from the true reward.



2409
2410 Figure 6: **Left.** Output images of p_{ref} sorted by the distance from the target color ($= -\text{reward}$).
2411 **Right.** Images sorted by the learned potential in $k = 2$.

2412 **Doob’s h-transform** We sampled the aligned images with 1000 diffusion steps. The guidance term
2413 of Doob’s h-transform was calculated in every 10 diffusion steps for faster sampling. We calculated
2414 the drift term of Doob’s h-transform once in 10 diffusion steps for faster sampling. In addition,
2415 We defined a decay rate $r_d = 0.95$ and a strongness $s = 5$ for $\nabla \log \rho_t$ and finally we added
2416 $r_d^{m'} \nabla \log \mathbb{E}[\exp(-sf_K(X_T^{\leftarrow}) \mid x_{10m\delta})]$ as a drift term in $l = 10m + m'$ th diffusion step to balance
2417 the computational cost and stability. The conditional expectation $\mathbb{E}[\rho_T(X_T^{\leftarrow}) \mid x]$ was calculated by
2418 Monte Carlo with 128 samples.
2419

2420 D.3 TILT CORRECTION FOR GENERATION OF MEDICAL IMAGE DATA
2421

2422 Our goal of this experiment was generating images with no rotation with an unconditional pre-
2423 trained model that generates rotated images. The objective was based on DPO. The rotation angle
2424 of each image was predicted with CNN. The summarized results are in Figure 11.

2425 **Dataset** 10000 images of Head CT (64×64 pixel) in Medical MNIST Lozano (2017) were leveraged.
2426 They include some rotated images, the angles are up to 90° . To aggravate the existing situation, we
2427 augmented the data by rotating images (up to 45°) from this dataset to be 40000. A predictor of
2428 angles were trained with the augmented dataset to define the reward in place of human preference
2429 due to preparation difficulties. The number of epochs was 10, 95% and 5% of the dataset were used
for training and validation, the training MSE loss was 3.79, and the validation MSE loss was 3.25.

2430
2431
2432
2433
2434
2435
2436
2437
2438
2439
2440
2441
2442
2443
2444
2445
2446
2447
2448
2449
2450
2451
2452
2453
2454
2455
2456
2457
2458
2459
2460
2461
2462
2463
2464
2465
2466
2467
2468
2469
2470
2471
2472
2473
2474
2475
2476
2477
2478
2479
2480
2481
2482
2483

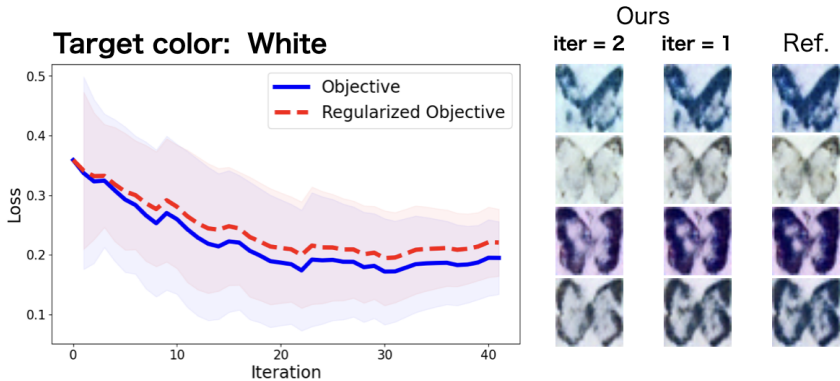


Figure 7: **Left.** The loss during DA for image generation alignment. “Objective”: DPO objective. “Regularized Objective”: “Objective” + $\beta D_{\text{KL}}(q||p_{\text{ref}})$, $\beta = 0.05$ **Right.** Examples of aligned image generation. “iter=2”: ours with $k = 2$ DA iterations, “iter=1”: ours with $k = 1$ DA iteration. “Reference”: samples from p_{ref} .

Note that there were rotated images in the original dataset, so the labels of the rotation angles made in the augmentation were noisy.

Pre-trained Autoencoder We pre-trained autoencoder from scratch. It encodes gray-scaled 64×64 pixels into latent 32×32 pixels. It only has convolution layers so that geometrical features were preserved for simplicity. The training data was 95% of augmented 40000 images and the validation data was 5% of them. This autoencoder was fed white-noised data to make the model robust with noise. The pretraining MSE loss is shown in the left side of Figure 8.

Latent Diffusion Model We also pre-trained a (latent) diffusion model based on Unet2DModel in Diffusers von Platen et al. (2022). Number of sampling steps was 1000. The beta scheduler was set to be squaredcos_cap_v2. In pre-training, we leveraged the augmented dataset up to 20000 images, the number of epochs was 15, the batch size was 8, the learning rate was 0.0001. The pretraining MSE loss is shown in right side of Figure 8 and the generated images are displayed in Figure 9.

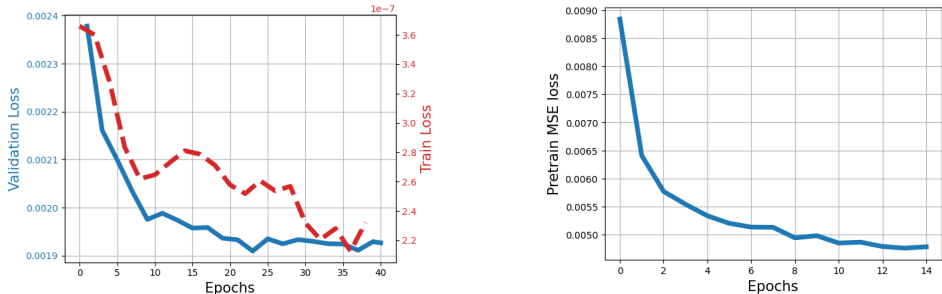
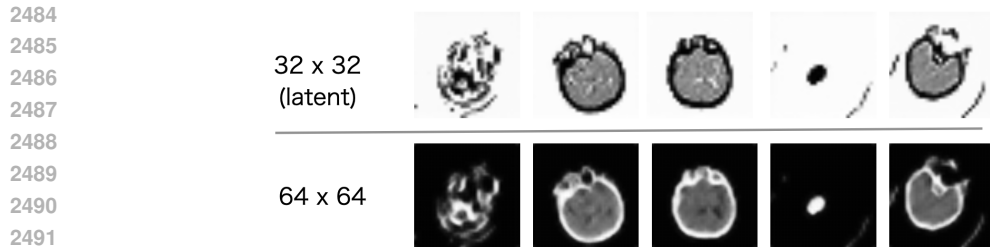


Figure 8: **Left.** The MSE loss in pretraining the Autoencoder. The solid blue line and the dashed red represent the validation loss and the train loss. **Right.** The MSE loss in pretraining the diffusion model.

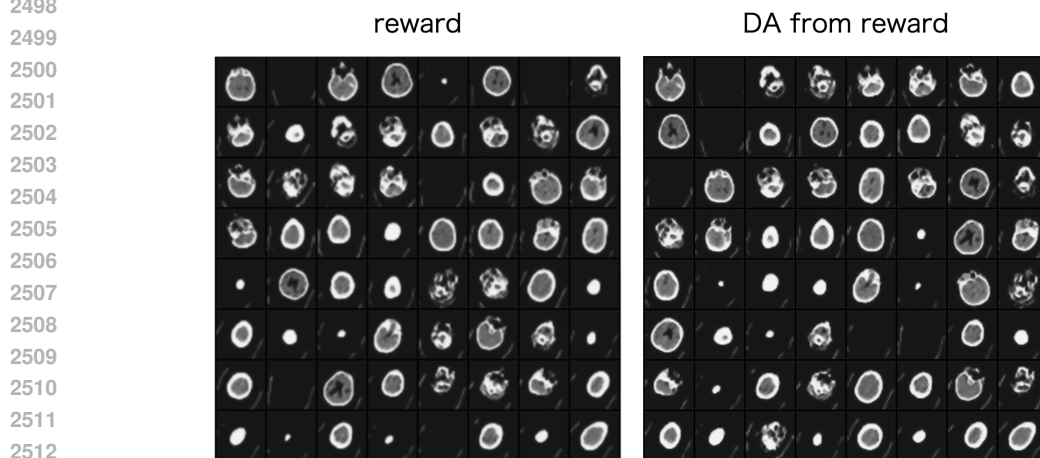
The objective The reward was defined to be $-|\text{predicted angle}|$ of the pre-trained predictor (in place of humans), described in the left side of Figure 10. 6400 samples from p_{ref} to calculate the expectation of F and $\frac{\delta F}{\delta q}$. β and γ were 0.01 and 0.1. The output of the functional derivative was clipped in ± 5 to stabilize the training step. In calculation of the DPO objective, the sample that has a higher reward (in the more vertical direction) is the “winning” sample.

Dual Averaging In each loop, f_k was trained by 6400 images from p_{ref} . All the generated images were reused during DA. The learning rate was 0.0001, the batch size was 64, and the number of



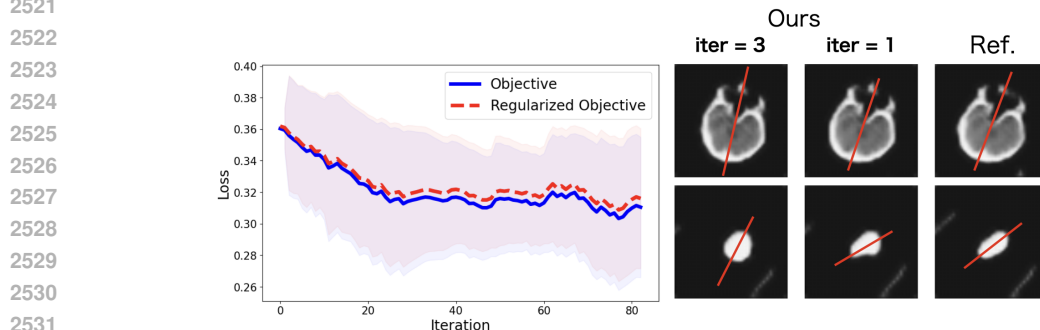
2493 **Figure 9: Top.** Outputs of pre-trained latent diffusion. **Bottom.** Decoded images of the outputs.

2494
 2495
 2496 epochs was 5. We compared the learned potential with the reference reward in Figure 10. We see
 2497 that DA iterations worked well to replicate the reference reward.



2514 **Figure 10: Left.** Output CT images of the pre-trained model, sorted by the absolute values of
 2515 estimated angles ($= -\text{reward}$). **Right.** Output CT Images sorted by the trained potential in the 3rd
 2516 loop in DA.

2517
 2518 **Doob’s h-transform** We sampled the aligned images with 1000 diffusion steps. The guidance term
 2519 of Doob’s h-transform was calculated once in 10 diffusion steps. Technical settings were the same
 2520 with . The conditional expectation was calculated by Monte Carlo with 128 samples.



2533 **Figure 11: Left.** The loss during DA for tilt correction. “Objective”: DPO objective. The target
 2534 point was $[2.5, 0]$. “Regularized Objective”: “Objective” + $\beta D_{\text{KL}}(q||p_{\text{ref}})$, $\beta = 0.01$ **Right.** Tilt-
 2535 corrected Head CT image generation. “iter=3”: ours with $k = 3$ DA iterations, “iter=1”: ours with
 2536 $k = 1$ DA iteration. “Reference”: samples from p_{ref} .

2537